NUCLEAR MAGNETIC RESONANCE IN SOME SOLID HYDROCARBONS

Robert G. Eades

A Thesis Submitted for the Degree of PhD
at the
University of St Andrews

1952

Full metadata for this item is available in
St Andrews Research Repository
at:
http://research-repository.st-andrews.ac.uk/

Please use this identifier to cite or link to this item:
http://hdl.handle.net/10023/14695

NUCLEAR MAGNETIC RESONANCE IN SOME SOLID HYDROCARBONS

being

a Thesis presented by

Robert G. Eades, B.Sc.

to the

University of St. Andrews

in application for the Degree

of Doctor of Philosophy.

ProQuest Number: 10171257

ProQuest 10171257

DECLARATION

I hereby declare that the following Thesis is based on the results of experiments carried out by me, that the Thesis is my own composition, and that it has not previously been presented for a Higher Degree.

The research was carried out in the Physical Laboratory of the United College of the University of St. Andrews under the direction of Dr. E.R. Andrew, F.R.S.E.

CERTIFICATE

I certify that Robert G. Eades, B.Sc., has spent nine terms at research work in the Physical Laboratory of the United College of the University of St. Andrews under my direction, that he has fulfilled the conditions of Ordinance No.16 (St. Andrews) and that he is qualified to submit the accompanying Thesis in application for the Degree of Doctor of Philosophy.

St. Andrews.   Director of Research.

CAREER

I matriculated in the University of
St. Andrews in October 1941, and followed a course
leading to graduation, obtaining the degree of
Bachelor of Science.   I recommenced my studies
in October 1947, after serving in the Royal Air
Force, and followed a course in Mathematics and
Natural Philosophy.   I obtained Postgraduate First
Class Honours in Natural Philosophy in June 1949.

In October 1949 I commenced research on the work
which is now being submitted as a Ph.D. Thesis.

CONTENTS

1. INTRODUCTION

Nuclear Magnetic Resonance in Relation to Problems of the Solid State.

The phenomenon of nuclear magnetic resonance is closely related to the molecular beam experiments and to microwave spectroscopy. Its significant feature is that the magnetic resonance principle, first applied to the molecular beam technique, has been extended to solids, liquids and gases in their normal physical states. In addition to providing yet another important method of measuring nuclear magnetic properties, this newer technique gives a means of investigating the establishment of the thermal equilibrium which is essential to the methods of obtaining very low temperatures; further, the resonance absorption spectrum yields information on crystal structures, phase transitions in solids and information about hindered rotation of molecules in solids. Thus the phenomenon can be used to study certain problems of the solid state. This thesis gives an account of such an application.

2.   THEORY

2.1.   General

Many nuclei possess an intrinsic angular momentum and an associated nuclear magnetic moment.   If the maximum measurable component of the angular momentum of the nucleus is denoted by $I\hbar$, and its magnetic moment by μ , and if a system of such spins is placed in a magnetic field $\underline{H}_o$ then for each of the spins there are $2I+1$ levels with energy spacing $\frac{\mu H_o}{I}$.   The nucleus at resonance in the investigations reported here is the proton, which has spin $\frac{1}{2}$.   Hence the energy separation of the two possible states is $2\mu H_o$:   these correspond to μ parallel or anti-parallel to the field $\underline{H}_o$.   Transitions between the two states are allowed and hence energy absorption can occur. For this to happen quanta of energy, $\Delta E = h\nu$, must be supplied from an electromagnetic field, viz

$$\Delta E = h\nu = 2\mu H_o$$

For magnetic fields H_o of a few thousand gauss, the frequency ν lies within the range 8 Mc/s to 30 Mc/s.   N. Bloembergen, et al (reference 1) have shown that radiation polarised at right angles to H_o is required to induce the transitions.

Stimulated emission will also occur, the nucleus involved returning to the lower of the two energy states. Since the

probabilities for absorption and emission are the same,
a net absorption of energy is only possible if there is
a surplus of spins in the lower energy state. This will
be the case providing there is some mechanism ensuring
that the spin system is at the same temperature as the
lattice.   There will then be a Boltzmann distribution
between the energy levels.   The mechanism by means of
which thermal equilibrium between the spins and the lattice
is established is called the 'Spin-lattice Relaxation
Process'.   The efficiency of such a process is measured
by the spin-lattice relaxation time, T_1; and the
establishment of equilibrium is characterised by an equation
of the form:

$$n = n_o \left(1 - exp - \frac{t}{T_1} \right) \tag{1}$$

where n is the existing difference in population
between the two levels and n_o is the equilibrium value
of this difference.   For protons in a field of 5500
gauss at room temperature, there are approximately one
million and four protons in the lower energy state for
every million in the higher state.

Provided the relaxation mechanism is able to maintain
this difference of population in the face of the competition
of the applied electromagnetic field, then a net absorption
of energy will continue.   It is from a study of the

variation of the absorption spectrum with temperature that information regarding molecular and crystal structures and motion within the solid is obtained. The spin-lattice relaxation time can also be readily measured as a function of the temperature of the sample; these measurements can also yield information about molecular motions occurring in the solid, since such motions may predominantly control the relaxation process.

It is now necessary to examine in more detail the origin and nature of the absorption spectrum and the spin-lattice relaxation process.

2.2. The Absorption Spectrum

For an isolated proton, placed in a magnetic field H_o, the frequency at which resonant absorption occurs is given by $h\nu = 2\mu H_o$. The protons in a solid, however, are not isolated in this sense, but are surrounded by a very large number of other protons each with a magnetic moment μ . Thus any particular proton experiences a field $\underline{H}_o + \underline{H}_{loc}$, where $\underline{H}_{loc}$ is the instantaneous sum of the fields of all its neighbours. $\underline{H}_{loc}$ is typically a few gauss, only the nearest neighbours being effective, since the z-component of the local field at a distance r from a dipole μ is given by

$$H_{loc_z} = \pm \frac{\mu}{r^3}(3\cos^2\theta - 1).$$

For a system of interacting protons, therefore, the resonance condition is :

$$h\nu = 2\mu(\underline{H}_0 + \underline{H}_{loc})$$

and the very narrow absorption line for an isolated spin is broadened into a spectrum which is a few gauss wide.

This picture is, of course, much simplified; but it does lead us to expect that the form and shape of the absorption spectrum will depend on both the arrangement of the protons within the molecule and the arrangement of the molecules in the crystal lattice.

Provided, therefore, that we can calculate theoretically the nature of the absorption spectrum to be expected from any given configuration of protons, then an examination of the resonance line will confirm postulated molecular and crystal structures. For simple cases where there are not more than three nuclei in the elementary interaction cell detailed perturbation calculations can be made. Examples of such work are given in references 2, 3, 4 and 5. For more complicated cases, the perturbation calculations are not suitable. Van Vleck has provided a more elegant method of interpreting the experimental data. His analysis (reference 6) relates the 'second moment' of the line shape function quantitatively to the structure of the sample. The 'second moment' is defined by him as the mean value of the square of the frequency deviation from the centre of

the resonance, the average being taken over the line shape function.

If ν_0 is the resonant frequency, the second moment is

$$\langle (\Delta \nu)^2 \rangle_{av} = \int_{-\infty}^{+\infty} (\nu - \nu_0)^2 \, g(\nu) \, d\nu$$

The line shape function $g(\nu)$ is normalised, i.e.

$$\int_{-\infty}^{+\infty} g(\nu) \, d\nu = 1$$

The technique employed in carrying out measurements (see section 3.2) is to vary the magnetic field at a fixed frequency. If the second moment is expressed appropriately in gauss^2, Van Vleck's theory leads to an expression :

$$\text{Second moment} = \frac{3}{2} \frac{I(I+1)}{N_R} g^2 \mu_0^2 \sum_{j>k} (3\cos^2\theta_{jk} - 1)^2 r_{jk}^{-6} + \frac{1}{3} \frac{\mu_0^2}{N_R} \sum_{j} \sum_{f} I_f(I_f+1) g_f^2 (3\cos^2\theta_{jf} - 1)^2 r_{jf}^{-6}$$

$$= \langle (\Delta H)^2 \rangle_{av}$$

where

$$\langle (\Delta \nu)^2 \rangle_{av} = \frac{g^2 \mu_0^2}{\hbar^2} \langle (\Delta H)^2 \rangle_{av}$$

g, I are the nuclear g-factor and spin of the nucleus

at resonance,

g_f, I_f are the nuclear g-factors and spins of the other nuclear species in the sample,

r_{jk} is the length of the vector connecting nuclei j and k,

N_R is the number of nuclei at resonance which are present in the group of nuclei to which broadening interactions are considered to be confined in evaluating $\langle (\Delta H)^2 \rangle_{av}$.

For a polycrystalline sample $(3\cos^2 \theta - 1)^2$ has to be averaged over a sphere. Also, since the samples examined in this work (with one exception) contained only one species of magnetic nucleus, we have finally :

$$\text{Second Moment of powdered sample} = \frac{6}{5} \frac{I(I+1)}{N_R} g^2 \mu_o^2 \sum_{j > k} r_{jk}^{-6} \quad \text{gauss}^2.$$

Using Bearden and Watt's values (reference 7), this gives

$$\text{second moment} = \frac{715.9}{N_R} \sum_{j > k} r_{jk}^{-6} \quad \text{gauss}^2.$$

These formulae have been used successfully by several workers. (See, for example, references 3 and 4).

So far in this section it has been assumed that the nuclei involved are at rest, except for the ever present thermal vibrations of the crystal lattice. Any motion of the nuclei will average out to some extent the magnetic

interactions and hence tend to narrow the observed line. The effect of motion in the lattice has been investigated by H.S. Gutowsky and G.E. Pake (reference 5), using results first obtained by N. Bloembergen et al. (reference 1). They introduce a reorientation frequency ν_c to define the average frequency of the molecular motion occurring and obtain the expression

$$(\delta\nu)^2 = A^2 \left(\frac{2}{\pi}\right) \tan^{-1}\left(\alpha \frac{\delta\nu}{\nu_c}\right) \qquad (2)$$

where $\delta\nu$ is the linewidth measured between maximum and minimum slope of the absorption line. ν_c is the reorientation frequency, and α is a constant of order unity. As $\nu_c \to 0$, then $\delta\nu \to A$ and the lattice is said to be effectively rigid. As ν_c increases and approaches the value A, $\delta\nu$ decreases. Now A is typically about 30 Kc/s hence the line is narrowed by relatively low frequency motion. E.R. Andrew (reference 8) has listed some forms of motion which may occur and the information which theory allows us to deduce from the experimental results :

"The various types of molecular motion about a rotational axis which may be encountered in a crystal include :

(i) Rotation

(ii) Quantum mechanical tunnelling through the potential barrier. The rotational axis must also be a symmetry axis if this motion is to be possible.

(iii) Rotational oscillation.

Provided the frequency of rotation, tunnelling or oscillation exceeds the minimum reorientation frequency, all these forms of motion cause a reduction of linewidth and of second moment.   Moreover, if the axis of rotation is one of three-, four-, or six-fold symmetry, the rotation in (i) need not be maintained all the time, provided the necessary number of reorientations are made per second. Thus a small fraction of the time may be spent in excited states of high rotational frequency and the remainder of the time in the various equivalent fixed positions.

The effect of rotation (including the non-continuous form just mentioned) on the second moment is identical with that of tunnelling about a three-, four-, or six-fold axis (reference 5) (except insofar as there may be a slight difference in the intermolecular contributions).   Second moment data are therefore unable to distinguish between these forms of motion".

Evidence obtained during this work indicates that in favourable cases molecules can spin about fixed centres of gravity, and may even to some extent diffuse through the crystal lattice (see section 4.2.5).

It can be said, therefore, that any form of molecular motion in the solid will reduce the second moment to some

fraction of the value calculated from Van Vleck's formula provided the motion takes place at a high enough frequency. The factor $(3 \cos^2 \theta - 1)/r^3$, occurring in Van Vleck's formula, must then be replaced by its mean value over the motion. The formula will then yield a theoretical second moment for the lattice in which motion is taking place, and this can be compared from that calculated from the experimental line shapes. The procedure is therefore :

(1) To obtain experimentally plots of the absorption lines at different temperatures.

(11) To calculate the second moment of these absorption lines and to plot a second moment v. temperature graph.

(111) To calculate the theoretical second moment using Van Vleck's formula - a procedure only possible when adequate information on the crystal structure of the sample is available.

(iv) To compare experimental and theoretical values of the second moment, postulating where necessary motions of molecules which would reduce the theoretical second moment to that found experiment--ally at any temperature.

This procedure is illustrated in sections 4.2 to 4.5.

2.3 **The Spin-lattice Relaxation Process.**

In the previous section we have considered a system of interacting nuclear spins. In a completely rigid lattice such a system would be thermally isolated and a net absorption of energy would not continue. The mechanism ensuring thermal contact between the spins and the lattice is therefore important.

If the nuclear spins and the lattice are to exchange energy, then there must exist at the nucleus oscillating magnetic fields which satisfy the resonance condition and which originate in the thermal motion of the lattice.   The ever present thermal vibrations of the lattice are relatively ineffective: this was shown by Heitler and Teller (reference 9) who applied Waller's theory (reference 10).   N. Bloembergen et al. (reference 1) included more general types of lattice motion in their treatment; they showed that, when excited, these motions are much more effective in bringing about spin-lattice relaxation than are the lattice vibrations.   A discussion of their treatment is reserved to section 4.2.6, where its application to present problems will also be consider--ed.   It is sufficient for the present to assume that there exists a mechanism coupling the spin system to the lattice, that the origin of this mechanism is in the thermal motion of the molecules, and that the efficiency of the coupling is measured by the spin-lattice relaxation time, T_1, as defined in section 2.1.

In the equation:

$$n = n_o \left(1 - \exp -\frac{t}{T_1} \right) \qquad (1)$$

which describes the population difference, n, of a system of proton spins, t seconds after being placed in an external magnetic field, n must be very nearly equal to n_o if we are to observe the full absorption intensity when we apply the

radio-frequency field.   (1) may be written as :

$$\frac{dn}{dt} = \frac{n_o - n}{T_1} \tag{2}$$

where dn/dt gives the rate of approach to equilibrium.
In the presence of an electromagnetic field we must subtract
a term from the right hand side to represent the rate at
which transitions to the higher energy state are being
induced.   If $W_{\frac{1}{2} \to -\frac{1}{2}}$ represents the probability of a single
transition - which makes a difference of 2 in the population
difference, then :

$$\frac{dn}{dt} = \frac{n_o - n}{T_1} - 2n\, W_{\frac{1}{2} \to -\frac{1}{2}} \tag{3}$$

The probability of a single transition $W_{\frac{1}{2} \to -\frac{1}{2}}$ is given by:

$$\frac{1}{4} \gamma^2 H_1^2 g(\nu)_{max} \tag{4}$$

(see reference 1)

where γ is the nuclear gyromagnetic ratio, $2H_1$ is the
amplitude of the radio-frequency field, and $g(\nu)$ is the
observed shape function of the absorption line.   In section
2.2. we saw that the shape and width of the absorption line
depended on the spin-spin interaction.   Accordingly $g(\nu)_{max}$
is conveniently expressed in terms of a quantity T_2, where

$$T_2 = \tfrac{1}{2} \, g(\nu)_{max} \qquad\qquad (5)$$

$1/T_2$ is then a measure of the linewidth of the resonance; T_2 itself measures the effieiency of the spin-spin relaxation.

Combining these results, and considering the equilibrium state defined by $dn/dt = 0$, we have :

$$0 = \frac{n_0 - n}{T_1} - n \, \gamma^2 H_1^2 \, T_2$$

$$\therefore \quad \frac{n}{n_0} = \frac{1}{1 + \gamma^2 H_1^2 T_1 T_2} \qquad\qquad (6)$$

Thus in the presence of the electromagnetic field, which is inducing transitions, the maximum steady state absorption is reduced by the saturation factor $1/(1 + \gamma^2 H_1^2 T_1 T_2)$. When $\gamma^2 H_1^2 T_1 T_2 \ll 1$ the full absorption intensity is observed. This saturation effect provides a method of determining T_1 when it is too short to be measured by more direct methods. This is discussed in section 4.2.6.

2.4. Summary of Section 2.

Briefly, then, we have seen that the fundamental resonance condition is $h\nu = 2\mu H_0$, and that the natural linewidth of the resonance for an isolated spin (typically 0.01 gauss) is swamped by the broadening due to the spin-

spin interaction.   Further, motion of the molecules in the lattice modifies this spin-spin interaction, thereby reducing the width of the absorption line.   Finally, we saw that this molecular motion can account for the relatively short spin-lattice relaxation times observed. From equation (6) it follows that the r.f. power supplied must be below a certain value if we are to observe the true absorption line.   Saturation of the sample does, however, provide a method of measuring T_1.

3. APPARATUS

3.1. General

The fundamental resonance condition, $h\nu_0 = 2\mu H_0$,
indicates that the frequency of operation ν_0 is proportional
to the magnetic field H_0 used.   But this does not mean that
an arbitrary choice of field or frequency decides the
operating conditions.   The intensity of the nuclear resonance
signal obtained from solids is in general small, being
comparable with noise voltages appearing in the detection
circuits.   Hence it is essential to have the optimum
experimental conditions if these weak signals are to be
recorded.   Bloembergen et al. (reference 1) developed an
expression giving the ratio of the nuclear signal obtained
to the R.M.S. noise fluctuations;   this shows that the ratio
is proportional to $\nu_0^{7/4}$, where ν_0 is the operating frequency.
Practical limitations in the design of associated detection
equipment make about 30 Mc/s an upper frequency limit.   Even
with this condition met, very careful design of the r.f.
circuits is necessary if useful results are to be obtained.
In the preliminary stages, an electromagnet was used to
supply the main field H_0.   The results recorded in this
thesis, however, have been obtained using the permanent
magnet designed by Dr. E.R. Andrew and Mr. F.A. Rushworth.

3.2. The Apparatus for detecting the Resonance Absorption.
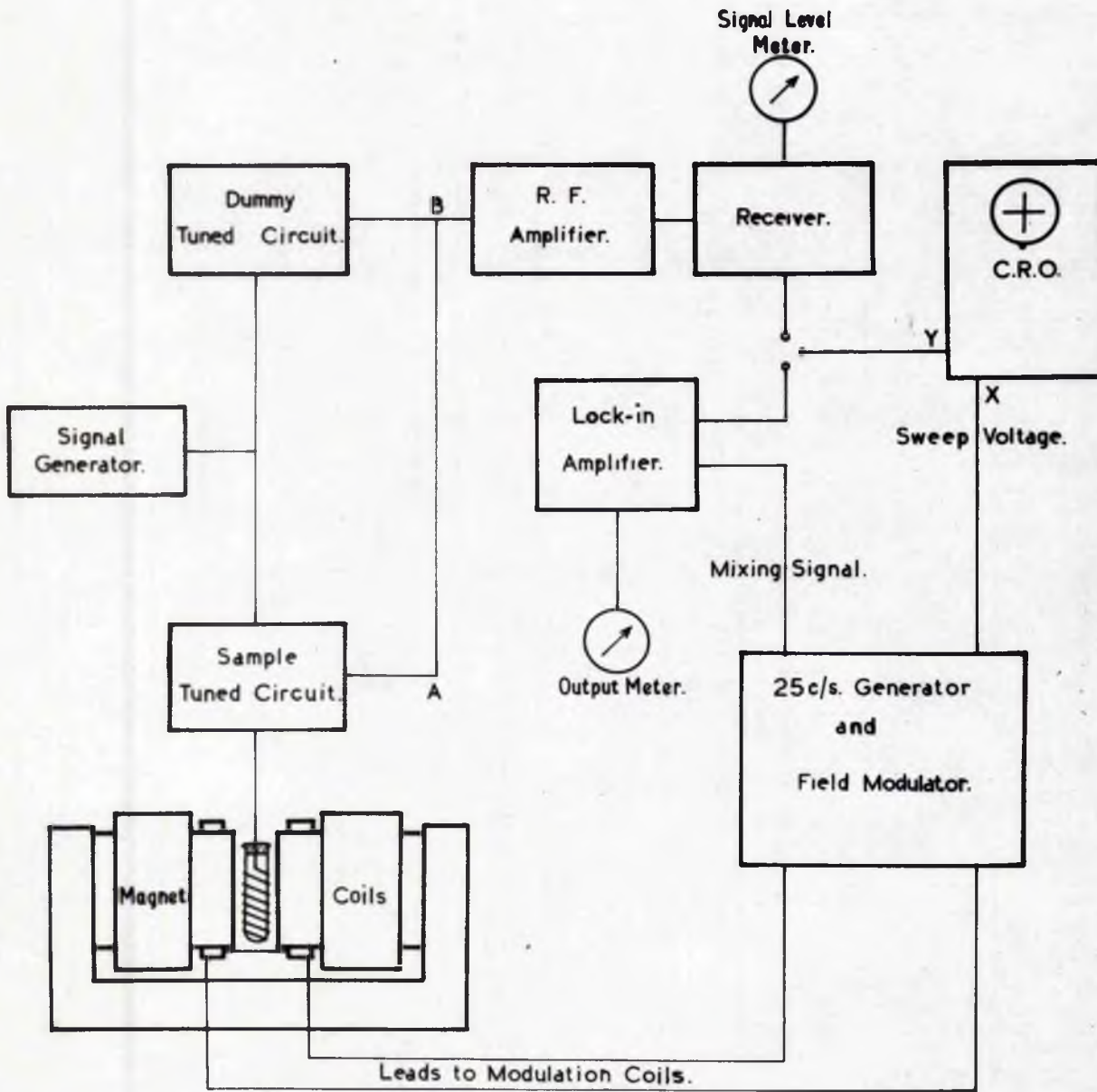
MODULATION BRIDGE.

Figure 1.

The resonant absorption of energy is detected by placing the sample under study in one arm of a radio-frequency bridge, part of which is located in the magnetic field H_o. A commercial Signal Generator supplies the quanta of radiation at a frequency ν_o, ν_o (or H_o in the case of the electromagnet) being adjusted until the resonance condition is met. The out of balance signal from the bridge is amplified and detected. The main magnetic field is modulated at 25 c/s, the amplitude of this modulation depending on the measuring technique being employed. Either the resultant field $H_o + H_m$, where H_m is the modulation field, is swept right through the resonance values twice in 1/25 second or the amplitude of the modulation is adjusted so that it is only a small fraction of the linewidth. In the first case, absorption of energy from a radio-frequency tuned circuit is occurring 50 times per second, giving an audio modulation of the r.f. carrier which is supplying the quanta of energy inducing the transitions. The audio modulation is in fact the absorption line shape which can be displayed on an oscilloscope if the X-plates are fed with a 25 c/s voltage correctly phased relative to the 25 c/s current in the field modulation coils. In this way narrow resonance lines can be readily observed.

With solid samples, however, the absorption line is generally several gauss wide and the maximum absorption intensity is correspondingly smaller. In order to plot out
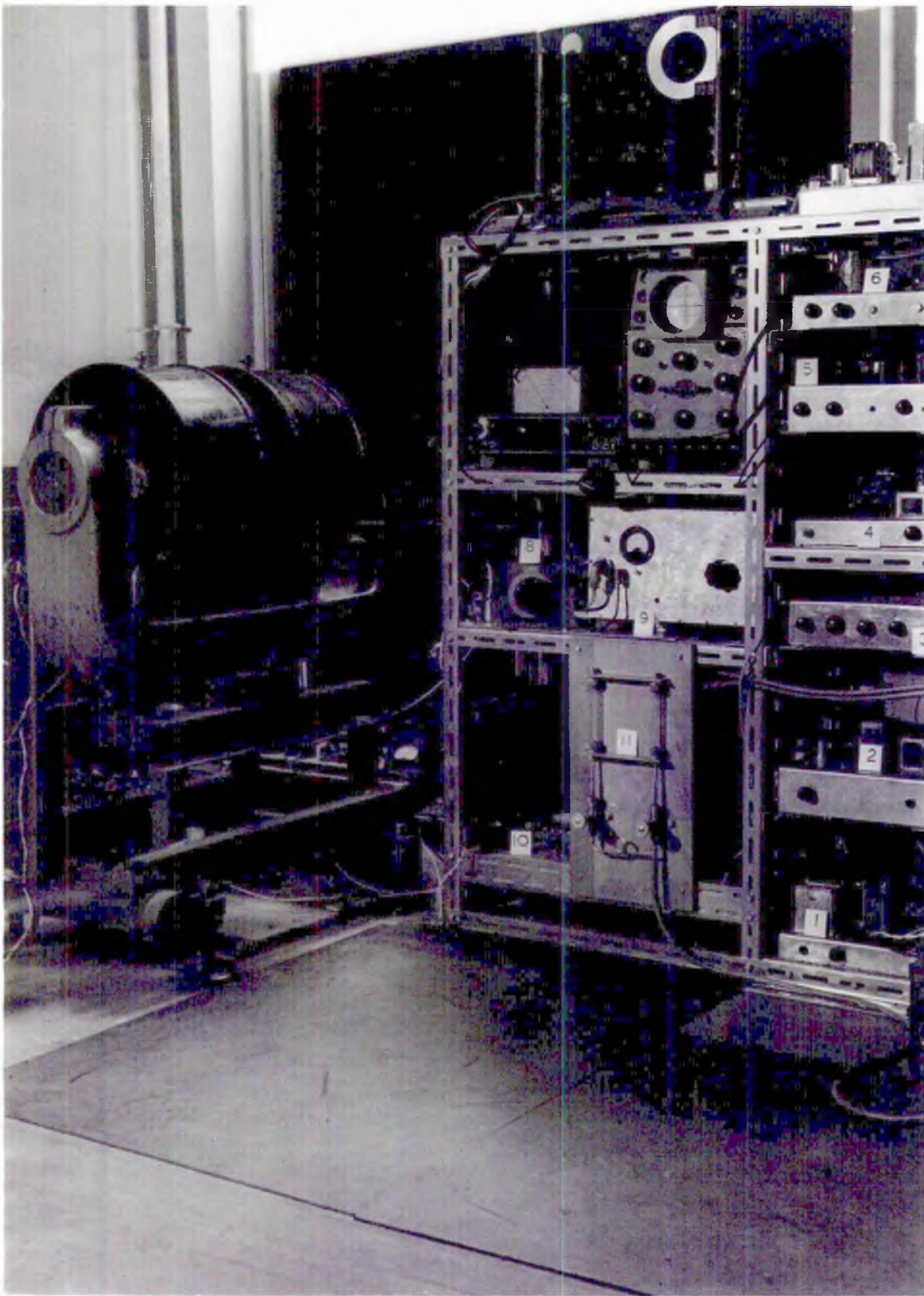
Figure 2.

these line shapes and to increase the sensitivity of the apparatus, a narrow band 'lock-in' amplifier is incorporated. This is used in conjunction with the small field modulation mentioned above. The main field is then shifted slowly through the resonance values. This device yields on the output meter (or recorder) the first derivative of the resonance line shape. The essential features of the modulation bridge are indicated schematically in figure 1; figures 2 and 3 are photographs of the main parts of the apparatus.

To the left of figure 2 can be seen the electromagnet. The oil circulating pump and the heat exchanger are further to the left and are not shown. On the rack is mounted most of the associated electronic equipment. Top left is the Signal Generator, Airmec type 701. Immediately below this are mounted the Receiver, Eddystone type 680, and the Cossor Oscillograph, model 1049. The other units are numbered and are as follows :

(1) Power supplies for the 25 c/s generator and Power Amplifier.

(2) The Power Amplifier, capable of supplying 15 watts at 25 c/s into a 200 ohm load.

(3) 25 c/s generator, consisting of a multi-vibrator and tuned amplifiers.

(4) Power supplies for the Lock-in Amplifier.

(5) The Lock-in Amplifier.
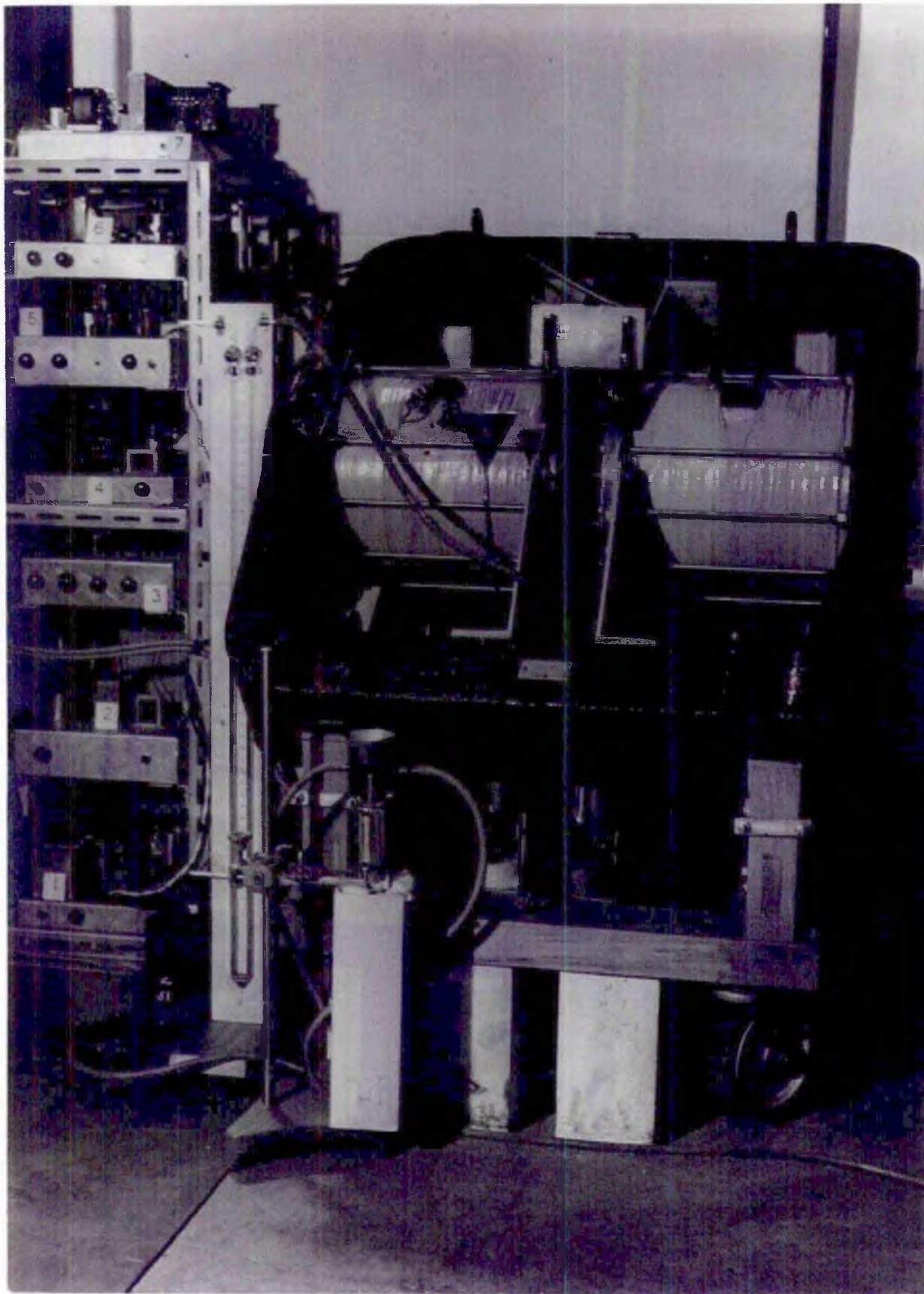
Figure 3.

(6) Phasing and transforming unit supplying the X-sweep for the C.R.O.

(7) High tension power supply for Eddystone receiver and Preamplifier.

(8) The 'dummy' unit of the R.F. Bridge.

(9) R.F. Preamplifier feeding the receiver.

(10) Stabilised power supply for the Signal Generator.

(11) Flow gauges for the gas cryostat used in cooling the sample.

Figure 3 shows the permanent magnet placed at the left right-hand side of the rack. The brass box containing part of the sample tuned circuit can be seen mounted above the gap. The coaxial lines connecting it into the R.F. bridge can be seen leaving it and running over the top portion of the yoke. The cryostat assembly with its pumping system cannot be seen clearly in the photograph. The manometer to the right of the magnet indicates the pressure under which the coolant - liquid nitrogen, air or oxygen - is boiling.

3.3. Details of the Apparatus.

In order to emphasise the important requirements of the apparatus some parts are described in more detail in the following sections.

3.3.1.   The Electromagnet.

This was obtained on loan from the Royal Society Mond Laboratory, Cambridge.   It has a resistance of 0.63 ohm, the total number of turns being 1000.   This means that fairly high currents are required to give suitable fields. For instance, with ν_0 = 25 Mc/s., a field of 5870 gauss gives resonance;   to obtain this a current of 21 amperes is required.   To plot out a line shape using the 'lock-in' amplifier takes up to 15 minutes and it is essential that over this interval the magnetic field remains sensibly constant - say within $\frac{1}{4}\pm$ gauss.   This, in fact, is a very stringent requirement, as the figures given below indicate.

A field drift can be considered as due to a combination of the following effects :-

(a)   a drop in voltage of the battery.

(b)   a change in the resistance of the leads - this includes change in value of any controlling resistance.

(c)   a change in resistance of the magnet coils.

Effects (b) and (c) are temperature effects;   there may also be a small effect due to the change in physical size of the magnet.   With the available battery, 24 volts, 200 A.H., the following are representative of the figures obtained for the field drift.   (The regulation resistance in each case was arranged to be zero;   the mean figures quoted are averages

taken over a period of one hour).

<u>Condition 1</u>.   Supply 16 volts, 200 A.H.

Mean current flowing	= 20.78 amps.
Lowest rate of battery voltage fall during complete discharge of accumulator	= 0.00138v/min.
Resultant rate of field fall	= 0.6 gauss/min.
Fall of field due to effect (c) after 8 hours running	= 0.3 gauss/min.

<u>Condition 2</u>.   Supply 12 volts, 400 A.H.

Mean current flowing	= 15.78 amps.
Lowest rate of battery voltage fall	= 0.00024v/min.
Resultant rate of field fall	= 0.1 gauss/min.
Fall of field due to effect (c) after 12 hours running	= 0.1 gauss/min.

The field drifts indicated by these figures prohibit the use of the 'lock-in' amplifier.   In order to obtain sufficient field stability it was necessary to use an oil circulation cooling system and to use the battery as a 6 volt, 800 A.H. supply.   The maximum field then obtainable was about 1800 gauss, corresponding to an operating frequency of about 8 Mc/s.   Under these conditions the field drift was about 0.2 gauss per hour.   Some preliminary experimental work was done at this frequency.

An attempt was made to stabilise galvanometrically the

current through the magnet coils.   This did not prove feasible with equipment immediately available and the imminent arrival of the permanent magnet made it unprofitable to spend more time on this project.

3.3.2. The Permanent Magnet.

The difficulties of maintaining a large field of 5 to 6 kilogauss constant are removed if a permanent magnet is used. The specifications of the magnet shown in figure 3 are :

Field: 5500 gauss.   Pole face diameter: 8 inches.
Gap width: 2 inches.   Field homogeneity in best
region: about 0.25 gauss per c.c.

The magnetic material is Alcomax III, the pole-pieces being built up from 90° circular segments.   The magnet poles are surrounded by the magnetising coils, and Armco iron recessed pole caps abutt on to the ends of the Alcomax III blocks and clamp them to the soft iron yoke; to obtain the high field uniformity the tips of the pole caps have specially shaped rims.

3.3.3. The Signal Generator.

The signal generator used is an Airmac instrument, Type 701.   It was found that there was a spurious amplitude modulation on the carrier of about one per cent.   This was eliminated by using a D.C. supply for the valve heaters and
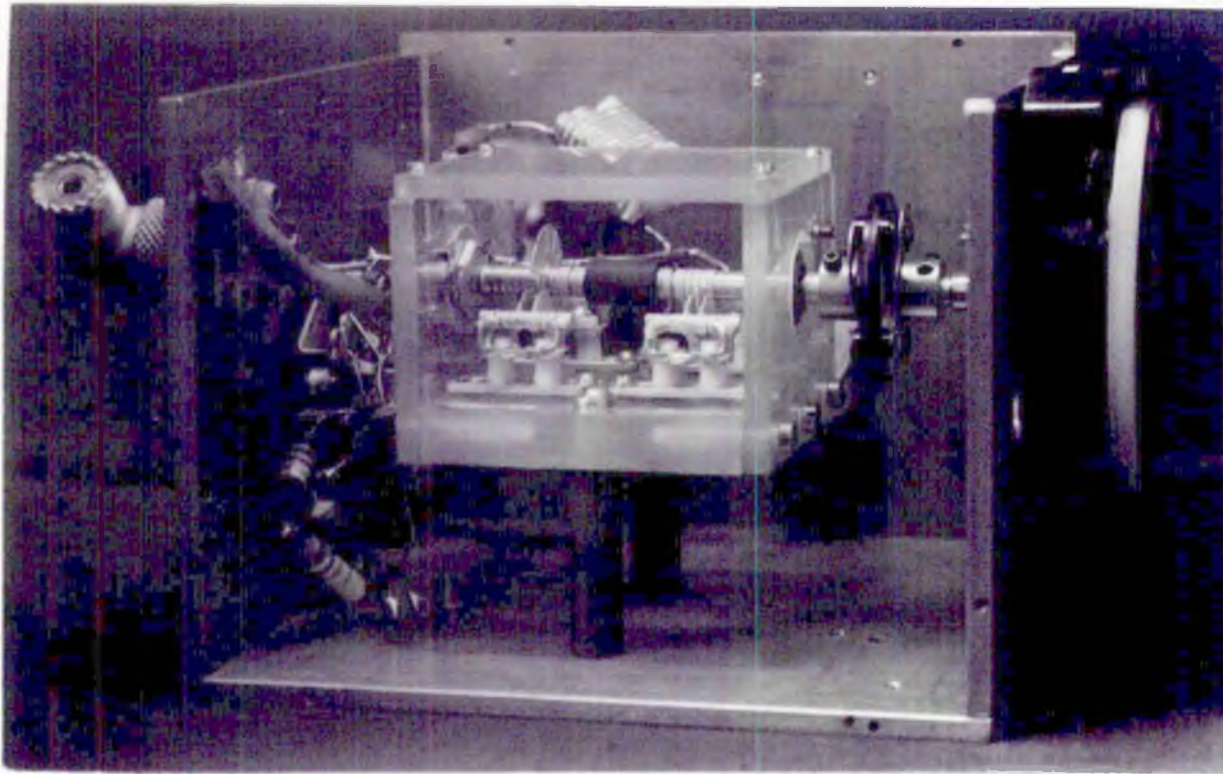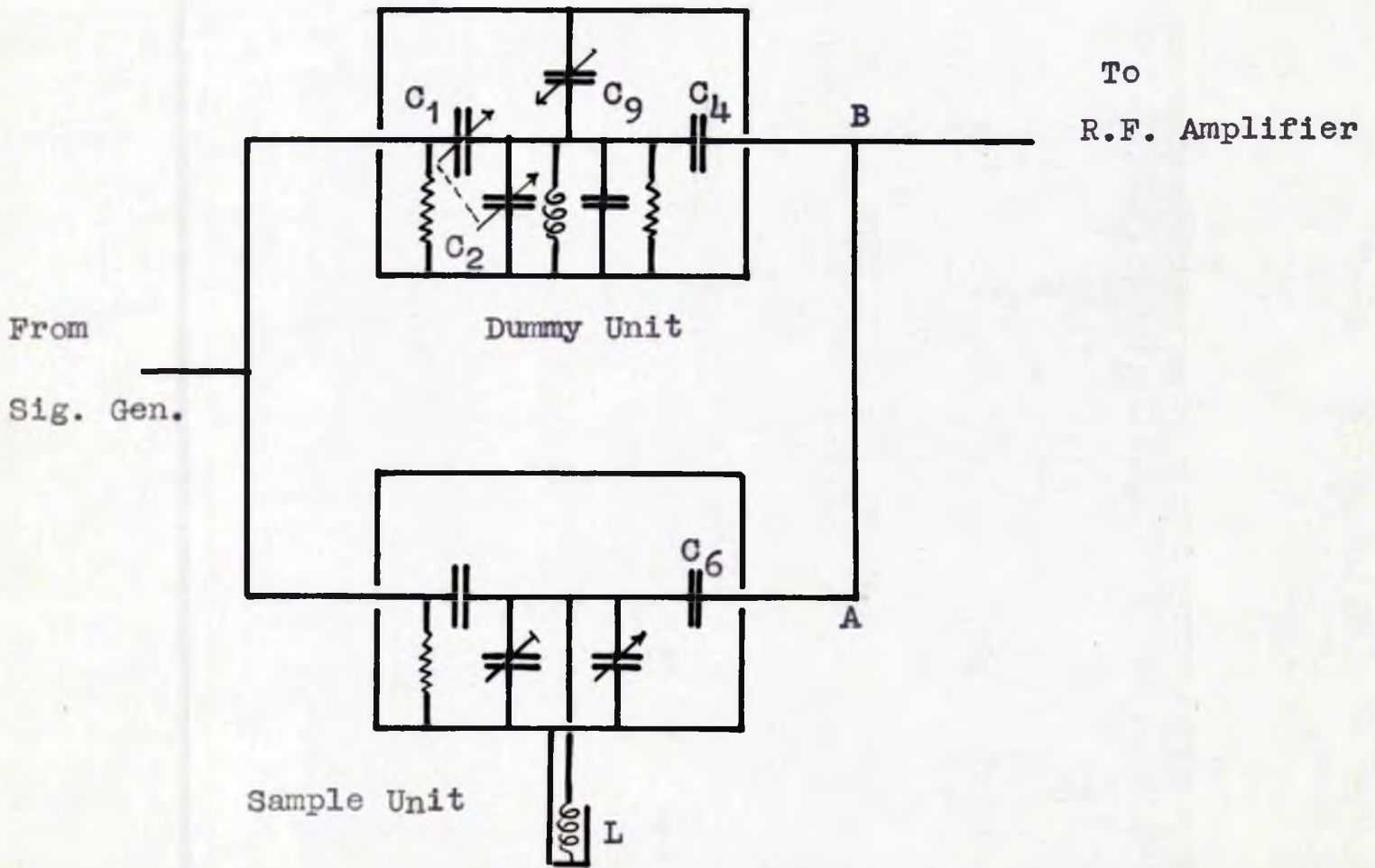
Figure 4.

Figure 5.

by building an external H.T. power supply, paying particular attention to the smoothing circuits. This supply was adequately stabilised, since the mains supply voltage varies by as much as 20%. The H.T. unit gives an output of 305 volts at 67 mA., the ripple voltage being 4mV peak to peak, and a 20% change in mains voltage gives a change of 0.03% in the output voltage.

3.3.4. The Radio-frequency Bridge.

The radio-frequency bridge consists of two units connected together with 50 ohm coaxial cable. The circuit arrangement is shown in figure 5.

The tuned circuits were constructed within closed boxes made of 3/16th inch brass sheet - heavy gauge copper wire was used for all internal connections, and care was taken to mount the components rigidly, since any mechanical vibration was found to give a spurious signal. Good bonding between the units and the connectors was found to be very important. With these precautions the bridge balance is stable up to 40 db., provided the temperature of the sample placed within L (figure 5) is constant.

An analysis of the conditions of balance and the signal obtained (reference 11) shows that the oscillograph will plot out the absorption curve if the bridge is unbalanced in amplitude, and the dispersion curve if it is unbalanced in phase. Approximate phase balance is obtained by including

the extra half wavelength of coaxial cable AB in one arm of the bridge. The variable condenser C_9 gives a fine phase balance control, while the ganged pair C_1 and C_2 give an approximately phase independent amplitude control. This is achieved by arranging the moving vanes of C_1 and C_2 180 degrees out of phase. Suitable condensers for C_1 and C_2 could not be obtained and it was necessary to make a unit. The section C_1 has to be completely insulated while the moving vanes of C_2 must be earthed, also stray capacities both between the units and from each to ground have to be kept very small. A satisfactory unit was made, each section having a swing of 1 to 4.8 pfs. Figure 4 shows this condenser mounted in the 'Dummy Unit' of the bridge.

3.3.5. The Radio-frequency Amplifier and Receiver.

The receiver in use in the apparatus is the Eddystone Communications Receiver, Type 680. To eliminate a small 50 c/s component in the audio output it was found necessary to use a D.C. supply for the valve heaters and to build a well smoothed H.T. supply unit; this unit also supplies a stabilised H.T. voltage for the R.F. Amplifier.

The latter is a single stage unit, employing an aligned grid pentode, Mullard type EF 54. Balanced input and output tuned circuits are used, these being inductively coupled to the coaxial feeders. A useful gain and a considerable improvement in the signal to noise ratio is obtained with

this unit.

Considerable care was, in fact, taken to have optimum coupling between the R.F. bridge and the preamplifier. To ensure this the noise factor of the preamplifier was measured as a function of the loading of its input circuit, a noise diode being used. The noise factor of the receiver (effectively that of the preamplifier, since it has a narrow bandwidth and a high gain) is given by the expression

$$N_r \quad = \quad 20 \, I \, R$$

where I is the anode current in amperes which, flowing through a resistance R ohms, doubles the total power indicated at the second detector of the receiver. This definition, and the technique of measuring N_r, follows those given by L.A. Moxon (reference 12). The resistance R in the noise diode circuit is connected across the input terminals of the preamplifier. The procedure then is :-

(a) The noise diode H.T. supply is switched off and the receiver R.F. gain is adjusted to give a convenient reading M_1 on a meter indicating second detector current. Conditions are now such as those which would exist if the receiver was perfect and the noise power available from the aerial of impedance R was $N_r kTB$ instead of kTB.
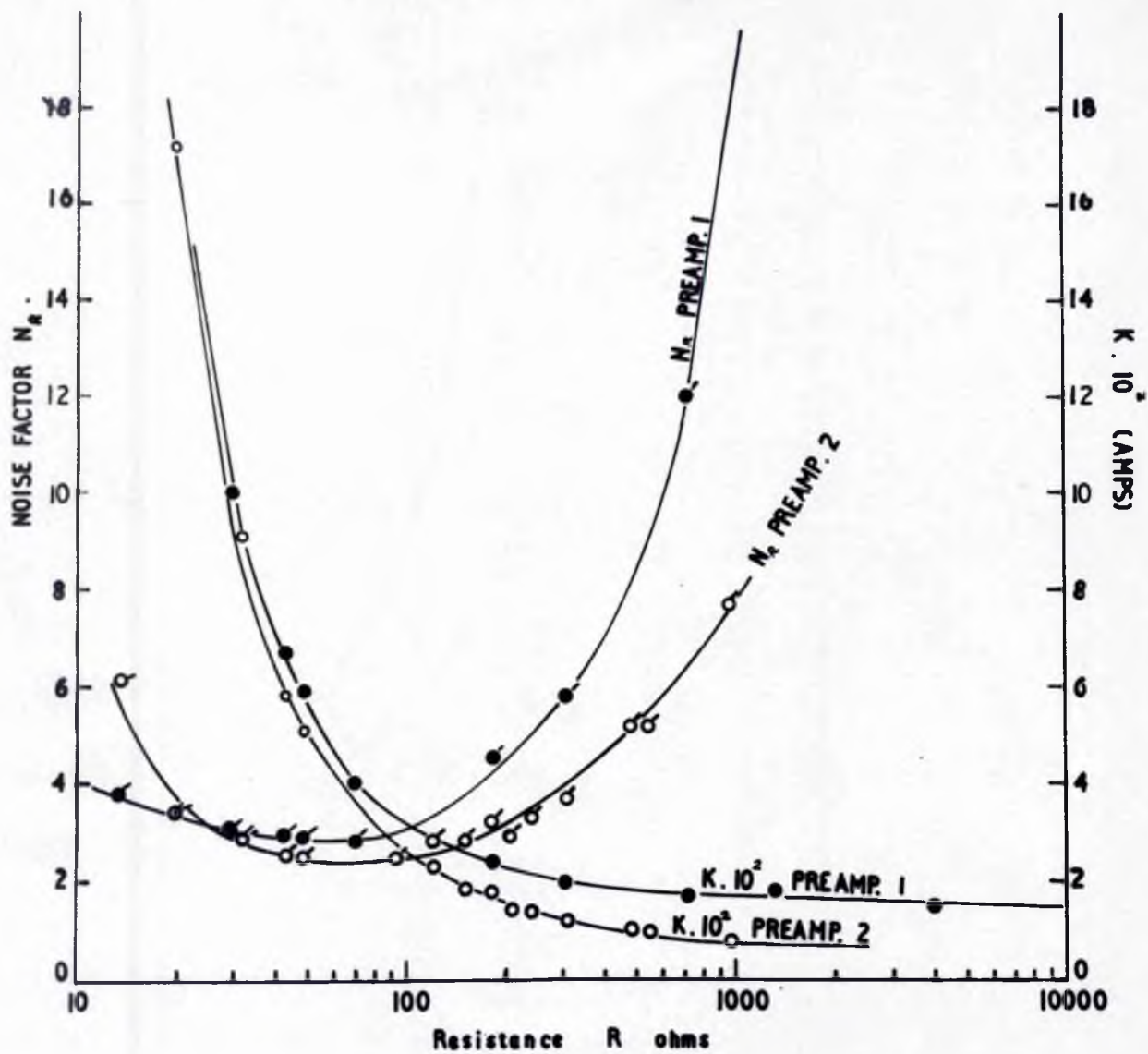
Figure 6.

(b) The noise diode current is now adjusted to a value I_1, making available an additional noise power 20 $I_1 R$ kTB.   The reading on the meter is now M_2, where M_2 is substantially greater than M_1.

(c) The receiver gain is now turned down until the meter reading is again M_1, the diode current being kept constant.

(d) Finally the noise diode current is increased to I_2 until the meter reading is again M_2.

In (a) and (b) M_1 and M_2 correspond to a noise power ratio $N_r/(N_r + 20 I_1 R)$, and in (c) and (d) to a ratio $(N_r + 20 I_1 R)/(N_r + 20 I_2 R)$.   These two ratios, being equal, give

$$N_r = \frac{20 I_1^2 R}{I_2 - 2I_1} = KR \text{ say.}$$

N_r and $K \times 10^2$ are plotted as functions of R for the two preamplifiers constructed in figure 6.

The noise diode circuit is then replaced by the connection from the R.F. bridge, and the value of $K \times 10^2$ is measured for different values of the coupling condensers, C_4 and C_6, (see figure 5).   The final value chosen was $C_4 = C_6 = 7$ pfs. N_r was then about 2.5.

3.3.6. The Narrow band, Lock-in Amplifier.

In order to increase the sensitivity of the apparatus a selective, lock-in amplifier is used. The form of the unit constructed follows very closely that described by R.H. Dicke (reference 13).

To plot out a line shape at any particular temperature, the bridge is balanced to the desired degree and the 25 c/s modulation of the main field is reduced to a small fraction of the linewidth. By means of field bias coils - the magnetising coils in the case of the permanent magnet - the field is gradually moved up to, and through, the region where the resonance absorption occurs. The absorption of energy from the coil results in a 25 c/s sinusoidal modulation of the R.F. carrier. Thus any absorption of energy appears as a 25 c/s audio output from the second detector of the receiver; noise signals cause distortion of this voltage. The output from the receiver passes through a selective amplifier to a balanced stage where it is mixed with a 25 c/s reference voltage suitably phased. The D.C. voltage at the output of the mixer stage depends on the amplitude and phase of the input signal. Random noise voltages are equally likely to effect the output in either direction so that their resultant tends to zero as the time constant of the output meter is increased. Actually a D.C. amplifier is included between the mixer stage and the meter ; thus the effective time constant of the meter is controlled by the
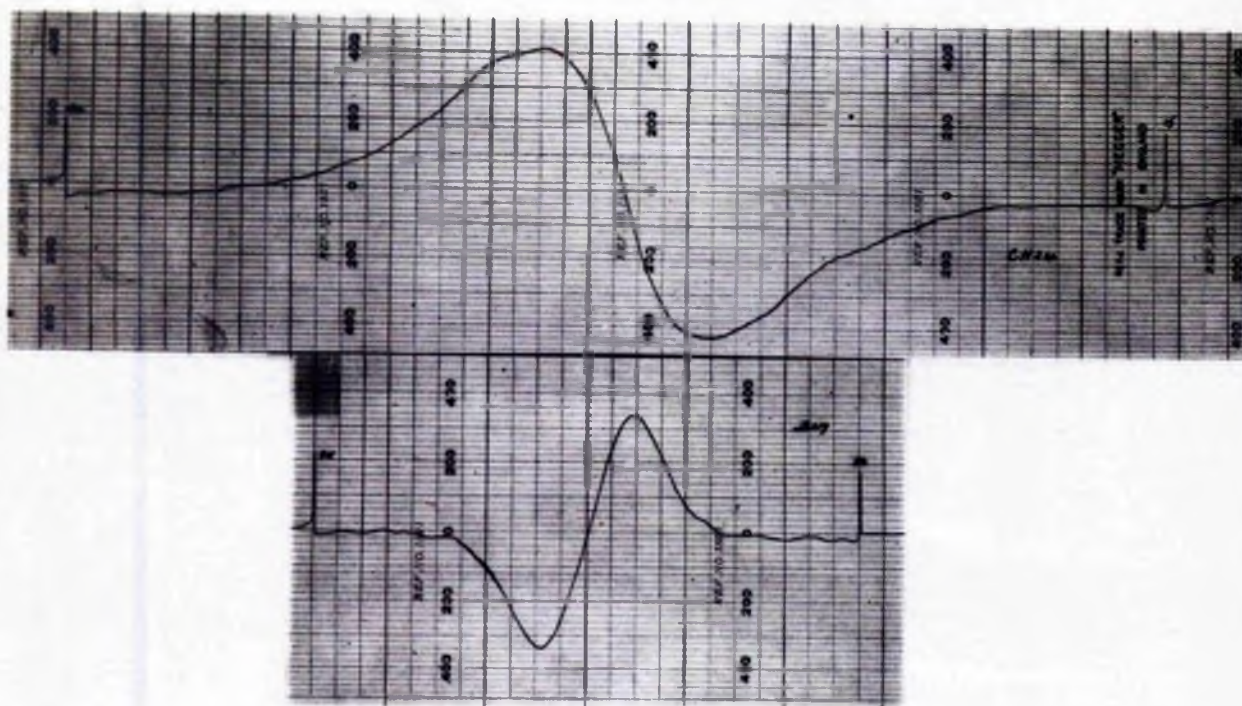
Figure 7.   Recorder plots.

        (a) Cyclohexene at 105°K.

        (b) Benzene at 205°K.

circuit connecting these two stages.   Two possible values were incorporated - 0.5 seconds, which is suitable for visual observation of the output meter, and 5 seconds, for use with the recording microammeter.   As a result of this measuring technique, the output meter indicates the first differential of the absorption line.

By applying to the field bias coils a voltage which is increased uniformly with time, the field is scanned at a constant rate.   The output from the lock-in amplifier is then applied to a recording microammeter, which traces out the differential of the absorption line shape.   The scanning rate is kept low so that the advantage of the long time constant in the lock-in amplifier may be used.   Calibration marks are put on the trace to give the scan rate in gauss/min. Examples of two traces are shown in figure 7.

3.3.7. The 25 c/s Generator and Field Modulating Equipment.

The 25 c/s generator consists of a multivibrator, followed by a two-stage selective amplifier employing symmetrical twin-T feedback networks (reference 14).   This method of obtaining a 25 c/s sinusoidal voltage, although cumbersome, has the important advantage that it is easy to fix the phase of the voltage relative to that of the mains supply voltage;   this eliminates beat voltages appearing in the output of the receiver.   Besides supplying the drive voltage for the field modulating equipment, the generator

gives the 25 c/s voltage necessary for the mixer stage of the lock-in amplifier (see figure 1).

The field modulating equipment consists of a power amplifier capable of delivering 15 watts at 25 c/s into the field modulation coils.   It is necessary that the waveform be good; to obtain this, two 807 valves are used in a push-pull circuit, the output transformer having a primary inductance of about 200 henries.

The modulating coils for the permanent magnet were wound on thin ebonite formers.   Each coil consists of 1000 turns of 22 s.w.g. wire; the coils can be seen in position in figure 9.

The oscillograph sweep voltage is also obtained from the secondary winding of the output transformer.

Calibration of Field Shift and Modulating Coils.

The field shift coils were calibrated first as follows: a narrow liquid resonance line was observed on the screen of the C.R.O., using a field modulation about 15 to 20 times the observed linewidth.   With no current flowing in the coils the frequency of the signal generator was adjusted until the resonance line was in the centre of the trace, the receiver being retuned and the bridge rebalanced to keep the signal visible on the screen.   When the signal was approximately central the modulation was reduced to about twice the linewidth; this made an accurate centering possible.   This was done and the frequency of the signal

generator was then determined by lightly coupling to the
bridge a heterodyne frequency meter, Type BC 221.   Adjust-
-ment of the frequency meter was ensured by varying its
frequency control until zero beat between the r.f. of the
signal generator and the het. oscillator was observed on
the screen of the C.R.O.   This procedure was repeated for
ten values of the current through the shift coils.   The
results obtained were fitted to a straight line, the slope
of which gave the frequency shift per unit current through
the shift coils.   Using Bearden and Watt's values (reference 7)
for h, Planck's constant = 6.62363×10^{-27} erg.sec.

μ proton = 1.521026×10^{-3} Bohr Magnetons.

1 Bohr Magneton = 9.27100×10^{-21} erg. gauss^{-1}.

and the relationship, $h \nu = 2 \mu H$, this was converted into a
field shift per milliampere.   The relative accuracy between
readings of the frequency meter was better than 0.01%.

Using this result, the modulation coils were calibrated.
Again a narrow liquid resonance line was employed.   Various
values of the modulation current were sent through the coils
and the change in the bias field current necessary to shift
the signal from one end to the other of the trace on the C.R.O.
screen was noted in each case.   This immediately gave the
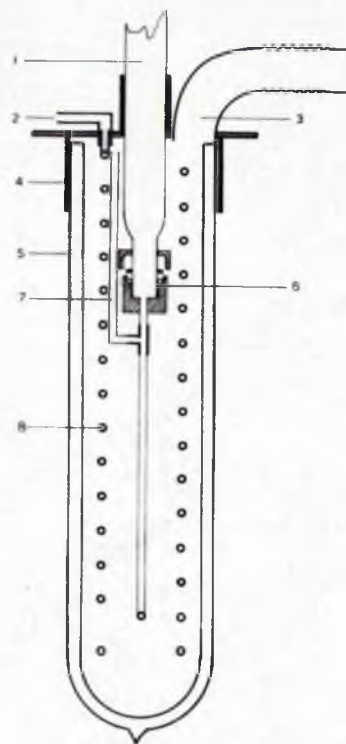peak to peak field swing for any value of the current through
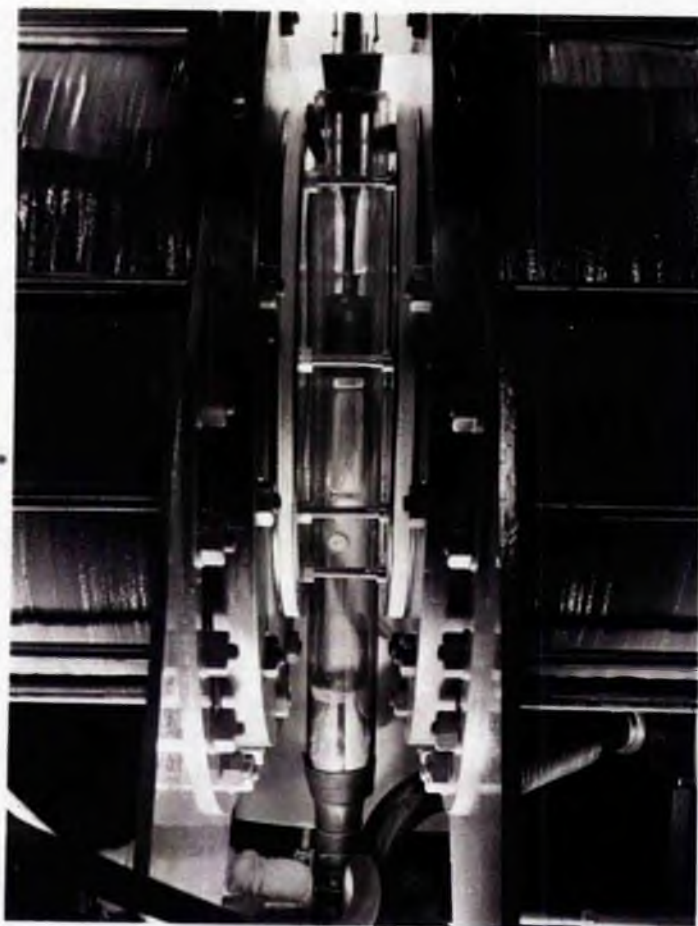the coils.

Figure 8.

GAS CRYOSTAT.

Figure 9.

3.3.8. The Cryostat.

The choice of a method of cooling the sample was determined by the requirements that (a) any temperature in the range 70° to 280°K be available, and (b) that the time taken to change from one temperature to another be kept reasonably short.   Since the thermal capacity of the assembly to be cooled was very low, a gas-flow type cryostat was an automatic choice.

This consists of two Dewar flasks, containing the following :-   No.1 - a closely wound spiral of 26 turns of 4 mm. german silver tubing.   No.2 - a section of this assembly is shown in figure 8.   The incoming gas is cooled in passing round the spiral in the first Dewar, which is filled with liquid oxygen or air.   The cold gas then enters the second cooling stage via the inlet pipe (2).   The temperature of the gas at this stage depends on the flow rate being used; generally it is about 110°K.   It is further cooled in passing through the spiral (8), which is immersed in liquid air or nitrogen.   The gas then passes up into the long Dewar tube (1), which is fixed to the spiral by a Gaco ring seal (6). The main Dewar (5) and the tube (1) are sealed with rubber gaskets to the top plate (4).   Outlet (3) is connected to the pumping line.

For use with the electromagnet a specially shaped Dewar tube was made; a straight tube can, however, be used with

the permanent magnet, and figure 9 shows this in position between the pole faces. The top plate of the second Dewar is just visible, together with the pumping line. Two sets of metal bellows were included in the line to reduce vibration of the cryostat. The front edges of the field modulating coils are also visible. These are clamped firmly against the large phosphor-bronze discs in which the pole caps are centred. The top part of the Dewar tube is unsilvered, and the small copper shielding can, which contains the R.F. coil L (figure 5) and sample, can be seen.

Without pumping the second Dewar, the lowest temperature attainable with this arrangement is 96°K, when the coolant is liquid oxygen. To further lower the temperature liquid nitrogen is used and the second Dewar is pumped; hydrogen is then used as a flow gas. This requires that the top of the Dewar tube be closed and provided with an exhaust tube for the cold hydrogen. A rubber stopper, sealed in, has been found quite satisfactory, provided that a small Dewar tube is used to lead the cold gas through the stopper into the exhaust line. This stopper, together with part of the small Dewar tube is also visible in figure 9.

This method of cooling has been found quite satisfactory and any temperature can be maintained reasonably constant in the range specified. Once the unit has cooled down, which takes a full 30 minutes, any subsequent change of temperature - obtained by adjusting the flow rate of the

gas in use - takes about 15 to 20 minutes.   This compares favourably with other methods.

4.   Experimental Results

4.1.   Programme.   Choice of Subjects for Study.

Nuclear Resonance methods can be applied with advantage to the study of solid hydrocarbons. Structural investigations by X-rays yield only the positions of the carbon atoms ; the positions of the protons have to be guessed.   Since, however, the inter-proton distances govern the local magnetic field, which itself controls the resonance linewidth if the lattice is effectively rigid, measurement of the second moment of the absorption line verifies the postulated positions of the protons.   Also information about molecular rotations can be obtained. Again this technique has an advantage over X-ray methods; these only yield such information if the molecule spends most of its time rotating.   The resonance line, however, is affected even if each molecule only spends a small fraction of its time rotating.

From the practical aspect, the high gyromagnet ratio of the proton makes the hydrocarbons good subjects for study, since this ensures a reasonable signal strength, (reference 1, Appendix), while the zero spin of the C^{12} nucleus makes the interpretation of the experimental results much easier.

It was intended, therefore, to study the hydrocarbons cyclohexane, benzene, benzene-d_1 and cyclohexene.   These

all have a six-membered carbon atom ring as skeleton. Experimental work on the first three of these has been completed and the results are discussed in detail in the following sections. A pure sample of cyclohexene could not be obtained in time and, therefore, the results recorded for this hydrocarbon cannot be considered to be so satisfactory : in fact, only exploratory spin-lattice relaxation time measurements have been made.

Cyclohexane is discussed first in section 4.2. In particular, the applicability of the theory derived by Bloembergen, Purcell and Pound to explain the observed relaxation times in terms of the motions occurring in the lattice is considered.

The interpretation of the experiment al results obtained with benzene and benzene-d_4 follows in sections 4.3 and 4.4, the procedure adopted being much the same as for cyclohexane. These two substances are found to behave in a very similar manner ; it had been thought that the 'weighting' of the molecule with the deuteron would affect more markedly the linewidth transition if tunnelling were occurring.

Finally the results obtained for cyclohexene are recorded.

SECTION 4.2.

CYCLOHEXANE

4.2 OYCLOHEXANE

4.2.1 Preparation of the Sample

The sample of cyclohexane examined was prepared by
Dr. E.R. Andrew.   Starting with B.D.H. Cyclohexane,
Special for Spectroscopy, a systematic fractional freezing
scheme was carried out, the accepted specimen coming from
the fifth and final stage of this process.   The freezing
point of the fraction was 6.44°C.

An estimation of the mole % purity of this sample
has been made from the measured depression of the freezing
point.   If :

N_a is the mole fraction of pure cyclohexane

ΔH is the molar heat of fusion = 633.8 cals/mole

R is the Gas Constant, taken as 8.314 joules/°C/mole

T_o is the F.Pt. of pure cyclohexane, taken as 6.57°C,
       the mean of the seven best reported values,

T is the F.Pt. of the specimen,

then

$$\ln N_a \;=\; -\,\frac{\Delta H(T_o - T)}{RTT_o}$$

$T_o - T = \Delta T = 0.13°K$ and $\ln N_a = 4.078 \times 10^{-3}\Delta T$

Taking $N_b = 1 - N_a$ = mole fraction of impurity, then

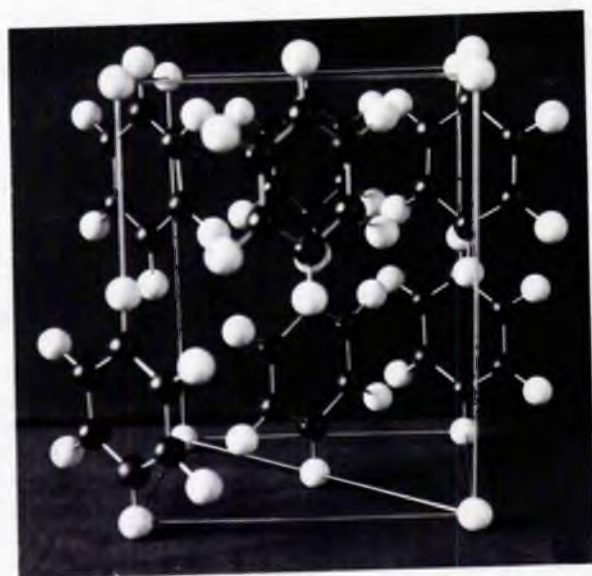$$\ln N_a = \ln(1 - N_b) = -N_b \;, \text{ since } N_b \ll 1.$$

Using the figures quoted, $N_b = 0.05$ mole % impurity.

CYCLOHEXANE MOLECULE.

Figure 10.

Benzene Unit Cell.

Figure 11.

4.2.2. Molecular Structure.

The molecular configuration assumed is the puckered ring model shown in figure 10. This model, which has D_{3d} symmetry with tetrahedral bond angles, is based on evidence obtained from X-ray studies, infra-red and Raman spectra and from electron diffraction experiments. X-ray workers (see, for example, references 15 and 16) were at most only able to say that a planar ring was unlikely, but recent evidence from infra-red and Raman spectra is more conclusive. Rasmussen (reference 17) has summarised the experimental work done prior to 1943 and confirms that a 'chair' D_{3d} form is well supported by these results. Beckett, Pitzer and Spitzer (reference 18) definitely confirm that this form predominates in gaseous cyclohexane at 25°C, while Hassel and Ottar (reference 19), using electron diffraction methods, also propose the highly symmetrical 'chair' or 'step' form, and suggest that the valence angles depart at most only slightly from the ideal tetrahedral value.

Summarising the results reported in references 19 to 26 the value of the C - C distance in the molecule has been taken as 1.54 ± 0.01 A., and the C - H distance as 1.10 ± 0.01 A.

4.2.3. Crystal Structure.

The crystal structure of cyclohexane has been determined by O. Hassel and A.M. Sommerfeldt (reference 27). The structure is cubic, with 4 molecules per unit cell. These

molecules have their centres of gravity at $\frac{1}{4}\frac{1}{4}\frac{1}{4}$, $\frac{3}{4}\frac{3}{4}\frac{1}{4}$, $\frac{1}{4}\frac{3}{4}\frac{3}{4}$, $\frac{3}{4}\frac{3}{4}\frac{3}{4}$, and their triad axes are the four cross diagonals of the cube, of side a = 8.76A. Hassel and Sommerfeldt also noted that at about 10° below the melting point the molecules appear to possess considerably more rotational freedom than at -40°C, the temperature at which they determined the structure. This rotational freedom was looked for by Carpenter and Halford (reference 28) using infra-red spectroscopic methods, but they found no evidence to confirm or deny such motion.

The only experimental results on which an estimate of the lattice contraction can be based are contained in references 27, 29 and 30. These give the following figures for the volume of the unit cell :

Temperature °K	Vol. $cm^3 \times 10^{-22}$	Reference
280	6.69	30
273	6.69	30
268	6.68	27
265	6.72	27
233	6.72 (?)	27
20	5.49	29

Thus the cell volume at 20°K is 82% of the volume at 273°K. This has to be compared with a figure of 90% for the benzene lattice for which some more figures are available. This difference is not unexpected, however, since there is a first order phase transition in cyclohexane at 186°K. For benzene there is a volume change of 13.5% on melting, compared with the figure of 5.7% for cyclohexane; thus an 8%

change of volume at the transition temperature is quite reasonable. Assuming, therefore, that such a change does take place, the volume of the unit cell at 100° to 110°K is 85% of the value at 273°K. This figure is good enough since, in fact, the actual crystal structure below the transition temperature is unknown. The effect of lattice contraction on the intermolecular contribution to the second moment for the rigid lattice is discussed in section 4.2.5.

4.2.4. Thermal Data.

A number of measurements have been made of the transition temperature, heats of transition and fusion, and of the specific heat as a function of temperature. These are given in references 31 to 34. Mean values are :-

Transition Temperature	=	186.10 ± 0.05°K
Heat of transition	=	1605 cal./mole.
Heat of fusion	=	630 cal./mole.

4.2.5. The Absorption Spectrum.

The first derivative of the absorption line shape has been plotted out at temperatures in the range 100 to 280°K, using the lock-in amplifier. This was done on lowering and raising the temperature, since it was found that supercooling of the solid through the transition temperature could occur. Since the cyclohexane is sealed in a small ampule, the
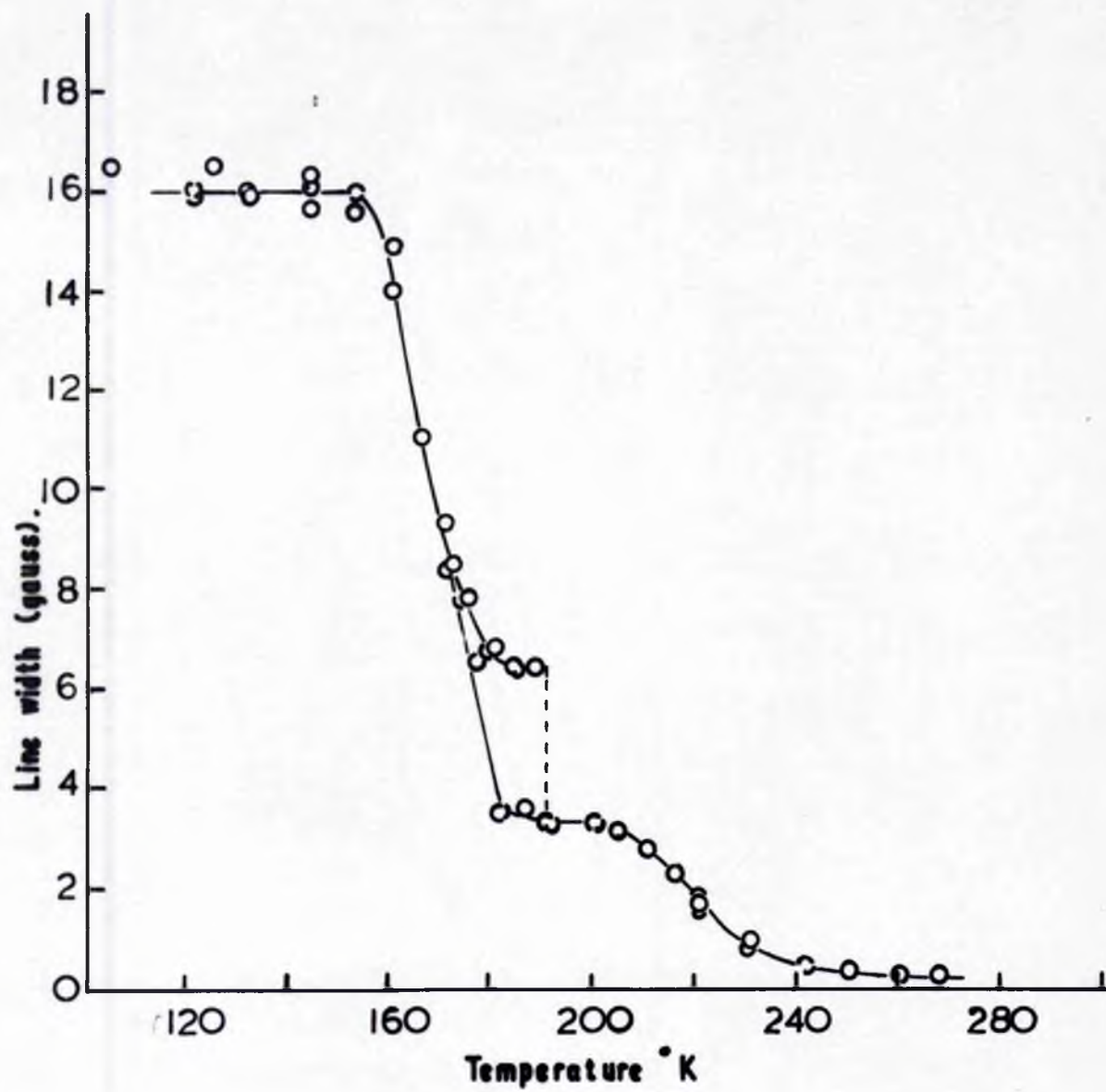
Figure 12.

temperature was measured by a thermocouple placed very close to the sample in the cold gas stream.

The linewidth, defined as the interval in gauss between points of maximum and minimum slope, is plotted as a function of the temperature in figure 12.

The second moments of the absorption lines have been calculated, and are plotted against the temperature of the sample in figure 13. Van Vleck defines the (2n)th moment of the line shape as :

$$\langle (\Delta \nu)^{2n} \rangle_{av} = \int_{-\infty}^{+\infty} g(\nu) \, (\Delta \nu)^{2n} \, d\nu$$

(See reference 6)

This can be written as :

$$\langle (\Delta \nu)^{2n} \rangle_{av} = \left| g(\nu) \frac{(\Delta \nu)^{2n+1}}{2n+1} \right|_{-\infty}^{+\infty} - \frac{1}{2n+1} \int_{-\infty}^{+\infty} (\Delta \nu)^{2n+1} \frac{dg(\nu)}{d\nu} \, d\nu$$

$$= - \frac{1}{2n+1} \int_{-\infty}^{+\infty} (\Delta \nu)^{2n+1} \frac{dg(\nu)}{d\nu} \, d\nu$$

since $g(\nu)$ vanishes except when ν is very nearly equal to ν_0 where ν_0 is the resonant frequency for a field H_0. Since, in practice, the frequency is fixed and the field H is varied, the expression for the (2n)th moment has to be written explicitly in terms of H : if $h = H - H_0$, then :

$$\langle (\Delta H)^{2n} \rangle_{av} = - \frac{k}{2n+1} \int_{-\infty}^{+\infty} h^{2n+1} \frac{df(h)}{dh} \, dh$$
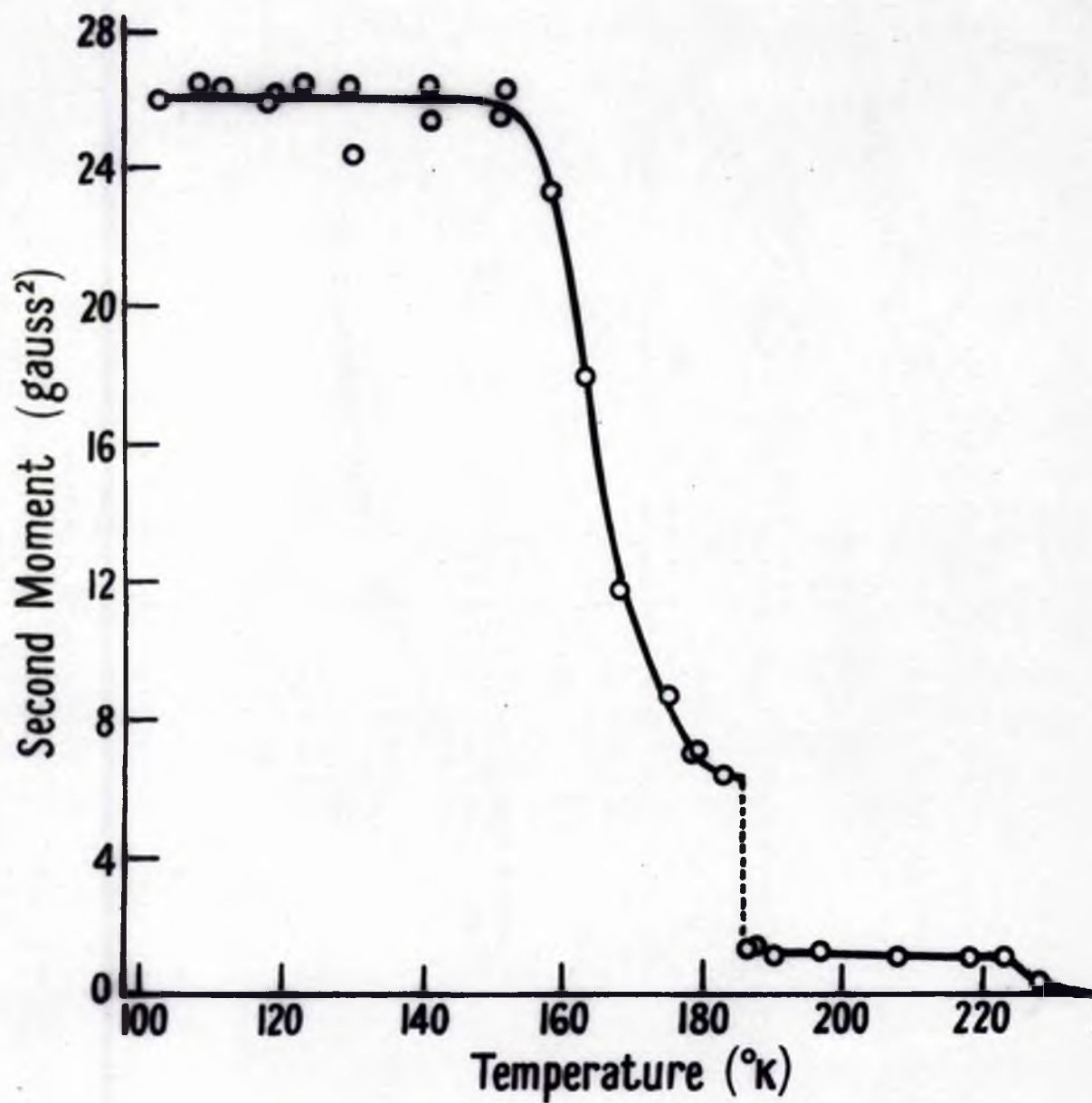
Figure 13.

Putting n = 1 to obtain the second moment, and normalising :

$$\text{Second Moment} = \frac{1}{3} \cdot \frac{\int h^3 \frac{df(h)}{dh} \, dh}{\int h \frac{df(h)}{dh} \, dh}$$

The quantity $df(h)/dh = F(h)$ is the quantity indicated in arbitrary units by the output meter of the lock-in amplifier. The integrals are evaluated using the trapezium rule, i.e.

$$\text{Second Moment} = \frac{\sum h^3 F(h)}{3 \sum h \, F(h)} \quad \text{gauss}^2.$$

This expression has been used throughout to calculate the second moment of the experimental line plots.

Below 150°K the second moment is constant (figure 13) indicating that the lattice is effectively rigid. The mean experimental value of the second moment between 100°K and 150°K is 26.0 ± 0.5 gauss^2. A theoretical value has been calculated assuming the molecular model discussed in section 4.2.2. This calculation consists of two parts : (a) the calculation of the intramolecular contribution, and (b) the calculation of the intermolecular contribution. Since

$$\text{Second Moment} = \frac{715.9}{N_R} \sum_{j>k} r_{jk}^{-6} \quad \text{gauss}^2. \quad \text{(see section 2.2)}$$

only the inter-proton distances are required. The 'intra'

contribution is 17.28 gauss^2, if one makes the reasonable assumption that the bond lengths are not contracted. There is some uncertainty, however, in the calculation of the 'inter' contribution as was indicated in section 4.2.3. The crystal structure was determined at 233°K ; a calculation of the 'inter' contribution using the unit cell size measured at that temperature gives only a lower limit of 7.40 gauss^2. Allowing a 5% linear contraction of the lattice the contribution becomes 13.44 gauss^2 ; this must be considered as an upper limit, since the change in structure at 186°K will in all probability increase the shortest proton-proton distances (now only 2 Å). If all the inter-molecular distances are considered to be contracted by 5%, an inter-contribution of 10.05 gauss^2 is obtained; this is a more reasonable value and compares with 9.6 gauss^2, a value based on the 'inter' contribution for normal hexane. (Dr. E.R. Andrew has related empirically the lattice energy of apolar molecular solids, such as n-hexane and cyclohexane, to the inter-molecular contribution to the second moment of the resonance spectrum of such solids).

The best value from these results is taken as 10.0 ± 1.5 gauss^2. Hence the total rigid lattice second moment is 27.3 ± 1.5 gauss^2. The agreement between the measured and calculated values provides general confirmation of the molecular structure assumed, namely D_{3d} symmetry, with bond

angles of 109°28', C - C bond lengths of 1.54 A and C - H bond lengths of 1.10 A.

Between 155°K and 180°K the absorption line narrows, the second moment falling to 6.4 gauss^2. The molecular motion most likely to set in is reorientation of each molecule about its triad axis. It is presumed that this motion is hindered in the sense that the molecules only occasionally are able to surmount the potential barrier opposing the motion - i.e., the motion is discontinuous, the molecules moving between their equilibrium positions.

The theoretical second moment for a lattice in which such motion is occurring has been obtained by modification of the Van Vleck formula (see Appendix 1): the intra-molecular contribution is reduced to 3.64 gauss^2 and the 'inter' contribution to 2.44 gauss^2. Owing to the very lengthy calculations involved in finding the effect of this motion of the 'inter' contribution, only a skeleton calculation has been possible. Hence the figure 2.44 gauss^2 is only a very reasonable estimate. The final theoretical value of the second moment for the non-rigid lattice is 6.1 $\pm$ 1.0 gauss^2, where these are safe error limits and include both the approximation mentioned and the doubt arising from the lack of knowledge of the crystal structure below the transition temperature. The agreement between the experimental and calculated values is satisfactory.

The solid-solid phase transition at 186°K is accompanied by a discontinuous change in the linewidth and second moment when the temperature is being raised. Some supercooling through the transition occurs if the temperature is being lowered ; this effect is shown in figure 12. The latent heat of transition is some 2½ times that at fusion, and indicates that a relatively large increase in molar volume occurs. This results in a loosening up of the structure which reduces the potential barriers hindering molecular reorientations. The reduction of the second moment to about 1.4 gauss^2 implies that the molecules can now reorientate about axes other than the triad. The possibility of a general motion about fixed centres of gravity is not unlikely. Unfortunately, averaging of the term $(3 \cos^2 \theta_{jk} - 1)/r_{jk}^3$ in the Van Vleck formula over such a motion is not feasible, and so an exact theoretical value for the second moment when such motion occurs cannot be calculated. In Appendix 2 approximate theoretical values of 1.11 and 1.32 gauss^2 are obtained. The experimental value falls from 1.5 gauss^2 at 190°K to 1.1 gauss^2 at 225°K. The agreement between these figures certainly gives weight to the suggestion that such a motion is occurring in the solid state at this temperature.

Between 220°K and 240°K the second moment again decreases. this time to a value less than 0.01 gauss^2. This indicates
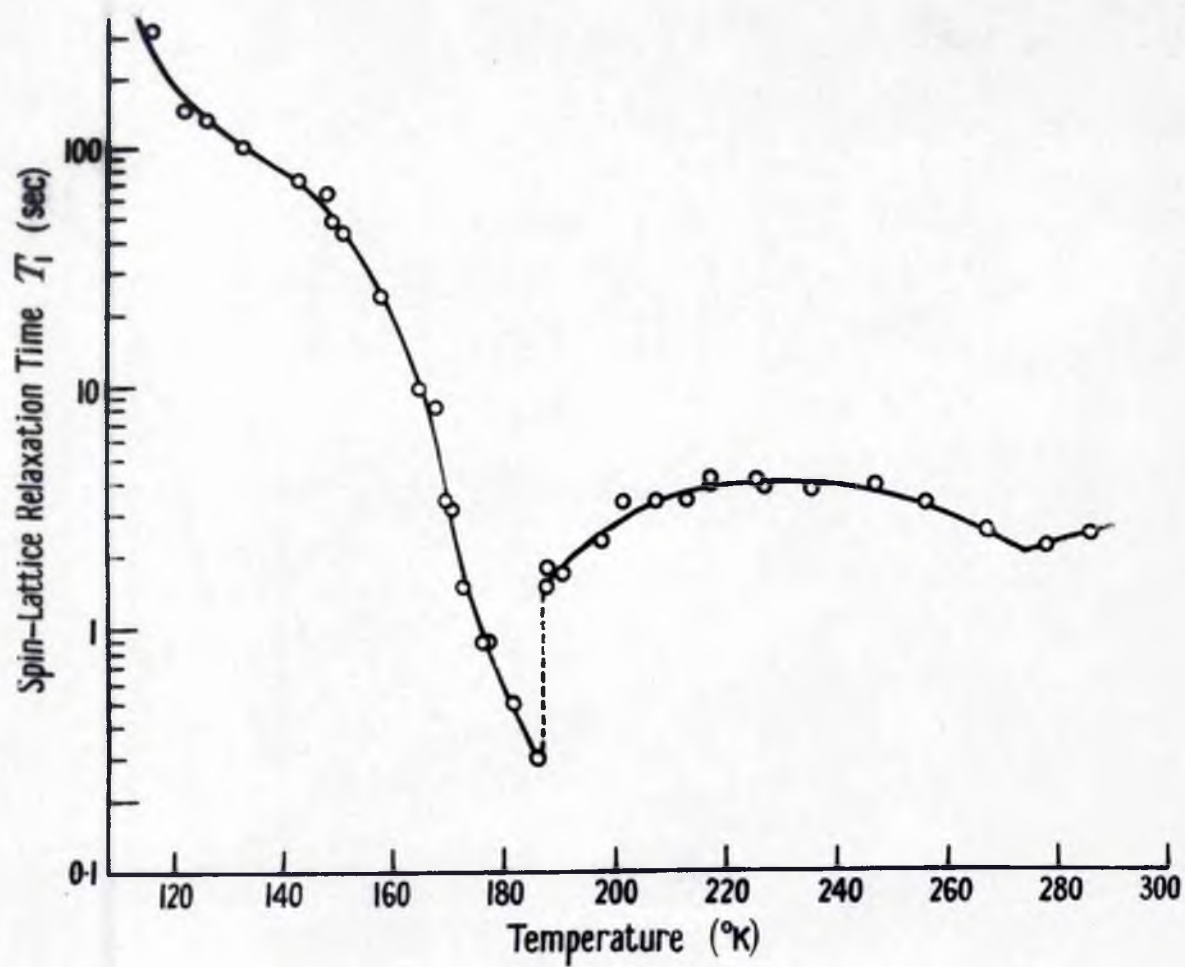
Figure 14.

a further increase in molecular freedom. In Appendix 3 it is shown that no form of motion about fixed centres of gravity can reduce the second moment below 0.05 gauss^2. It is thus necessary to postulate that above about 230°K the molecules can diffuse through the lattice. Hassel and Sommerfeldt (reference 27) noted that their X-ray pictures taken at approximately 270°K differed markedly from these taken at 233°K, presumably due to this effect. If, in fact, this process is occurring, one requires to suppose that, at about 225°K, the molecules make approximately 5×10^4 random jumps per second each of the order of 5 A, since the same considerations must apply to this process as were discussed for molecular reorientation in section 2.2. This gives an average displacement of the centre of gravity of the molecule of 10^{-5} cm/sec.

4.2.6. <u>Spin-lattice Relaxation Time Measurements</u>.

The spin-lattice relaxation time T_1, introduced in sections 2.1 and 2.3, has been measured between 120°K and room temperature. A plot of T_1 against temperature is shown in figure 14.

The method used to determine T_1 at any particular temperature depends on (a) its order of magnitude and (b) whether or not the true width of the absorption spectrum can be measured. Three methods have been used for cyclohexane:

(1) A direct measurement of T_1 is possible if it is

greater than about 30 seconds. To do this a high R.F. level is used so that, in equation (6), section 2.3, $\gamma^2 H_1^2 T_1 T_2$ becomes very much greater than unity. The observed absorption intensity falls to zero, and the signal disappears. The R.F. level is then reduced by a factor of 100 and the subsequent regrowth of the signal observed on the output meter. The slope of a plot of the meter reading against time, on semi-log paper, gives the value of T_1 at the temperature of the measurement. Relaxation times up to 1000 seconds have been measured in this way.

(2) An indirect method has to be used for times shorter than 30 seconds and is that discussed by Bloembergen et al. (reference 1, pp. 689-692). For cyclohexane, case 2 applies, the minimum value of the product $\omega_m T_1$ being about 25. The basic assumption made in this method is that the same degree of saturation is associated with the same intensity of absorption; that is, $\frac{1}{2}$ intensity occurs when $n = \frac{1}{2}n_0$, or $\gamma^2 H_1^2 T_1 T_2 = 1$. Thus for two values of the temperature denoted by A and B

$$(H_1^2 T_1 T_2)_A = (H_1^2 T_1 T_2)_B$$

where $2H_{1A}$ is the R.F. amplitude which reduces the observed signal to half of its maximum value at temperature A, etc. The ratio $(T_2)_A / (T_2)_B$ is obtained from the ratio of the linewidths at the two temperatures, and H_1 is proportional

to the signal generator output. The proportionality factor
is determined by measuring T_1 at a temperature at which
both methods (1) and (2) can be used. This saturation
method could not be used above 230°K for cyclohexane.
At this temperature the linewidth is of the same order of
magnitude as the field inhomogeneity over the sample;
there is then no simple way of measuring T_2.

(3) However, the extreme narrowness of the absorption
spectrum ensures a very good signal to noise ratio, which
allows the absorption signal to be displayed on the screen
of an oscilloscope. Method (1) is then used, the regrowth
of the signal being filmed with a cine camera. The values
of T_1 at temperatures above 230°K have been obtained in
this way; there is good agreement between the T_1 values
obtained by methods (2) and (3) at 230°K, the change-over
temperature. T_1 was also measured at two values above the
melting point, and these points are included in figure 14.

The interpretation of the temperature dependence of
T_1 is based on the treatment of spin-lattice interaction
given in reference 1. Briefly this is as follows :

The position coordinates of the nuclei vary with time
due to the motion of the molecules of which they are part.
Motion of one nucleus j relative to another k sets up
at k an oscillating magnetic field with a frequency
spectrum characteristic of the motion. This spectrum

contains components which can induce transitions. For
the case of protons with $I = \frac{1}{2}$ the general formula for
the spin-lattice relaxation time due to dipole-dipole
interaction is

$$\frac{1}{T_1} = \frac{3}{2} \gamma^4 \hbar^2 I(I+1) \left[J_1(\nu_0) + \tfrac{1}{2} J_2(2\nu_0) \right] \qquad (1)$$

This is equation (34) in reference 1. Here γ, $\hbar$ and I
have their usual significance and J_1 and J_2 are the
intensities of the Fourier spectra of the position
coordinates involved. These spectra are expressed as
functions of a single correlation time τ_g for all
coordinates. That is :

$$J(\nu) = \langle F(t)F^*(t) \rangle_{av} \frac{2\tau_c}{(1 + 4\pi^2\nu^2\tau_c^2)} \qquad (2)$$

where $F(t)$ is the instantaneous value of the position
coordinate considered. From (1) and (2),

$$\frac{1}{T_1} = \frac{3}{2} \gamma^4 \hbar^2 I(I+1) \left[\frac{2\langle F_1 F_1^*(t)\rangle_{av}\tau_c}{1 + \omega^2\tau_c^2} + \frac{\langle F_2 F_2^*(t)\rangle_{av}\tau_c}{1 + 4\omega^2\tau_c^2} \right] \qquad (3)$$

Bloembergen et al applied this to water, assuming that
only one neighbour of a given proton was important and
that this neighbour was at a fixed distance b. Hence

$$\langle F_1 F_1^* \rangle = \frac{2}{15} b^{-6} \qquad \langle F_2 F_2^* \rangle = \frac{8}{15} b^{-6}$$

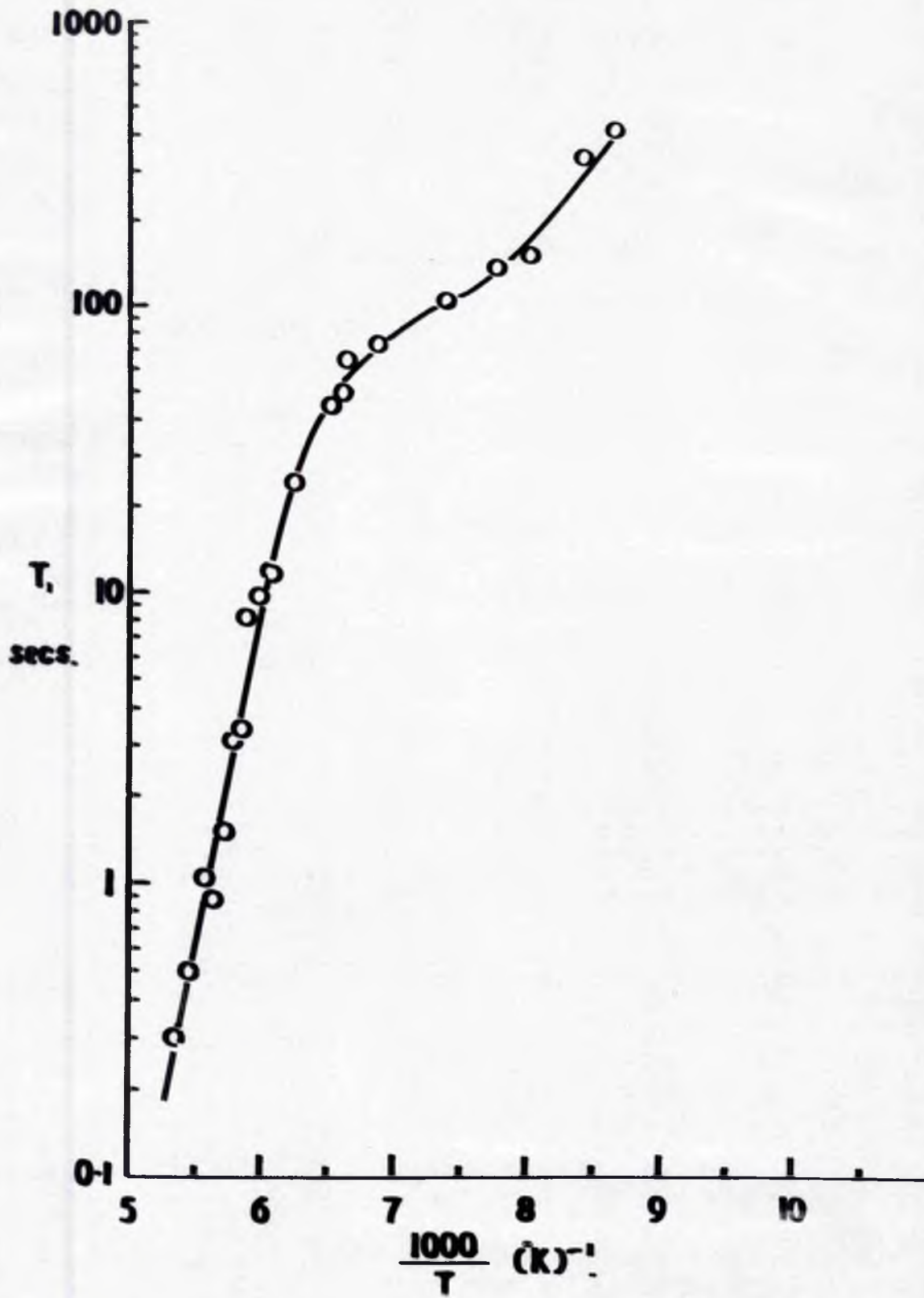Figure 15.

giving

$$\frac{1}{T_1} = C_1 \left[\frac{\tau_c}{1 + \omega^2 \tau_c^2} + \frac{2\tau_c}{1 + 4\omega^2 \tau_c^2} \right] \tag{4}$$

where

$$C_1 = \frac{3}{10} \frac{\gamma^4 \hbar^2}{b^6} \tag{5}$$

When $\omega\tau_c = 1/\sqrt{2}$, T_1 is a minimum and equal to $3\omega/2^{3/2} C_1$. Thus C_1 can be evaluated. However, in cyclohexane, the transition at 186°K prevents the minimum being observed and so C_1 cannot be directly found in this way.

Below 186°K, however, $\omega^2\tau_c^2 \gg 1$, since T_1 is increasing rapidly with decreasing temperature. Then

$$T_1 = \frac{2\omega^2 \tau_c}{3C_1} \tag{6}$$

and if $\tau_c = \tau_0 e^{E/RT}$, which implies a potential barrier of height E hindering the reorientation process, then

$$T_1 = \frac{2\omega^2 \tau_0}{3C_1} e^{E/RT}$$

and $\qquad \log T_1 = \log \frac{2\omega^2 \tau_0}{3C_1} + \frac{E}{RT} \log e \tag{7}$

If, then, the theory is a fair description of the relaxation mechanism, a plot of $\log T_1$ against the reciprocal of the absolute temperature, T, should give a straight line; figure 15 shows this plot. From the

transition temperature 186°K down to 165°K a linear
relationship exists as predicted. This is just the
temperature range in which the first reduction of the
linewidth occurs. Below 165°K, however, log T_1 is less
than predicted, indicating that T_1 is shorter than is to
be expected from this one mechanism alone. The effective-
ness of another process (or processes) is now showing up.
The slope $\frac{E}{R} \log_{10} e$ of the straight line portion yields
the value of 11 ± 1 Kcal/mole for E , the height of the
potential barrier restricting motion about the triad axis
of the molecule. Equation (7) also gives a value for
$1/\nu_o C_1$, where $\nu_o = 1/2\pi \tau_o$,

$$\frac{1}{\nu_o C_1} = 1.77 \times 10^{-29} \ \sec^3. \quad \text{(for E = 11 Kcal/mole)}$$

(8)

The linewidth transition associated with the onset
of the motion about the triad axis has been synthesised
using the value for barrier height obtained from the
relaxation time measurements. Gutowsky and Pake (reference 5)
proposed this idea, but they simply used the barrier height
as a fitting parameter. Equation (15) of reference 5 is :

$$(\delta\nu)^2 = B^2 + C^2 \left(\frac{2}{\pi}\right) \tan^{-1} \left\{ \propto \frac{\delta\nu}{\nu_c} \right\} \quad (9)$$

where $\delta\nu$ is the linewidth measured between points of
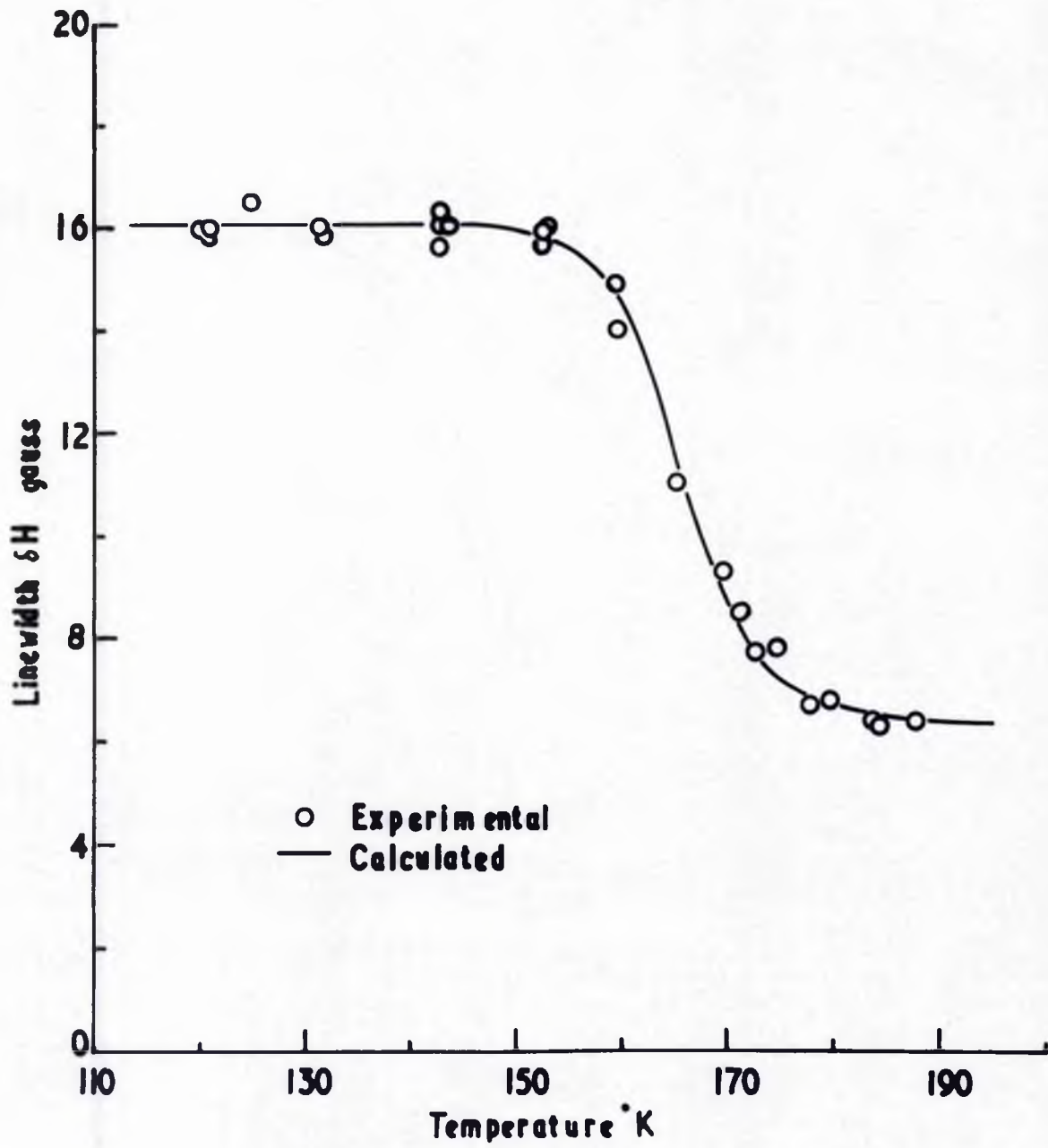maximum and minimum slope of the absorption line ; ν_c is

Figure 16.

correlation frequency = $1/2\pi \tau_c$; α is a constant of
order unity. At low temperatures $\nu_c \to 0$ and $\delta\omega \to \overline{\sqrt{B^2 + \sigma^2}}$;
this is the rigid lattice linewidth. At high temperatures
$\nu_c \to \infty$ and $\delta\omega \to B$. That is, equation (9) describes
a linewidth transition from a value $\sqrt{(B^2 + \sigma^2)}$ to a
smaller value B, this reduction being due to the onset
of a specific motion.

To compute the linewidth transition, ν_0 , appearing
in (8), has to be calculated from the experimental data.
$\nu_0 = \nu_c \exp\left(\frac{E}{RT}\right)$ is substituted in (9), which is then
rearranged to read :

$$\exp\left(\frac{E}{RT}\right) = \frac{h\,\nu_0}{\alpha\,\gamma\beta.\delta H}\tan\frac{\pi}{2}\left[\frac{(\delta H)^2 - B^2}{\sigma^2}\right] \tag{10}$$

where δH is the linewidth expressed in gauss. Values
for δH are then substituted and the corresponding values
of the temperature calculated. The smooth curve in figure
16 is a plot of (10) obtained in this way. The agreement
with the experimental values, which are also shown, is good.

Calculation shows that the minimum value of the
relaxation time (= 0.05 seconds) would have occurred at
205°K.

A value for σ_1 (equation 5) has been calculated
assuming that the relative motion of the neighbour proton
in the same OH_2 group predominates the relaxation process.
(This assumption is similar to that made by Bloembergen
et al). The value obtained is 5.05×10^9 sec^{-2}. This has

to be compared with a value of 3×10^9 obtained experimentally. An error factor of two, which embraces both the uncertainties in α and E and in the graphical analysis, must be quoted for this result. In view of the simplifying assumptions made, the agreement between these figures is reasonable and allows us to conclude that the spin-lattice relaxation process over the temperature range 165°K to 186°K is in the main controlled by the relative motion of the two protons in the CH_2 groups in the molecules.

Above the transition temperature, the mean frequency of reorientation is greater than 23.4 Mc/s, the operating frequency, since T_1 is now increasing with increasing temperature. A further decrease in T_1 accompanies the onset of the proposed 'diffusion' process around 240°K. The absence of a measurable discontinuity in T_1 (and, for that matter, in the second moment) at the melting point emphasises the marked freedom of the molecules in the solid state at this temperature.

SECTION 4.3.

BENZENE

4.3. BENZENE

4.3.1. Preparation of the Sample.

The sample of benzene examined was kindly supplied by Professor Everett of University College, Dundee, and was prepared as follows.   Starting with AnalaR grade benzene, the sulphur compounds were first removed; the benzene was then fractionally frozen twelve times and finally distilled.   The melting point of the sample was 5.52°C.   This gives an estimated impurity content of 0.005 mole% if the true melting point is taken as 5.53°C, the value measured by workers at the National Bureau of Standards. (reference 55).   A small additional amount of impurity may have been introduced in transferring the benzene to the specimen ampule.   The sample examined, however, certainly contained less than 0.05 mole% impurity (cf. cyclohexane).

4.3.2. Molecular Structure.

The generally accepted model has been assumed, namely that the six carbon atoms form a plane hexagon and that each carbon has a side bond hydrogen atom. Thus a plane hexagon of protons is formed, the molecule having a hexad symmetry axis in addition to its six diad axes. The values assumed for the C-C bond length (1.39A) and the C-H bond length (1.08A) are those used by E.R. Andrew (reference 8). The C-C bond length is that found by L.O. Brockway and J.M.

Robertson (reference 60) and the C-H bond length is
intermediate between 1.09A for -C-H and 1.07A for =C-H
(reference 23). These values are well supported by the
recent electron diffraction experiments of I.L. Karle
(reference 43).

4.3.3. Crystal Structure.

The crystal structure of solid benzene has been
determined by E.G. Cox (reference 44). The unit cell is
orthorhombic, and at -22°C has dimensions, a = 7.44A,
b = 9.65A and c = 6.81A. : it contains four molecules which
are arranged with their planes parallel to the b axis and
making angles of 40 degrees with the plane (100); figure 11
shows a model of the unit cell. The smallest inter-molecular
carbon-carbon distance for this structure is somewhat larger
than usually found in organic compounds.

The unit cell dimensions have been determined at various
temperatures in the range 20°K to 273°K (references 45 to 49
and 51 to 54), and A. Euken and E. Lindenberg have measured
the mean expansion coefficient for approximately 20° intervals
in the range 193°K to 273°K (reference 50). From these
results the volume of the unit cell at 80°K has been estimated
to be 95.2% of Cox's value; i.e., there has been a linear
lattice contraction of 1/3.(4.8)% = 1.6%.

Benzene, unlike cyclohexane, does not undergo a change
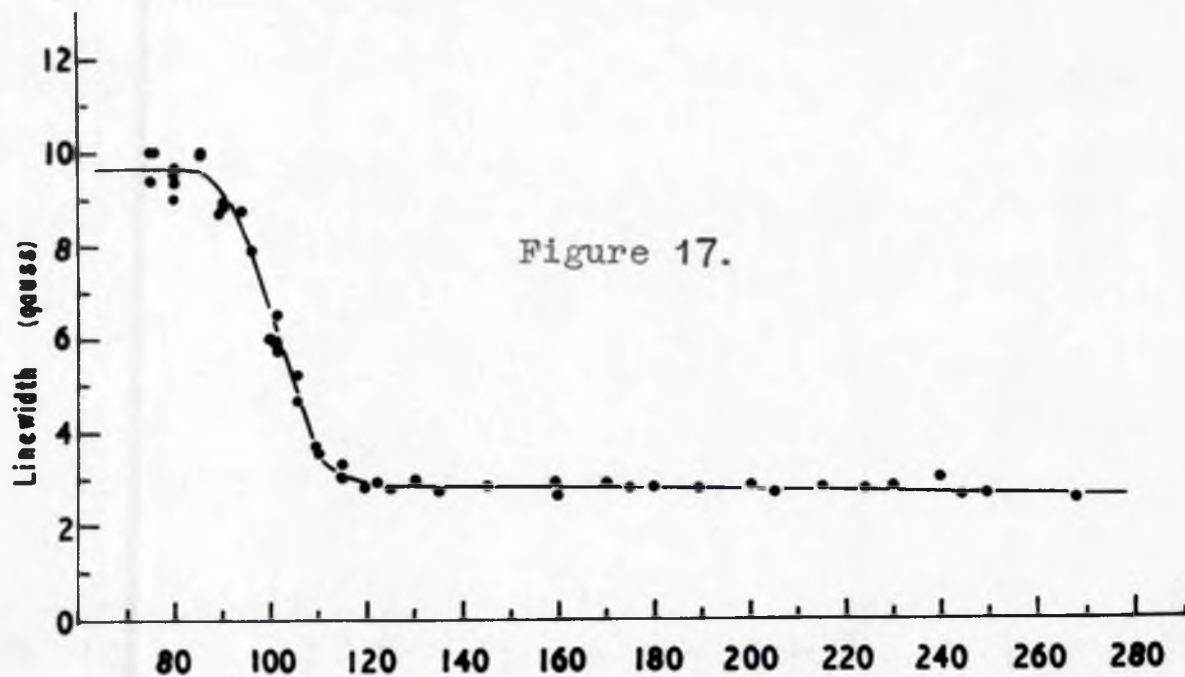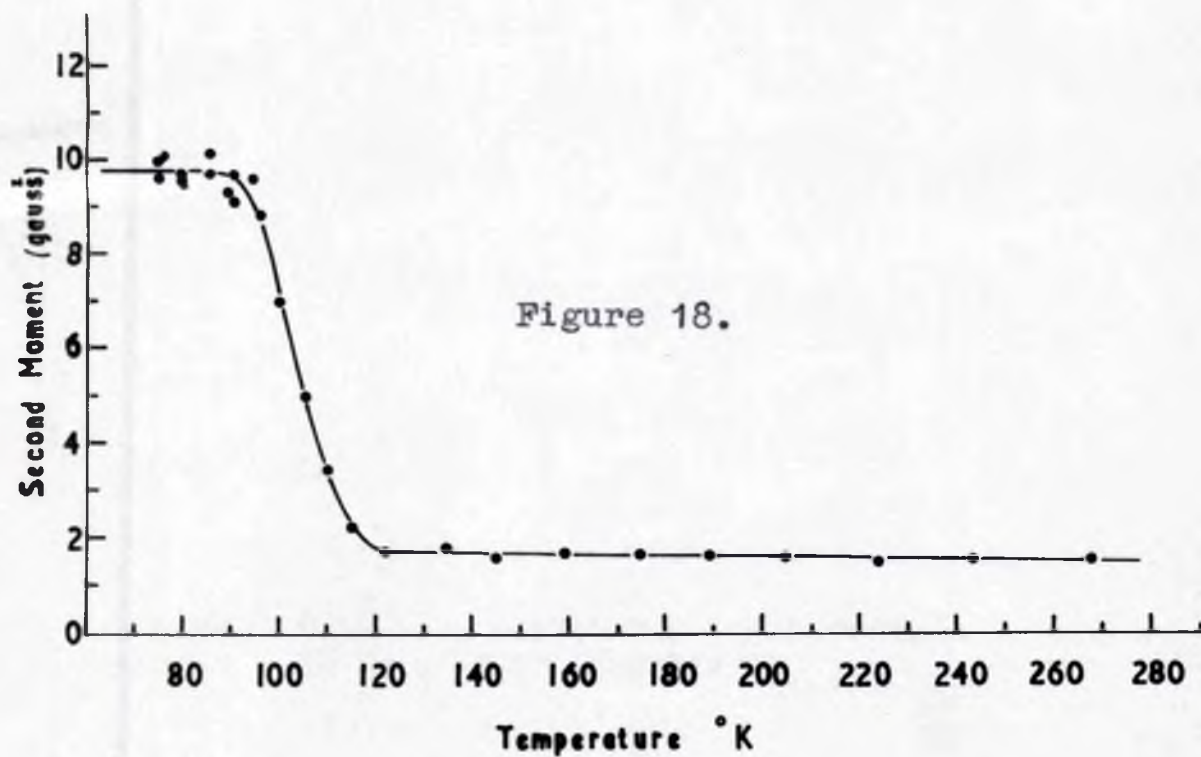of crystal structure in the temperature range covered.

Figure 17.

Figure 18.

4.3.5. The Absorption Spectrum.

Using the lock-in amplifier and field-scanning device the first derivative of the absorption line was recorded at temperatures in the range 75°K to 268°K, and from these plots the linewidths and second moments have been calculated. (The lower plot in figure 7 is the recorded first derivative of the absorption line in benzene at 205°K). Figures 17 and 18 show the temperature variation of the linewidth and second moment respectively.

The second moment is constant below 85°K indicating that the lattice is effectively rigid. The mean experimental value for the rigid lattice is 9.75 ± 0.25 gauss^2. A theoretical value has been calculated assuming the molecular and crystal structures discussed, and assuming a linear lattice contraction of 1.6%. The intra-molecular contribution is 3.29 gauss^2, and the inter-molecular contribution 6.52 gauss^2, giving a total calculated value of 9.81 gauss^2. This is in good agreement with the experimental value.

The signal to noise ratio obtained with benzene was somewhat less than that for cyclohexane. However, the low field-scanning rate enabled the long time constant coupling circuit to be used to the output stage of the lock-in amplifier, and this effected a very marked improvement. It appears, therefore, that the small discrepancy between the calculated and measured values of the rigid lattice

second moment reported by E.R. Andrew (reference 8) was due to the limitations of the recording technique and to the use of too large a field modulation amplitude in an attempt to improve the signal strength.

The Absorption line narrows between 85°K and 135°K and the second moment falls to 1.7 gauss^2. The molecular motion most likely to occur appears to be reorientation about the hexad axis which is normal to the plane of the molecule. Angular oscillation and reorientation about the diad axes cannot, however, be completely excluded. The effects of reorientation about the hexad axis on both the 'intra' and 'inter' contributions to the second moment have been calculated (see Appendix 1). The 'intra' contribution is reduced from 3.29 gauss^2 to 0.82 gauss^2, and the 'inter' contribution from 6.52 gauss^2 to 0.91 ± 0.5 gauss^2, giving a total reduced second moment of 1.7 ± 0.5 gauss^2.

Reorientation about one of each of the two types of diad axis has also been considered. The effect on the 'intra' contribution is the same for both, reducing it to 1.13 gauss^2. The effect of reorientation about the diad axis parallel to the b axis of the unit cell on the 'inter' contribution is to reduce it to 1.71 ± 0.5 gauss^2, thus giving a total reduced value for the second moment of 2.8 ± 0.5 gauss^2. Motion about the other diads is likely to yield essentially similar values. Hence reorientation about one diad alone appears insufficient to reduce the second moment to the
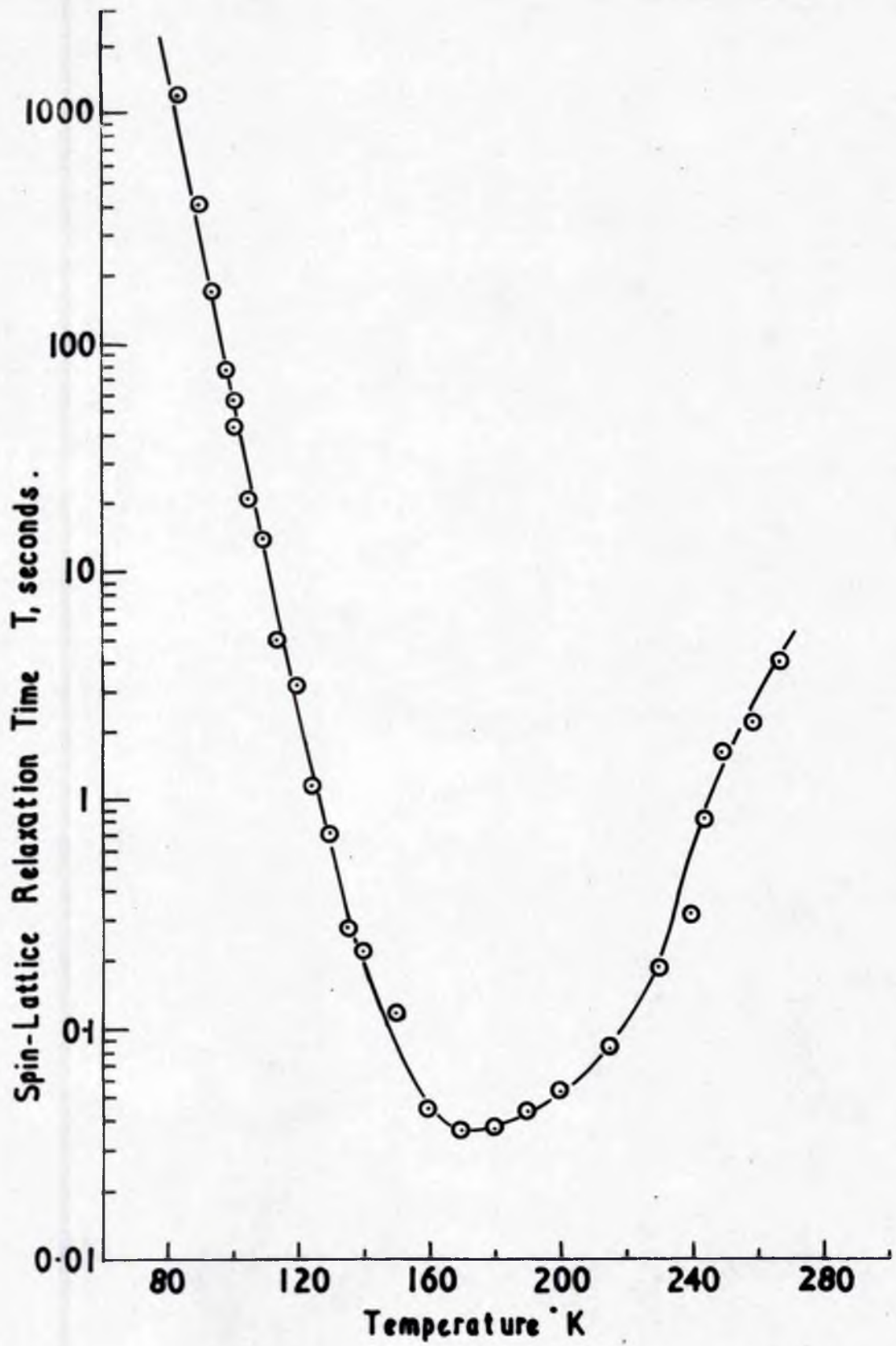
Figure 19.

observed value. Motion about the hexad axis alone, however, does give a reduced second moment which agrees well with that observed experimentally.

It seems, therefore, that the motion occurring initially is a discontinuous rotation of the molecules about their hexad axes. Angular oscillations and occasional reorientations about the diad axes may also occur, together with vibration of the centres of gravity of the molecules and of the nuclei within the molecules. One or more of these possible motions are probably responsible for the gradual decrease in the second moment between $135°K$ and $268°K$ (1.7 to 1.5 gauss^2). In section 4.3.7 it is shown that the proposed motion about the hexad axis is not incompatible with the interpretations of the Raman spectra given by A. Fruhling, I. Ichishima and S. Mizushima (references 56 and 57).

4.3.6. Spin-lattice Relaxation Time Measurements.

The spin-lattice relaxation time has been measured and is shown as a function of the temperature in figure 19. Below $101°K$ the relaxation times were long enough to measure directly (see section 4.2.6). Above this temperature the saturation technique was employed; since, however, the linewidth remains considerably greater than the field inhomogeneity over the volume of the sample, it was not necessary or, in fact, feasible to use the cine film method.
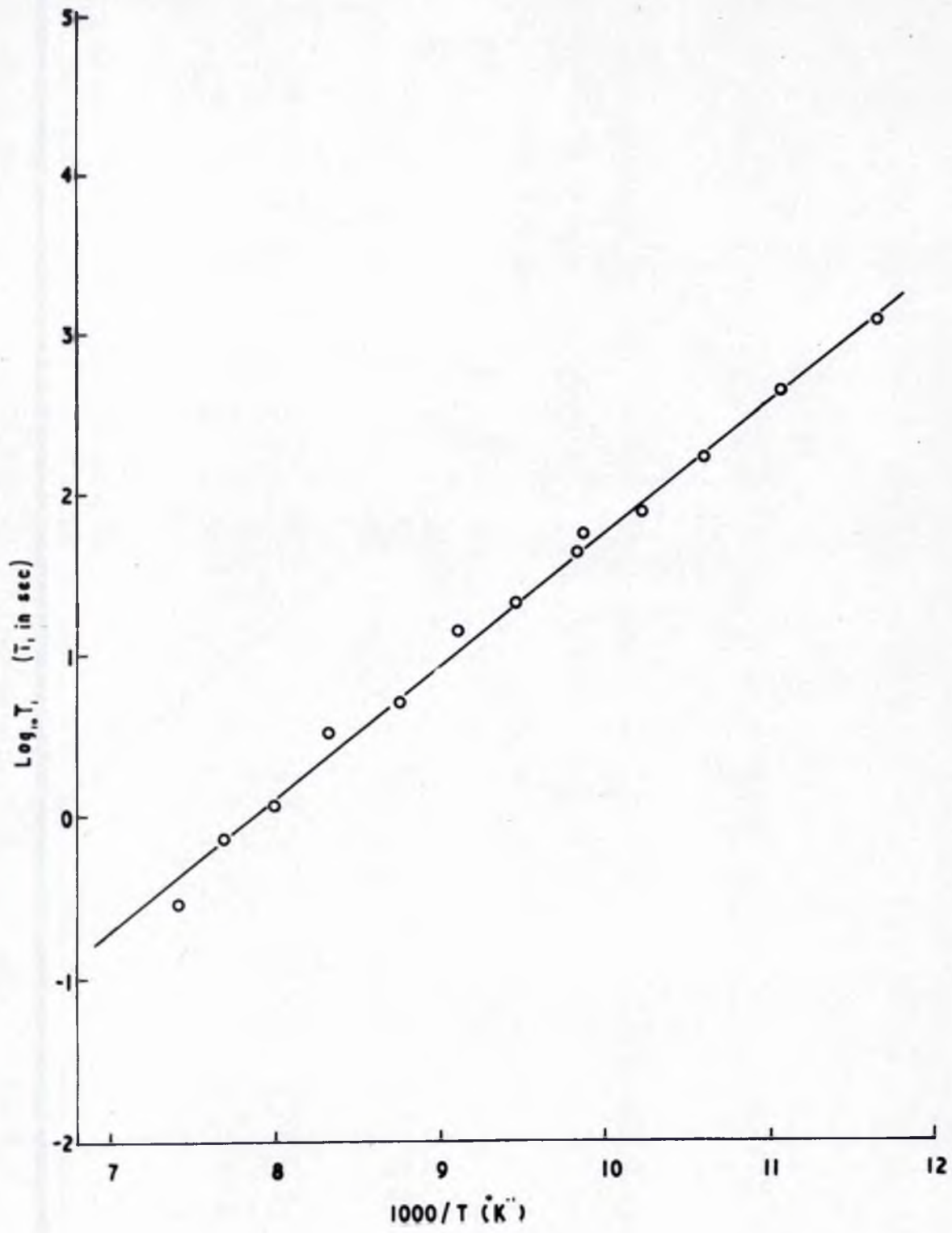
Figure 20.

The interpretation of the relaxation time data
follows that outlined for cyclohexane. Since, however,
no polymorphic change occurs, the minimum value of T_1
is observed. The values of $\log T_1$ have been plotted
against the reciprocal of the absolute temperature for
the region where T_1 is increasing rapidly with decreasing
temperature. Equation 7, section 4.2.6 applies :

$$\log T_1 \;=\; \log \frac{2\,\omega^2\tau_o}{3\mathcal{G}_1} \;+\; \frac{E \log e}{R} \; \frac{1}{T}$$

This assumes that the so-called barrier height E is
independent of the temperature; to a first approximation,
at least, this will be true over the limited temperature
range 75°K to 135°K. Figure 20 shows this plot; the
straight line has been fitted using a least squares
calculation and gives the value for E of 3.74 ± 0.20 Kcal/
mole. This represents the height of the potential barrier
hindering the reorientation about the hexad axis.

Combining the linewidth data and the value obtained
for E, $\nu_o = \frac{1}{2\pi\tau_o}$ has been calculated. This has been done
by re-writing equation 9, section 4.2.6 as

$$\alpha \frac{\delta\nu}{\nu_c} \;=\; \tan\frac{\pi}{2} \left[\frac{(\delta H)^2 - B^2}{C^2} \right] - t \tag{1}$$

Since $\quad \nu_o = \nu_c\, e^{E/RT} \quad$ and $\quad h\nu = 2\mu H \quad$ then :

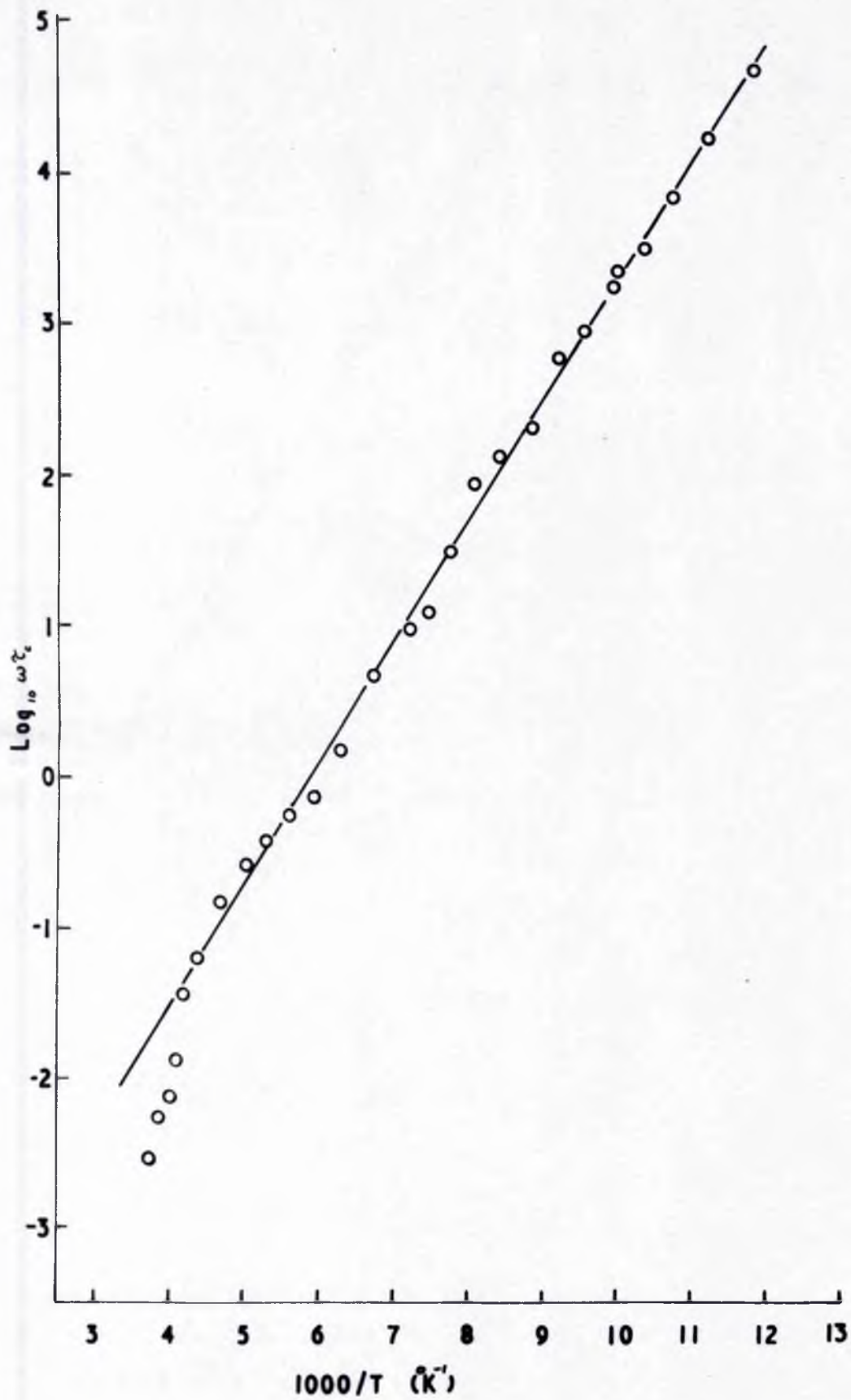$$\nu_o \;=\; \frac{\alpha\gamma\beta}{h} \; \frac{\delta H}{t} \; e^{E/RT} \tag{2}$$

Figure 21.

which gives on substituting known quantities :

$$\log \frac{\delta H}{E} = -0.8165 \frac{1000}{T} - \log \frac{\alpha \gamma \beta}{h \nu_0} \tag{3}$$

The experimental values of $\log \frac{\delta H}{E}$ were then plotted against the corresponding values of 1/T and the constant $\log \frac{\alpha \gamma \beta}{h \nu_0}$ in equation (3), adjusted to give best fit. From this constant the value of ν_0 in terms of the quantity α has been calculated; again α is a constant of order unity embracing both the doubts in the integration limits used in forming equation (1) and a factor intimately connected with the line shape of the resonance. Using the value of ν_0 so obtained, the calculated minimum value of T_1 is 0.126 α seconds.

The measured T_1 values have been converted into values using the expression

$$\frac{1}{T_1} = C_1 \left[\frac{\tau_c}{1 + \omega^2 \tau_c^2} + \frac{2\tau_c}{1 + 4\omega^2 \tau_c^2} \right]$$

If the barrier height is considered constant, then $\tau_c = \tau_0 e^{E/RT}$ as above. Thus

$$\log \omega \tau_c = \log \omega \tau_0 + \frac{E}{R} \log e \cdot \frac{1}{T} \tag{4}$$

where ω is the operating angular frequency. From (4) we see that a plot of $\log \omega \tau_c$ against 1/T should be a straight line and should have a slope equal to that of the $\log T_1$ v. 1/T plot. That this is essentially true over most
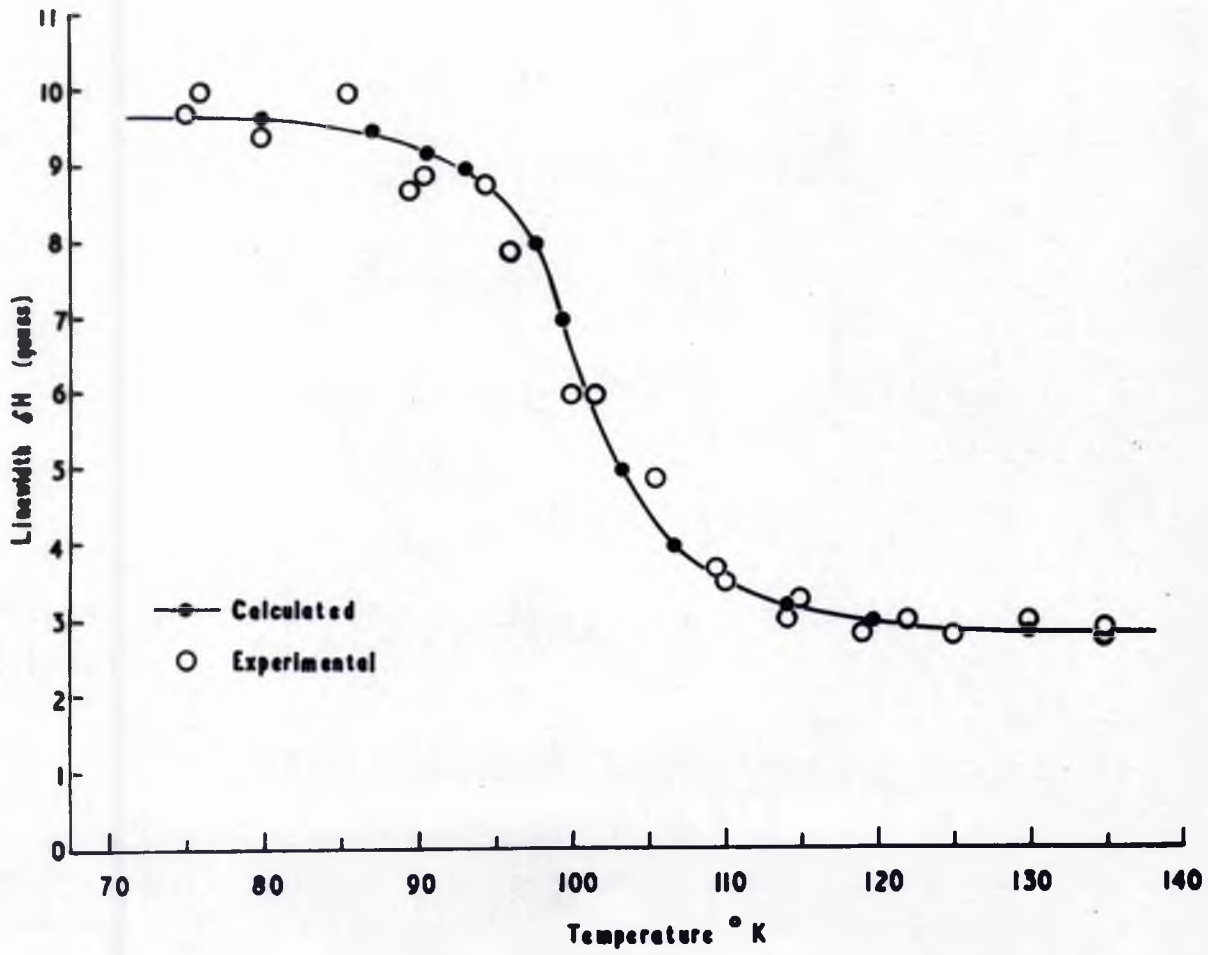
Figure 22.

of the temperature range covered can be seen from figure 21.
The straight line has, in fact, been drawn with a slope
corresponding to 3.74 Kcal/mole. The divergence of the
experimental points at the high temperature end of the
plot indicates that τ_c is becoming shorter than predicted
by equation 4 ; this is equivalent to saying that the
barrier height is less than at lower temperatures.

Using the calculated value of T_1 min., the linewidth
transition has been synthesised as described in section
4.2.6 for cyclohexane. Figure 22 shows that calculated
and experimental values are in agreement, indicating
consistency in the analysis.

The interpretation of the relaxation time data is
therefore satisfactory provided it is assumed that α has
the value 0.29, or, of course, that a systematic error
occurs in measuring T_1 near the minimum. Individual
measurements of T_1 well removed from the minimum are
reliable to within ± 15% : within this range the saturation
technique used to measure T_1 corresponds to Case 2
discussed by Bloembergen et al. in reference 1. The
criterion of case 2 is that $2\pi \nu_m T_1 \gg 1$, where ν_m is
the field modulation frequency, in this case 25 c/s. In
fact even at the minimum $2\pi \nu_m T_1 \doteq 6$, thus still being
somewhat greater than unity. Consequently T_1 values,
calculated from the saturation curves assuming case 2
throughout, are certainly unlikely to be more than 30% out.

Thus the total probable error in the measured value of
T_1 min. is about 35%. The value of α , therefore, must
be assumed to be about 1/3. If, as proposed by Bloembergen
et al (reference 1, p.699), the integration limits assumed
in formulating (1) are taken as $\pm 2\Delta\nu$, where $\Delta\nu$ is the
R.M.S. linewidth, then α has the following values :

Line shape	$\alpha = 2\frac{\Delta\nu}{\delta\nu}$
Gaussian	1.0
Sinusoidal	0.72
Half sinusoid	0.44
Triangular	0.41 (min.)

Above and below the linewidth transition temperature the
experimental values of $2\frac{\Delta\nu}{\delta\nu}$ for benzene are 0.90 and 0.65
respectively, giving a mean value of about 0.80. On the
whole it is considered that the integration limits $\pm 2\Delta\nu$
are rather generous : any reduction of these, of course,
reduces the values of α given above. Thus the experimental
value of $\alpha = 0.3$ is not unreasonable when the experimental
uncertainty in T_1 is also taken into account.

4.3.7. Correlation with the observed Raman Spectrum.

Four lines have been found in the Raman spectrum of
solid benzene. The three independent investigations made
to date (references 56 to 58) have produced results which
agree well as to the frequency of the lines. However, there
has not been the same agreement on the interpretation of the

spectrum.   Quoting only Fruhling's results as representative:

Temperature °C	Lines in cm^{-1}				Half-widths in cm^{-1}			
	ν_1	ν_2	ν_3	ν_4	$\delta\nu_1$	$\delta\nu_2$	$\delta\nu_3$	$\delta\nu_4$
0	35	63	69	105	8	15	8	20
-37	45	69	78	112				
-50	47	70	82	110				
-75	52	71	86	117	6	9	6	7
-85	53	74	?	117				

Fruhling, for instance, considers ν_1 and ν_2 are the lines
due to the oscillation of the molecules about their hexad
axes, whereas Ichishima and Mizushima consider that, since
the line(s) due to oscillation about the hexad axis might
be expected to become broader and weaker at higher
temperatures due to molecular reorientation, ν_4 represents
the hexad oscillation.

What, however, is fundamentally important is that a
Raman line is observed which is very likely to be due to
the angular oscillation of the molecules about their hexad
axes. If, say, the line due to such an oscillation has
frequency ν_R , then in the presence of reorientation it
can only be observed if $\nu_R > \nu_c$, where ν_c is the average
reorientation frequency of the molecules. Further, if the
Raman line has an observed width $\delta\nu_R$, then the even more
stringent requirement that $\delta\nu_R$ is greater than ν_c must

be fulfilled. Considering the linewidths at 0°C obtained by Fruhling, $\delta\nu_R$ is about 3×10^{11} c/s. This has to be compared with the experimental value found for ν_c from the relaxation time measurements. At -5°C, this is 8.1×10^9 c/s. Thus ν_c is certainly less than $\delta\nu_R$, and the reorientation about the hexad axis proposed in this investigation is compatible with the published interpretations of the Raman spectra (references 56 and 57).

Extrapolating the measured $\sim\nu_c$ values to 0°C gives a value of $\nu_c = 2.4 \times 10^{10}$ c/s. For the ν_4 line, $\delta\nu_R = 6 \times 10^{11}$ c/s : thus the ratio $\delta\nu_R/\nu_c$ is not very large, and perhaps the marked broadening of the ν_4 line between -75°C and 0°C is due to the reorientation effect, as suggested by Ichishima and Mizushima.
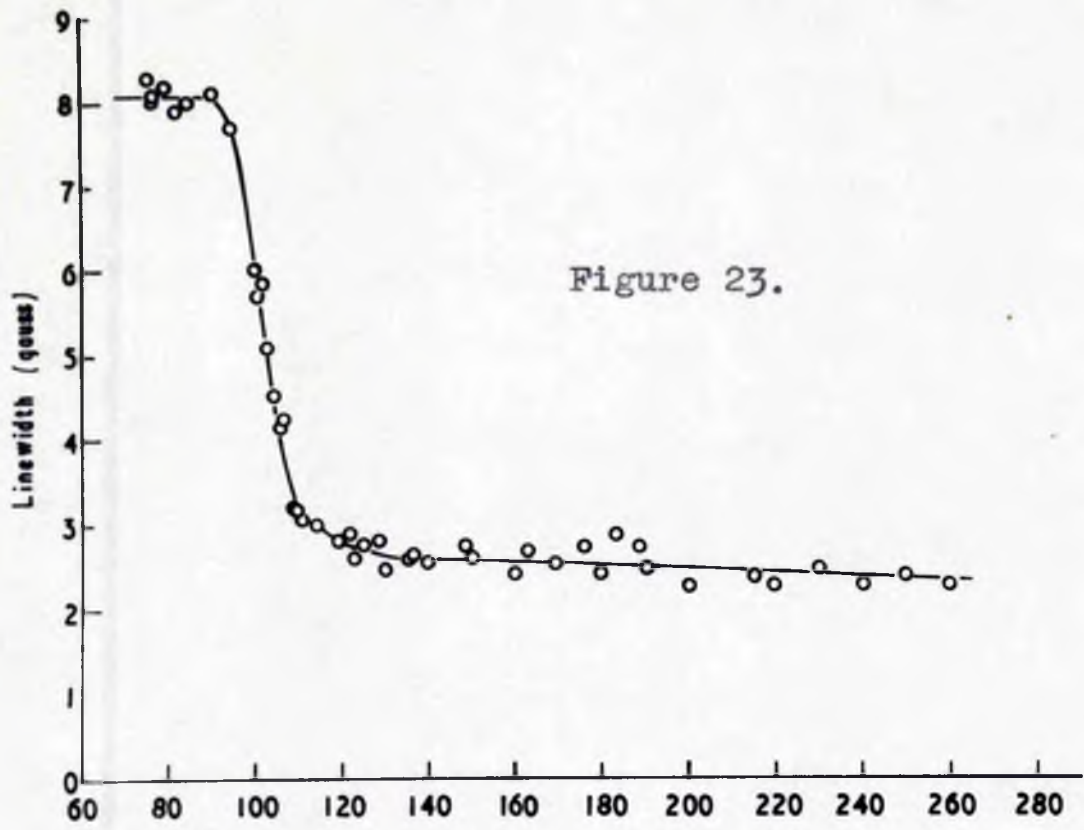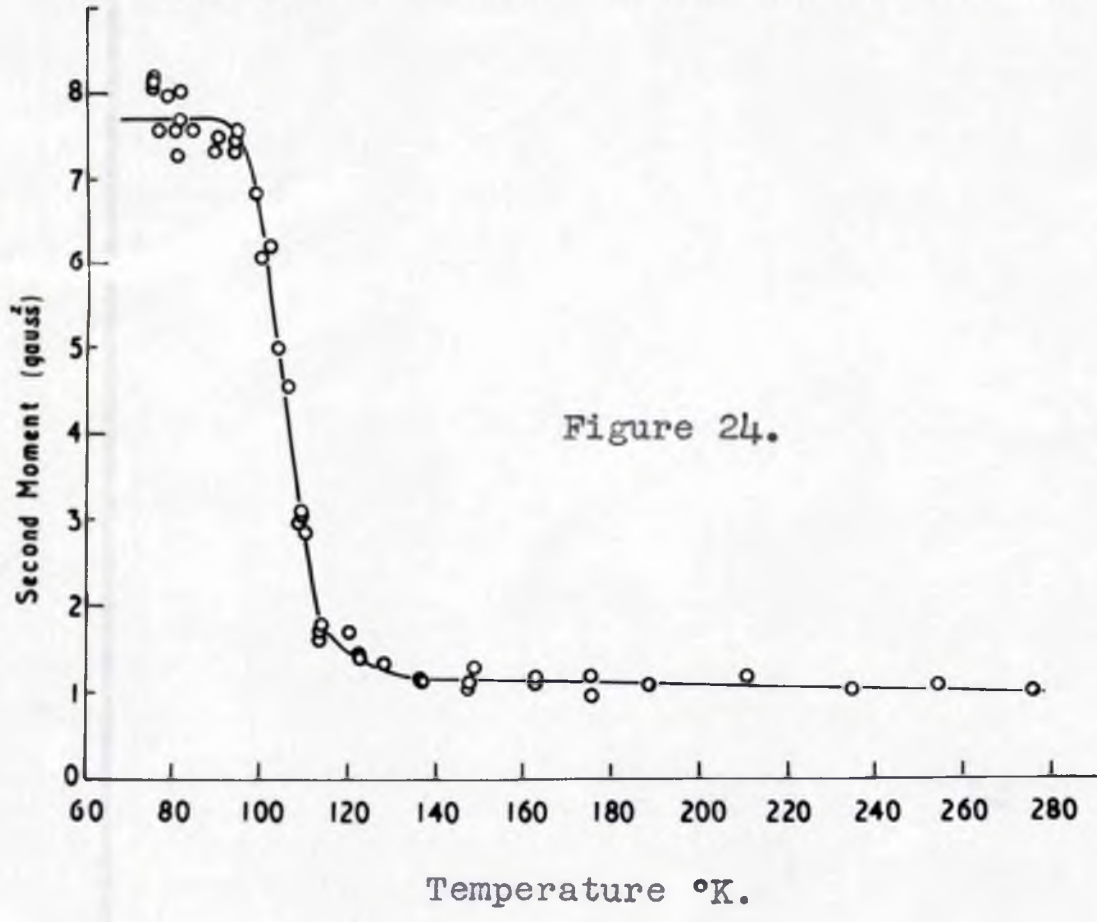
SECTION 4.4

BENZENE - d_1

Figure 23.

Figure 24.

Temperature °K.

4.4   BENZENE - d$_1$

4.4.1   General

The specimen examined was kindly supplied by Professor Ingold, University College, London.

The important difference between this substance and the others examined is that here there are two species of nuclear magnets present in the crystal lattice. Hence both the proton and deuteron resonances could have been observed ;   in fact, only the proton resonance was examined.

4.4.2   Molecular and Crystal Structures.

The following reasonable assumptions have been made about the molecular and crystal structures :

   (a)   The molecule is planar as for benzene and the dimensions are also identical.

   (b)   The crystal structure also remains unaltered except in so far as there is now one deuteron randomly distributed in each molecular group of six sites.

4.4.3   The Absorption Spectrum.

The measured width and second moment of the absorption line are shown as functions of the temperature in figures 23 and 24. Below 85°K the lattice is effectively rigid

(cf. benzene), the mean experimental value of the second moment being 7.77 ± 0.25 gauss^2. The calculation of the corresponding theoretical value differs somewhat from that for cyclohexane and benzene since the presence of the deuterons has also to be considered. The form of Van Vleck's formula used (see section 2.2) is :

$$\text{Second Moment} = \frac{6\,I(I+1)}{5\,N_R} \cdot g^2\beta^2 \sum_{j>k} r_{jk}^{-6} + \frac{4\beta^2}{15 \cdot N_R} \sum_{j;f} \frac{I_f(I_f+1)}{r_{jf}^6}\, g_f^2$$

Here the second term represents the contribution from the deuterons. This gives for the 'intra' contribution 2.65 gauss^2, of which only 0.02 gauss^2 comes from the second term. Since a random distribution of the deuterons over the six available sites in each molecule has been assumed, so far as the 'inter' contribution is concerned each site can be considered to accommodate 5/6th of a proton and 1/6th of a deuteron. Accordingly, the proton-proton contribution is 5/6th of that in the case of benzene, while the proton-deuteron contribution is 1/6th of that of benzene multiplied by the reduction factor

$$\frac{\frac{4}{15}\; I_f(I_f+1) \cdot g_f^2}{\frac{6}{5}\; I(I+1) \cdot g^2}$$

from equation (1) above.

The 'inter' contribution at 80°K is, therefore, 5.46 gauss^2, and the total calculated second moment for the rigid lattice is 8.11 gauss^2. The agreement between the experimental and theoretical values is reasonably good and supports the
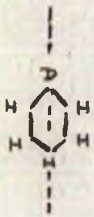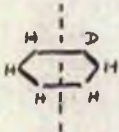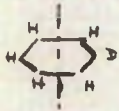
assumptions made in the previous section.

Between 85°K and 135°K the absorption line narrows
and the second moment falls to 1.2 gauss^2.   Thus the
linewidth transition occurs in the same temperature
interval as in benzene. In view of the similarity of
behaviour of the two substances, the effect of motion
about an axis perpendicular to the plane of the molecule
has been calculated. The intra-molecular contribution
to the second moment is reduced to 0.66 gauss^2 while
the new 'inter' contribution is 0.75 ± 0.4 gauss^2 ; the
latter figure has been obtained by assuming the reduced
'inter' contribution (0.91 gauss^2) found for benzene.
Thus, when motion about the pseudo-hexad axis occurs, the
total calculated second moment is 1.4 ± 0.4 gauss^2, which
is in reasonable agreement with the experimental value,
1.2 gauss^2, at 135°K.

The second moment falls slightly between 135°K and
276°K. This may again be due to angular oscillations and
occasional reorientations about the diad axes of which
there are now four, one true diad and three pseudo diads.
The effect on the 'intra' contribution of reorientation
about these axes has been considered. The effect on the
'inter' contribution has not been considered in detail but
an approximate value will be 5/6th of the corresponding
contribution for benzene, namely 1.4 gauss^2.

These results are listed below :

Axis		Contributions 'Intra' 'Inter' (gauss^2)		Total Second Moment (gauss^2)
	True Diad	1.31	1.4	2.7
	Pseudo-diad 1.	0.71	"	2.1
	Pseudo-diad 2.	0.93	"	2.3
	Pseudo-diad 3.	0.87	"	2.3

Vibration of the centres of gravity of the molecules and of the nuclei within the molecules could also contribute an effect as the temperature is further raised. The main linewidth transition, however, appears to be due to the onset of molecular reorientation about the pseudo-hexad axis.
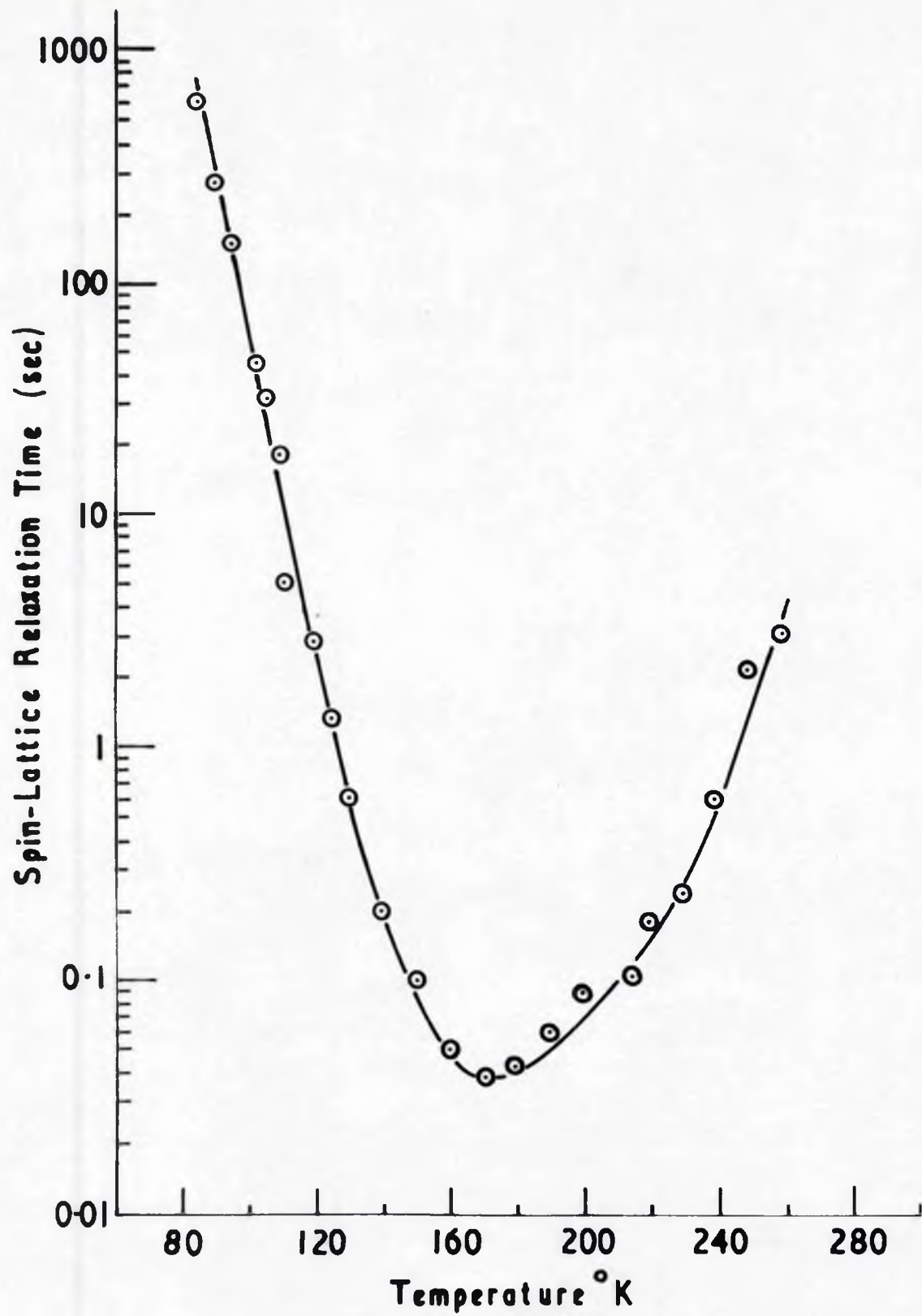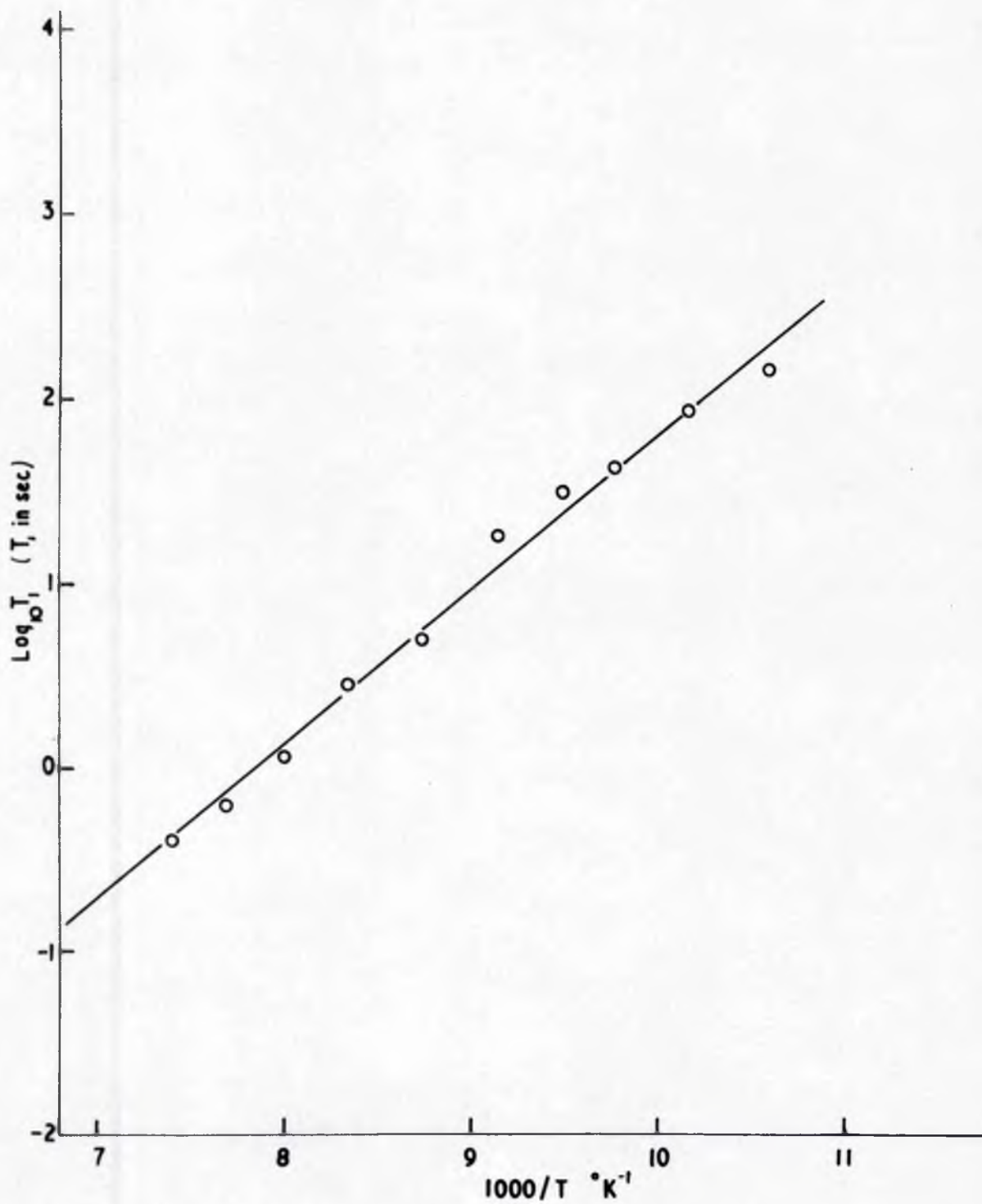
Figure 25.

Figure 26.

4.4.4 Spin-lattice Relaxation Time Measurements.

The spin-lattice relaxation time has been measured
and is shown as a function of the temperature in figure 25.
The methods used to obtain T_1 and the interpretation of
the experimental data follow precisely those for benzene.
Again the first step has been to obtain a value for E,
the barrier height opposing the reorientation about the
pseudo-hexad axis; figure 26 shows the plot of log T_1
against the reciprocal of the absolute temperature. Two
points (at 90°K and 85°K) have not been plotted. At
these temperatures the measured T_1 values were definitely
lower than expected and accordingly they were not included
in the least squares analysis used to obtain the best
value of E from the experimental points. The fact that
T_1 is less than expected below about 90°K makes it
necessary to assume that some additional relaxation
mechanism is becoming more important (cf. cyclohexane
below 165°K). The value obtained for E is 3.90 ± 0.20
Kcal/mole. This has to be compared with 3.74 Kcal/mole
for benzene.

The calculated minimum value for T_1 is 0.105 $\propto$
seconds. Since the observed minimum value is 0.039
seconds and since there is no reason to expect a large
experimental error, $\propto$ again must have a value of ~1/3.

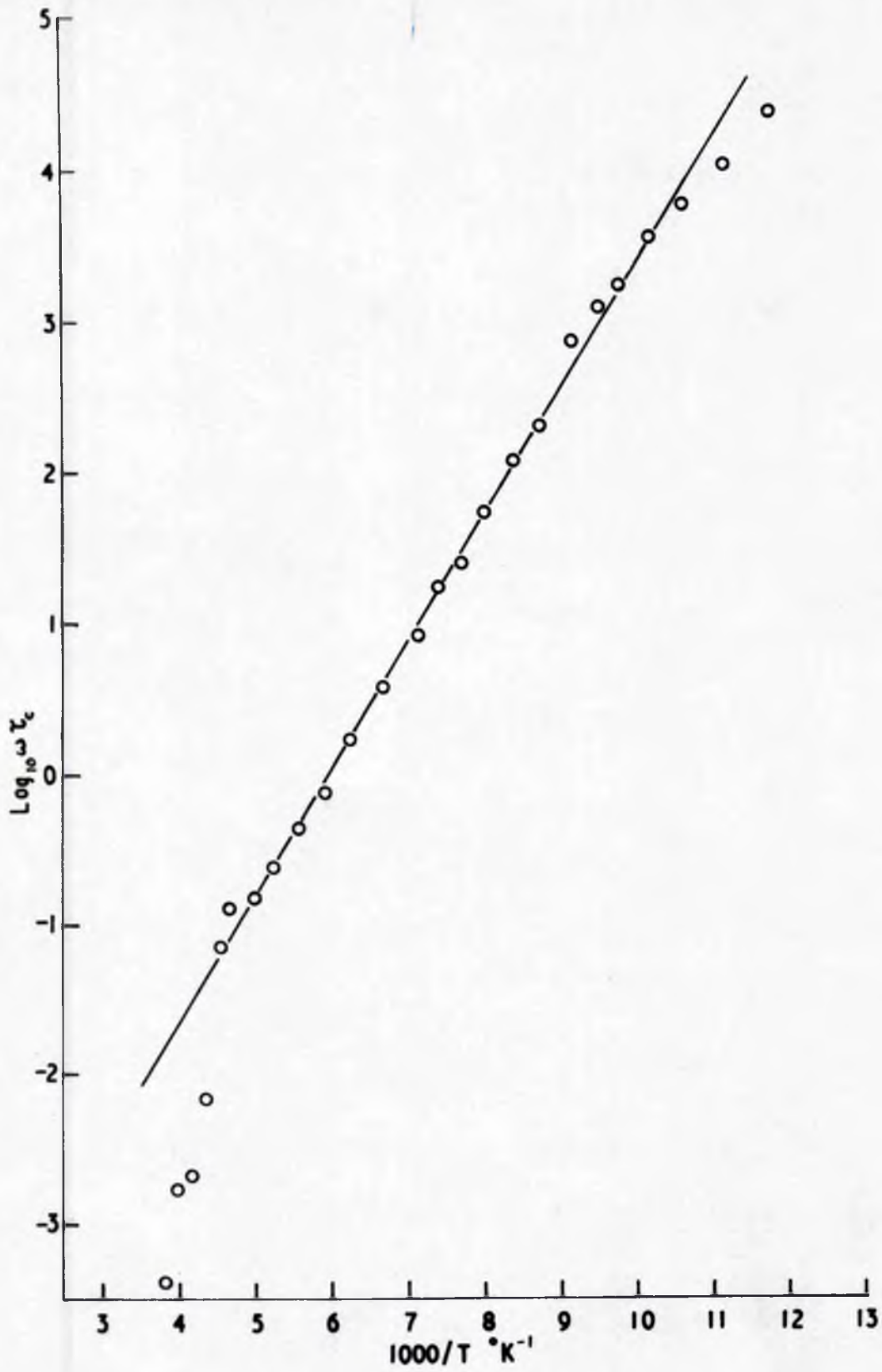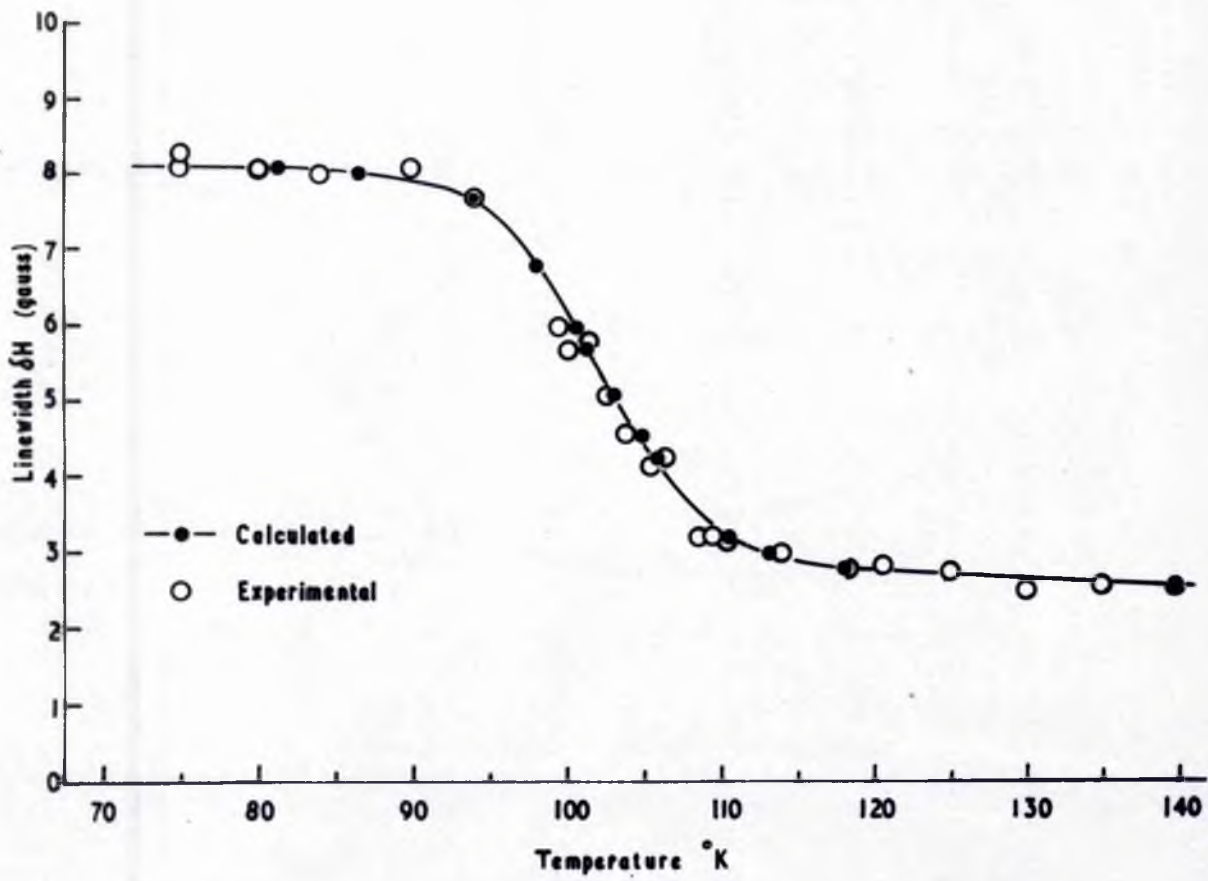The measured T_1 values have been converted into ~τ_c

Figure 27.

Figure 28.

values and these are plotted against the reciprocal of
the absolute temperature in figure 27. A straight line
has been drawn with a slope corresponding to E = 3.90
Kcal/mole. The experimental points fit this line well
over most of the temperature range investigated, indicating
that the barrier height E is effectively constant. There
is, however, a marked departure at both ends of the plot.
At the low temperature and the experimental values of T_1
are less than predicted by the linear relationship; thus
it appears that another mechanism is partially
controlling the relaxation mechanism below about 90°K.
At the high temperature end the divergence of the points
indicates that the potential barrier opposing the
reorientation about the pseudo-hexad axis is decreasing
quite rapidly with increasing temperature.

Finally, the linewidth transition has been reconstructed
using the calculated value of T_1 min. This is shown in
figure 28 together with the experimental points.

The marked similarity in the behaviour of benzene
and benzene-d_1 suggests it is unlikely that quantum-mechanical
tunnelling about the hexad axis is responsible for the
reduction of the linewidth between 85°K and 135°K.
E.R. Andrew and D. ter Haar (reference 59) have investigated
the difference in tunnelling rates of the two substances.
This depends on the difference in moments of inertia of the

two molecules and upon the assumptions made about the
angular width of the potential barrier opposing the
free reorientation of the molecules. It has been shown
that for angular widths greater than about three degrees
this difference is at least 20%.   While, of course, it
is less than this for very narrow barriers, which are
considered unlikely, it rises fairly rapidly as the barrier
width is increased, and at the maximum width of about
thirty degrees the tunnelling rate for benzene is between
two and three times that for benzene - d_1.   These figures
support the view that tunnelling does not play an important
role here.

SECTION 4.5

## CYCLOHEXENE

4.5 CYCLOHEXENE. C_6H_{10}.

Two samples have been examined; both were of the
highest purity grade obtainable commercially in the United
Kingdom, but no reliable figures of their percentage
compositions could be obtained. One sample was supplied
by B.D.H. and the other by I.C.I., designated 'spectroscopic-
ally pure'. It is evident, however, from the experimental
observations - see section 4.5.5 - that the relaxation
mechanism is being affected by the impurity centres in the
lattice; but it is very unlikely that the impurity content
is sufficient to modify the rigid lattice line shape. Thus
some useful information is available from the observations
reported in the following sections. Since, however, there
is some doubt of the validity of the relaxation time
measurements and of the temperatures at which the linewidth
transitions occur, a full interpretation of the experimental
data is not attempted.

4.5.1 Molecular Structure.

The molecular structure assumed is based on evidence
obtained from both chemical reaction rate experiments and
spectroscopic studies.

J. Boerseken and J. Stuurman (reference 35) have shown
that in velocity of oxidation experiments cyclohexene behaves
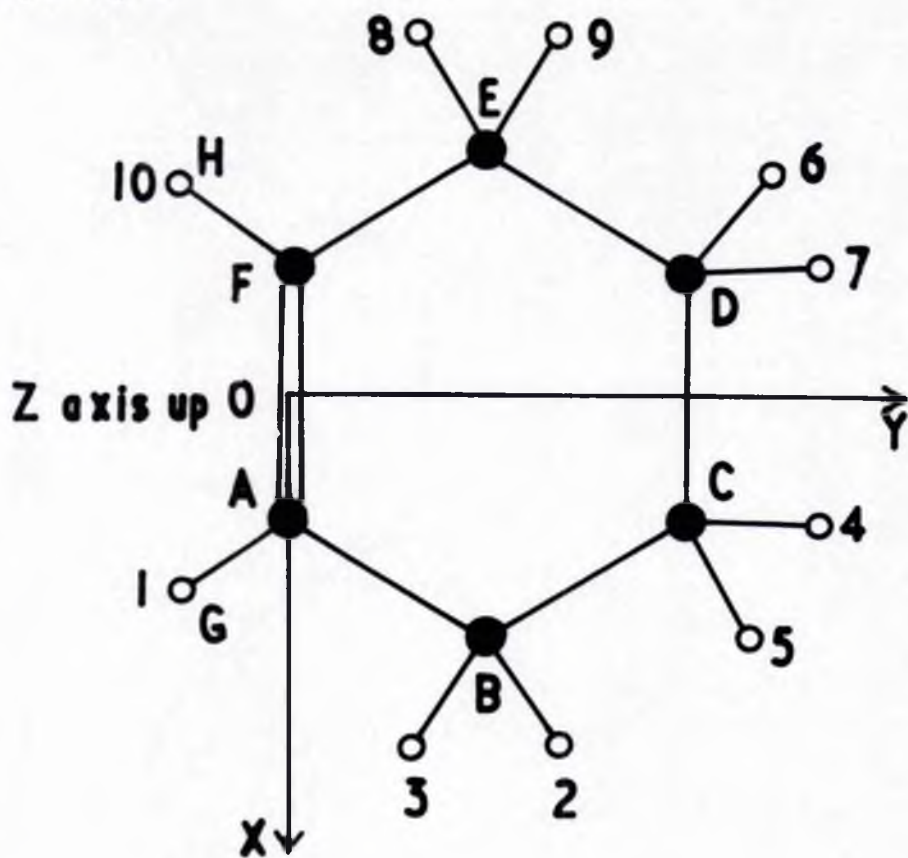exactly like hexene-3; i.e., the cyclic hydrocarbon behaves
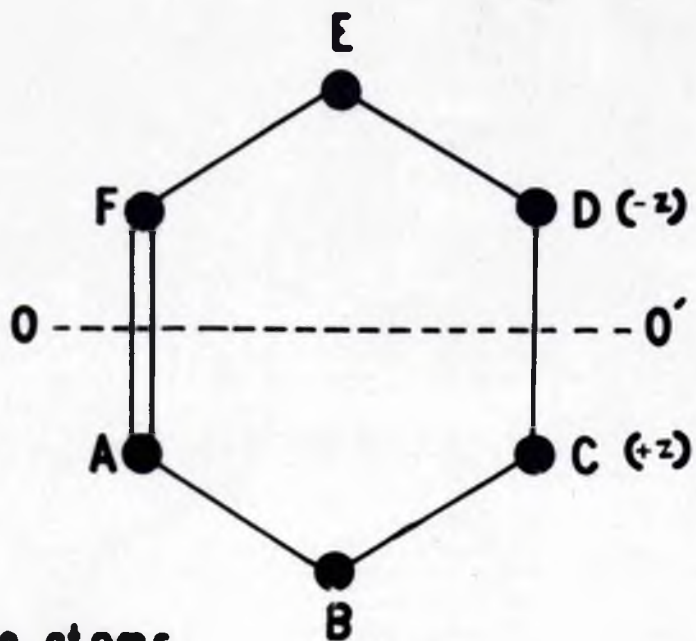
Figure 29.

exactly as if no ring closure had taken place. This indicates the absence of a marked ring tension and rules out the possibility of a planar structure. Boerseken and Stuurman suggest that four of the six carbon atoms lie in one plane, the other two being placed at equal distances above and below this plane. Beckett, Freeman and Pitzer (reference 36) conclude from their spectroscopic studies that cyclohexene probably has one predominant configuration with C_2 symmetry; Lister (reference 37) also suggests such a form.

The Proposed Model:

In figure 29, A,B,C,D,E and F are the six carbon atoms. The C = C bond length (A to F) is taken as 2a and the C - C bond length as 2b. Carbon atoms A,B,E and F lie in one plane, while atoms C and D lie respectively above and below this plane by the same amount. Angles ABC and DEF are assumed tetrahedral, and angles BAF and AFE are denoted by β, and angles BCD and CDE by γ. Since OO' is an axis of 2-fold symmetry, then (see Appendix 4),

$$\cos \gamma = \frac{\frac{28ab}{3} \sec\beta - 2a^2\sec^2\beta - \frac{26b^2}{3} - (2a\tan\beta - 4b\sin\beta)\sqrt{(a^2\sec^2\beta - \frac{16ab}{3}\sec\beta + \frac{24b^2}{3})}}{4b^2} \quad (1)$$

If the reasonable assumption is made that the angles at C and D are also tetrahedral, i.e. γ = 109°28', equation (1) gives β = 123°29'.

The coordinates of the six carbon atoms and the ten protons with respect to the system of axes shown in figure 29

were calculated assuming this geometry ; the $\geq$ C-H bond length was taken as 1.10 A (cf. cyclohexane), and the $\diagdown$ C - H as 1.07 A.; the angles GAF and HFA were taken as 123°29'. The z-coordinates of the carbon atoms C and D are then ± 0.425 A.

The only relevant X-ray data comes from a recent paper by R.A. Pasternak (reference 38). Here a brief account is given of work done on δ- pentachlorocyclo--hexene; the carbon atom skeleton is essentially that proposed above, although the results obtained by Pasternak are not very convincing. The measured C - C distances are definitely low, indicating a cramping of the model; it is therefore not surprising that he finds z-coordinates for atoms C and D somewhat smaller also, ± 0.367 A. (mean). The mean value of the angle $\diagup$ C $\diagdown$ obtained is 124°.

4.5.2 Crystal Structure.

The crystal structure of cyclohexene has not been determined; Pasternak (reference 38) has found that the δ- pentachloro- derivative has a monoclinic structure. But the introduction of the relatively large chlorine atoms will modify the lattice constants and his results, therefore, cannot be used for cyclohexene itself.

4.5.3 Thermal Data.

A first order phase transition occurs at 138.8°K (reference 39 and 40) and the melting point of the pure substance is 169.66°K (reference 41). Recorded heats of fusion and transition are 9.582 and 12.367 cal/gm. respectively. Although the difference is not so great as in cyclohexane, the heat of transition is still larger than the heat of fusion. A small discontinuity at least was therefore expected in the second moment and relaxation time v. temperature curves at 138.8°K. When this was not observed, an attempt was made to observe the transition thermally using a 'differential thermo-analyser' of the type described by Hassel and Hveding (reference 42).

In this instrument the substance to be investigated is brought into contact with a large heat reservoir - in this case a block of copper, with a silver plated cavity for the specimen. The temperature of the reservoir is slowly raised and the difference in temperature between the reservoir and the specimen is measured. By placing the copper block well down in the Dewar tube and adjusting the cold gas flow rate, the temperature rise was maintained at about two degrees per minute.

Melting of the specimen was clearly indicated by a rise in the standing temperature difference between the specimen and the block. The transition at 139°K, however, involving a larger latent heat, was not observed.
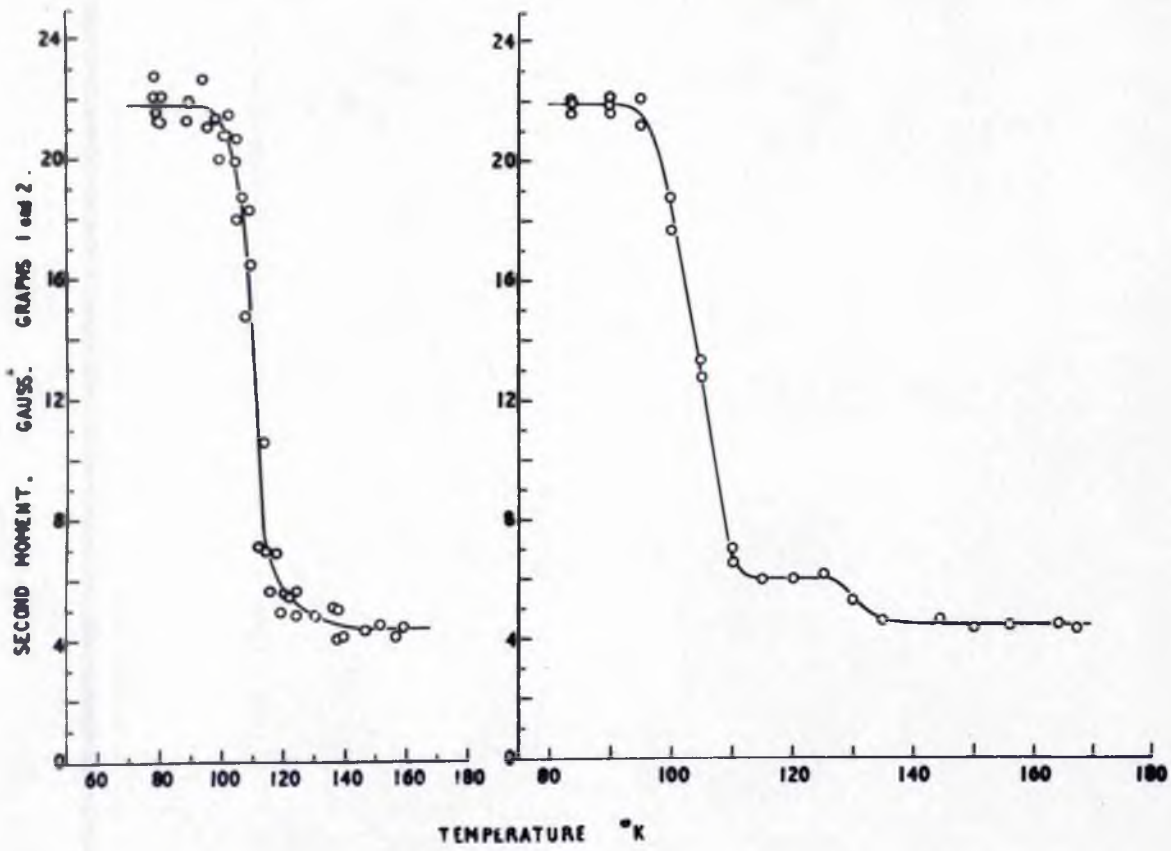
Figure 30.

4.5.4 The Absorption Spectrum.

The absorption line shape of the two samples has been examined between 78°K and 166°K.

The B.D.H. sample was investigated before the install--ation of the recorder and before the spin-lattice relaxation times had been approximately measured.   In fact it was the first specimen to be examined at 23.4 Mc/s; consequently the experimental conditions were not ideal. In particular, the optimum R.F. levels were not used, resulting in a poorer signal to noise ratio than obtained with the I.C.I. sample. The existence of the very long skirts on the absorption line was also partly missed.   These points account for the scatter of the second moment values calculated from these early observations, and shown in figure 30.

The results of the measurements on the I.C.I. sample are also shown in figure 30.   These were obtained under optimum experimental conditions and the improvement in the signal to noise ratio was very marked.   A typical line plot taken during this set of observations is shown in figure 7, (upper plot).   It is confidently expected that these results will be more nearly substantiated when the measurements can be repeated with a pure sample.   It is significant, however, that the rigid lattice second moments for the two samples agree well, as do the final smaller values assumed prior to melting.   There is, however, no evidence of a discontinuity around 139°K.

The mean experimental value for the rigid lattice second moment - using both sets of results - is 21.9 ± 0.3 gauss^2. Since the crystal structure is unknown, only an approximate theoretical value can be calculated. For the molecular configuration proposed, the 'intra' contribution is 13.8 gauss^2 The 'inter' contribution will be less than that for cyclohexane: assuming that there is no marked difference in the packing of the crystal lattices for the two substances, a rough value is obtained by reducing the values for cyclohexane in the ratio of the numbers of protons in the two molecules. This gives a value 8.3 ± 2.0 gauss^2 for the 'inter' contribution, and a total of 22.1 ± 2.0 gauss^2.

If it is assumed that the molecular configurations used in sections 4.2.2 and 4.3.2 for cyclohexane and benzene are correct - and they certainly are not far out - then the calculated intra-molecular contributions together with the mean experimental values of the rigid lattice second moments give 'experimental' values for the 'inter' contributions. A value for the 'inter' contribution for cyclohexene can then be calculated by assuming that a regular decrease is to be expected as the series cyclohexane, cyclohexene, cyclohexadine and benzene is traversed; such a decrease is to be expected from lattice energy considerations. Hence :

'Inter' contribution for cyclohexane $= 8.7 \pm 0.5$ gauss^2
      "   "   "   benzene $= 6.4 \pm 0.3$ "

                          Difference $= 2.3 \pm 0.6$ "

'Inter' contribution for cyclohexene $= 6.4 \pm 0.3 + \frac{2}{3}(2.3 \pm 0.6)$

$$= 7.9 \pm 0.5 \text{ gauss}^2$$

Theoretical second moment for cyclohexene $\quad = 21.7 \pm 0.5$ "

To these error limits, which only include the experimental uncertainties, must be added those arising from the assumptions that the molecular configurations are correct and that the decrease in the 'inter' contribution is regular in the series cyclohexane to benzene. These are difficult to estimate but safe limits of ± 2.0 gauss^2 are proposed. Thus the mean calculated value is 21.9 ± 2.0 gauss^2.

Until the crystal structure of cyclohexene is determined below the transition temperature, it is not possible to say more than that these results further substantiate the proposed molecular structure.

The second moment of the I.C.I. sample falls between 95°K and 115°K to 6.0 gauss^2. Molecular motions which might occur include rotation about the diad axis OO' (figure 29) and rotation about an axis parallel to the Z-axis (figure 29). Motion of each molecule about its diad axis reduces the 'intra' contribution to 8.0 gauss^2 (Appendix 5). This motion cannot alone account for the observed value. Motion about an axis perpendicular to the plane containing the four carbon atoms reduces the 'intra' contribution to 4.12 gauss^2. Motion about the corresponding axis in cyclohexane reduced
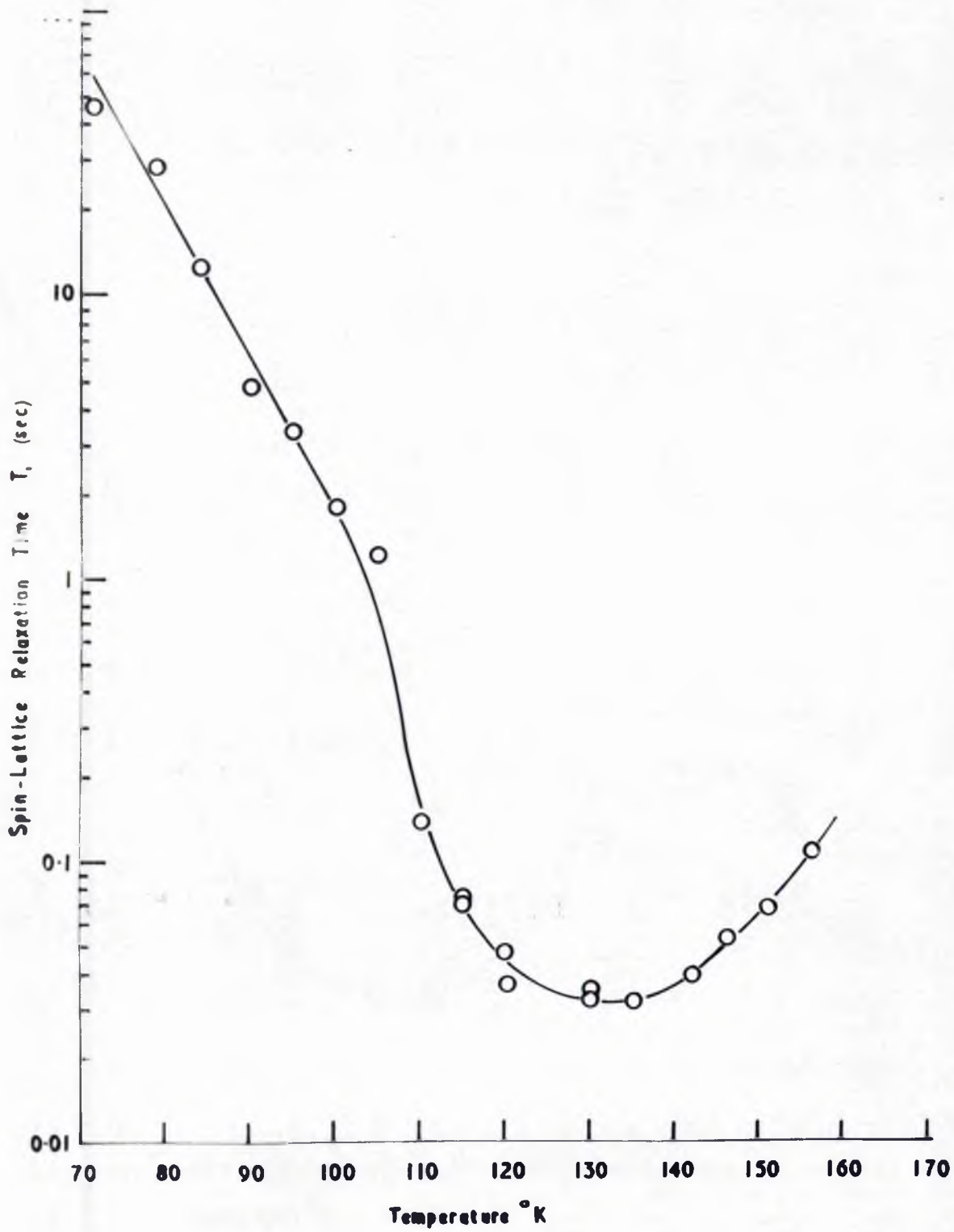
Figure 31.

the 'inter' contribution by a factor 0.244. Using this figure for cyclohexene gives a reduced 'inter' contribution of 1.9 gauss^2. Thus the approximate theoretical second moment value for the lattice in which this motion is occurring is 6.0 gauss^2. Apart from the uncertainty in the molecular configuration, the error in this figure is that of the 'inter' contribution; for this an error factor of about two must be stated. Thus the final value is 6.0 ± 2.0 gauss^2. This figure certainly supports the suggestion that such molecular motion may be occurring. The form of the additional motion responsible for the further reduction of the second moment around 130°K is not clear. In fact, due to the lack of symmetry of the molecule, combinations of various motions may occur, no single form being preferred other than, perhaps, those already considered.

4.5.5 Spin-lattice Relaxation Time Measurements.

Some measurements were made with the B.D.H. sample and are shown in figure 31. As mentioned earlier there is no hint of the phase transition around 139°K. The value of the relaxation time at 75°K for the I.C.I. sample was only about 4 seconds - that is, nearly a factor of ten shorter than for the B.D.H. sample. In view of this, and of the lack of information on the purity of the samples, it was decided to postpone these measurements until a pure sample was available.

It is hoped that a specimen will be obtained from the National Bureau of Standards so that this work can be completed in the near future.

5. SUMMARY

The variations with temperature of the nuclear magnetic resonance absorption spectra of cyclohexane, benzene, benzene-d_4 and cyclohexene have been examined between 75°K and 280°K. Also the spin-lattice relaxation times have been measured as a function of the temperature for the first three of these substances.

Proposed molecular and crystal structures are confirmed by the agreement between the experimental and calculated rigid lattice second moment values.

In all four cases above a certain temperature the linewidth of the absorption spectrum is less than the rigid lattice value due to the occurrence of molecular motion in the lattice, and it appears that these motions are predominantly responsible for the relatively short relaxation times observed.

The height of the potential barrier opposing reorient--ation of the cyclohexane molecule about its triad axis has been found to be 11 ± 1 Kcal/mole. In the case of benzene and benzene-d_4 motion about the hexad axis is hindered by barrier heights of 3.74 ± 0.20 and 3.90 ± 0.20 Kcal/mole respectively.

To carry out these measurements a conventional 'radio-frequency bridge' type of apparatus has been developed.

In conclusion, the author wishes to record his sincere

6.   Appendices

1.   Effect on the 'intra' and 'inter' molecular contributions to the second moment of non-continuous molecular motion about a symmetry axis.   Application to cyclohexane and benzene.

2.   Effect on the 'intra' and 'inter' molecular contributions to the second moment of continuous motion of the molecules about their centres of gravity. Application to cyclohexane.

3.   Minimum value of the second moment for cyclohexane if the molecules have fixed positions in the lattice.

4.   Molecular model for cyclohexane.

5.   Reduction of the 'intra' contribution to the second moment due to motion about a diad axis of the molecule.

Figure 32.

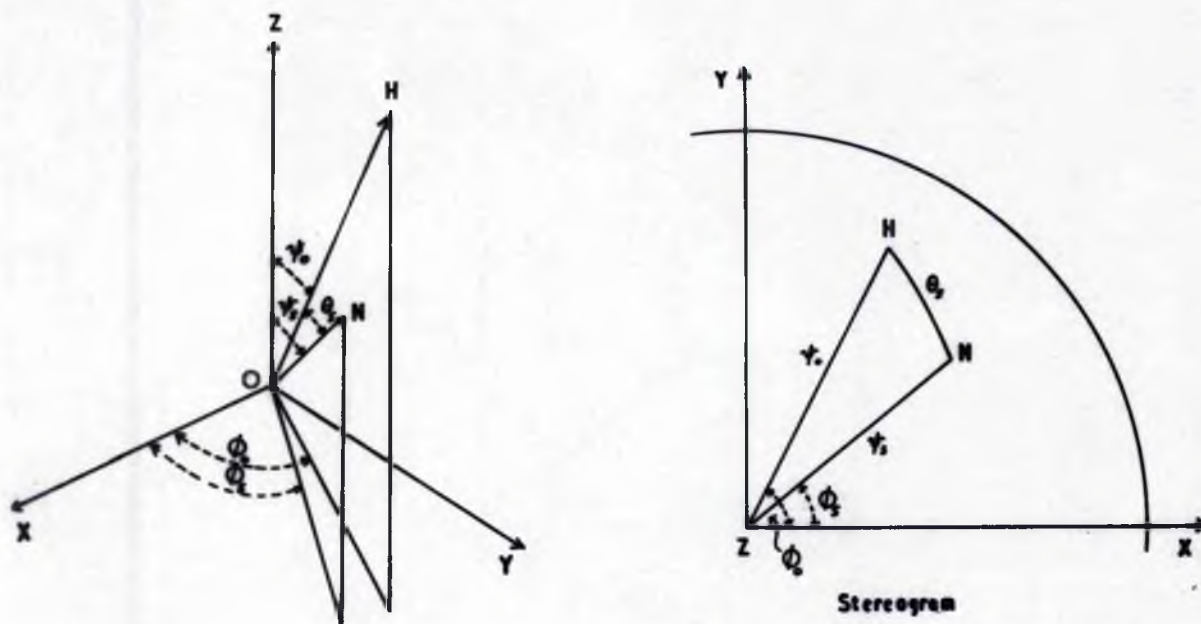One moving nucleus is in one of its equivalent positions
at the origin.

Pole of the stereogram is Z axis of the crystal.

H   Direction of the external magnetic field.

N   Direction of second nucleus in one possible position.

ϕ_o Azimuth of H.

ϕ_s Azimuth of N.

γ_o Polar angle of H.

γ_s Polar angle of N.

θ_s Angle between H and internuclear direction.

Appendix 1.

Effect on the 'intra' and 'inter' molecular contributions to the second moment of non-continuous molecular motion about a symmetry axis.

The effect of motion of this form on the 'intra' contribution has been studied by Gutowsky and Pake ; their result is given in Appendix 5.

In this appendix a formula is derived which enables the 'inter' contribution also to be calculated for the non-rigid lattice. The analysis is due to E.R. Andrew (reference 61).

Figure 32 applies ; the theory of spherical triangles gives :

$$\cos \theta_s = \cos \psi_0 \cos \psi_s + \sin \psi_0 \sin \psi_s \cos(\phi_s - \phi_0)$$

If
$$\mathcal{J}_s = \frac{3\cos^2\theta_s - 1}{r_s^3} \quad , \text{ then}$$

$$\mathcal{J}_s = \frac{3}{r_s^3}\left[\cos^2\psi_0 \cos^2\psi_s + \frac{1}{2}\sin 2\psi_0 \sin 2\psi_s \cos(\phi_s - \phi_0) + \sin^2\psi_0 \sin^2\psi_s \cos^2(\phi_s - \phi_0)\right] - \frac{1}{r_s^3}$$

This expression has to be averaged over the molecular motion occurring. If each molecule can take up 'n' equivalent positions, then

$$\bar{\mathcal{J}} = \frac{1}{n}\sum_{s=1}^{n} \mathcal{J}_s$$

$$\bar{\mathcal{J}} = A\cos^2\psi_0 + B\sin 2\psi_0 \cos\phi_0 + C\sin 2\psi_0 \sin\phi_0 + D\sin^2\psi_0 \cos^2\phi_0 + E\sin^2\psi_0 \sin 2\phi_0 + F\sin^2\psi_0 \sin^2\phi_0 - G$$

where

$$A = \frac{3}{n} \sum \frac{\cos^2 \psi_s}{r_s^3} \qquad B = \frac{3}{2n} \sum \frac{\sin 2\psi_s \cos\phi_s}{r_s^3} \qquad C = \frac{3}{2n} \sum \frac{\sin 2\psi_s \sin\phi_s}{r_s^3}$$

$$D = \frac{3}{n} \sum \frac{\sin^2 \psi_s \cos^2 \phi_s}{r_s^3} \qquad E = \frac{3}{2n} \sum \frac{\sin^2 2\psi_s \sin 2\phi_s}{r_s^3} \qquad F = \frac{3}{n} \sum \frac{\sin^2 \psi_s \sin^2 \phi_s}{r_s^3}$$

$$G = \frac{1}{n} \sum \frac{1}{r_s^3}$$

$(\bar{y})^2$ appears in the second moment formula (see section 2.2).
Hence $(\bar{y})^2$ has to be formed and ϕ_o and ψ_o averaged for
over all values since the sample is polycrystalline; i.e.
ϕ_o is averaged over a circle, and ψ_o over a sphere.
This gives :

$$\overline{(\bar{y})^2}^{\phi_o \psi_o} = \frac{1}{5} A^2 + \frac{4}{15} B^2 + \frac{4}{15} C^2 + \frac{1}{5} D^2 + \frac{4}{15} E^2 + \frac{1}{5} F^2 + G^2 + \frac{2}{15} AD$$

$$+ \frac{2}{15} AF - \frac{2}{3} AG + \frac{2}{15} DF - \frac{2}{3} DG - \frac{2}{3} FG$$

$$= f(A, B, C \cdots G)$$

For a nuclear pair rigidly separated by a distance r_o,

$$\bar{y}^2 = \frac{4}{5} r_o^{-6}$$

Hence $\qquad \dfrac{\bar{y}^2 \text{ moving}}{\bar{y}^2 \text{ stationary}} = \rho = \dfrac{f(A, B, C \cdots G)}{\frac{4}{5} r_o^{-6}}$

and

$$\frac{\rho}{r_o^6} = \frac{1}{4}\left(A^2 + D^2 + F^2 + 5G^2 \right) + \frac{1}{3}\left(B^2 + C^2 + E^2 \right) + \frac{1}{6}(AD + DF + AF)$$

$$- \frac{5}{6}(AG + GF + GD)$$

Hence, when motion of this form is occurring, each term in the summation $\sum 1/r_{jk}^{6}$ appearing in the second moment formula for the rigid lattice has to be replaced by the value of this expression when calculating the intermolecular contribution to the second moment.

Application to Cyclohexane.

Motion of the cyclohexane molecules about their triad axes means that there are nine terms in the summations involved in evaluating A, B, C ....G. Thus the application of this result to even a relatively simple case involves very lengthy calculations. Further, pairs of protons which are relatively distant in the rigid lattice and which, therefore, give only a very small contribution to the second moment can, by the molecular motion, be brought relatively close to each other. Accordingly, an accurate theoretical value for the 'inter' contribution can only be obtained by applying the results of this appendix to a very large number of internuclear distances; this involves a prohibitively large amount of calculation. A reasonable estimate of the 'inter' contribution has been obtained as follows :

Group 1. Proton-proton distances less than 3A.

The nine shortest distances, 2.3A to 2.93A have been treated exactly. These give a total contribution of 0.066 x 10^{46} cm^{-6}. to $(\sum r_{jk}^{-6})$ (non-rigid) compared with 2.920 x 10^{46} cm^{-6}.

for the rigid lattice.

Group 2. Distances greater than 3A but less than 5A.

Here 39 nuclear pairs have to be considered. Six of
these are considered incidently in group 1 : two show
slightly increased contributions for the non-rigid lattice,
since appreciable time is spent in positions which are
closer together. The others show a larger decrease, for,
although one of the nine distances in each case is much
shorter, the others are much larger.   Most of the remaining
33 pairs have their other eight distances over 5A. A net
decrease in the contribution from this group is to be
expected. Applying the mean reduction factor 2.2 - obtained
from the six pairs calculated - the contribution from group
2 is 0.399 x 10^{46} cm^{-6}.   Groups 1 and 2 give a total 'inter'
contribution of 0.71 $gauss^2$.

Group 3. Distances greater than 5A.

12 distances have been worked out incidently in
group 1. All give an increased contribution, the factor of
increase varying from 2 to 8. These distances are all in the
range 5.0 to 7.2 A, which in the rigid lattice case gives
67% of the contribution from the protons over 5A. But these
cannot be said to be representative distances since the pairs
come much closer together during reorientation than the other
distances in this interval do. Also, some quite remote pairs
will come in relatively close, and for them the factor of

increase will be large.

On the whole an increase is to be expected but will not
be large : a factor of two is likely. The contribution from
the proton-proton distances greater than 5A for the rigid
lattice is 0.86 gauss^2. Hence, for the non-rigid case,
this contribution is 1.72 ± 1.0 gauss^2, giving :

'Inter' contribution to the second moment when the molecules
are reorientating about their triad axes = 2.44 gauss^2 ± 1.0
gauss^2.

Application to Benzene.

1. Motion of the benzene molecules about their hexad axes
means that there are 36 terms in the summations involved in
evaluating the reduced inter-molecular effect. Although by
calculating r' for three selected proton pairs, all the
proton-proton distances under 5A in the rigid lattice are
covered, still an exact theoretical value for the contribution
in the non-rigid lattice cannot easily be obtained. (cf.
cyclohexane). Again proton pairs which are relatively distant
in the rigid lattice can, by the molecular motion, be brought
quite close to each other. Thus it would be necessary to
consider all distances up to about 10A individually if an
exact value is to be calculated. A reliable estimate of the
'inter' contribution has, however, been computed as follows :

Group 1. Distances less than 5A in the rigid lattice.

The 37 shortest distances in the summation $\sum\limits_{j>k} r_{jk}^{-6}$ for

the rigid lattice have been treated exactly and give a new total contribution of 0.19 gauss^2. Some 20 distances greater than 5A are incidently treated here.

Group 2. Distances between 5A and 6A.

Here 53 proton pairs have to be considered; of these twelve are treated incidently in group 1, and for all these the closest distance of approach is 3.16A or below. The mean value of the reduction factor for these is very nearly unity; the remaining 41 pairs come in no closer than 5.04A, and in general move much further apart than in the rigid lattice. On the whole for these a slight reduction is to be expected. Group 2 contributes 42% of that from the proton pairs greater than 5A apart in the case of the rigid lattice.

Group 3. Distances greater than 6A.

Range 6A to 7A : this group contributes 22% in the rigid lattice case (cf. group 2). Seven proton pairs with r_{jk} in this range have been considered incidently in group 1. These show a mean factor of increase of two; but, since these move to within 5A, they are not representative of this sub-group as a whole. The majority of pairs will give a decreased contribution by moving out beyond 7A during the reorientation process. Here again the net contribution will not differ much from that for the rigid lattice.

For distances over 7A (normally contributing 36%), an

increase by a factor of about two is to be expected.

Combining the groups 2 and 3 a net increased effect of about 30% is to be expected from this analysis. Thus the new contribution from the pair distances greater than 5A is 0.72 ± 0.5 gauss^2, giving a total 'inter' contribution of 0.91 ± 0.5 gauss^2, and a total reduced second moment of 1.7 ± 0.5 gauss^2. (The reduced 'intra' contribution is calculated using the formula of Gutowsky and Pake, quoted in Appendix 5 ; this gives a reduced 'intra' contribution of 0.82 gauss^2).

2. Motion of the benzene molecules about their diad axes : Here again the contribution from pairs less than 5A apart has been found exactly ; the new contribution is 0.99 gauss^2. This treatment again incidently considered some distances greater than 5A, and, in all cases, showed that their residual contributions were greater than in the case of rotation about the hexad axis. Thus, if the figure 0.71 ± 0.5 gauss^2 is accepted for the contribution from pairs greater than 5A apart, the net result will tend to yield a minimum value for the 'inter' contribution to the second moment when such molecular reorientation is occurring. Since the reduced 'intra' contribution is 1.13 gauss^2, the reduced second moment is 2.84 gauss^2.

Appendix 2.

Effect on the 'intra' and 'inter' molecular contributions to the second moment of continuous motion of the molecules about all axes through their centres of gravity.

Such motion would reduce the 'intra' contribution to zero. The effect on the 'inter' contribution, however, is not so drastic. For a continuous motion about any particular axis, the summations appearing in Appendix I for A, B, ... G are replaced by integrals which generally require graphical solutions. For the case of rotation about a number of axes as here, the integrals prove yet more unwieldy, so that even an approximate solution is not feasible.

A reliable estimate of the expected value of the 'inter' contribution for cyclohexane when such motion is occurring has been obtained as follows :

In Appendix I, the dominant factor in the calculation which gives the reduced 'inter' contribution is $1/r_s^3$: accordingly, it is reasonable to expect that $G = \left\langle 1/r_s^3 \right\rangle$ av will give a useful measure of the reduction of the second moment contribution. Examination of the working done in applying the results of Appendix I shows that the angular variables which enter the terms only introduce a further reduction factor of about 2.

The contribution for the rigid lattice depends on $1/r_o^6$,
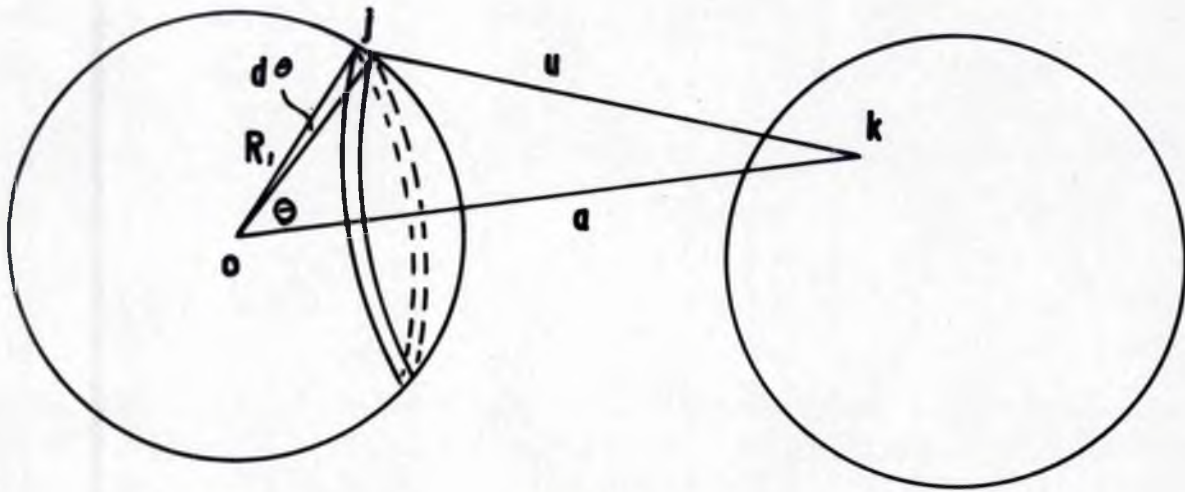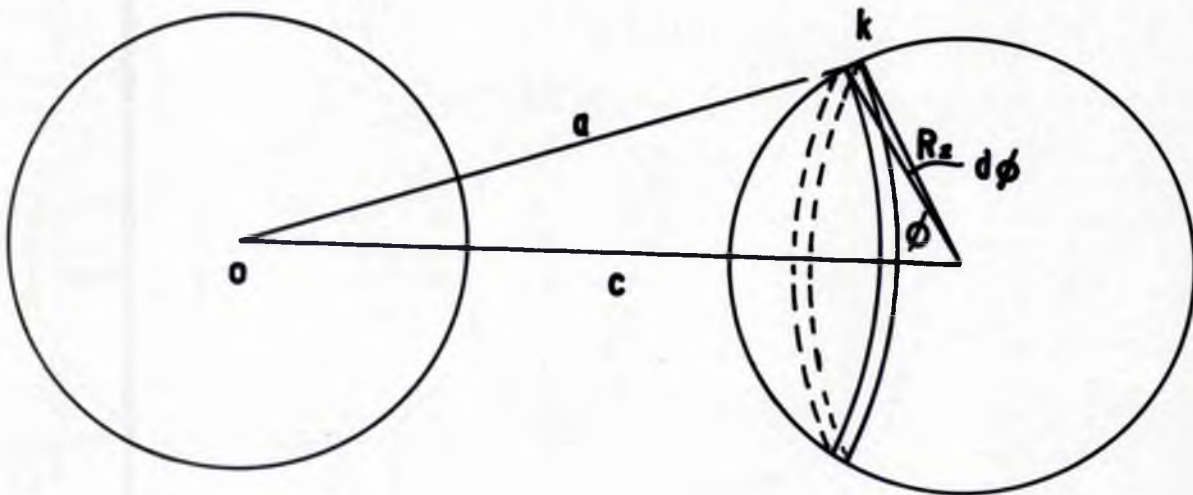
APPENDIX 2.

Figure 33.

Figure 34.

so that the contribution for the non-rigid lattice will
be of the order $x \langle \frac{1}{r_3^3} \rangle_{av}^2$, where x is a factor of order
unity which takes into account the neglected angular terms.
From the exact calculations made for distances less than 3A,
a mean value of $x = 0.63$ is obtained.

$\langle 1/r_s^3 \rangle$ av can be simply evaluated for the motion under
consideration ; for there are two types of protons in the
molecule of cyclohexane. The protons in each group are at
a certain distance from the centre of gravity of the molecule;
thus they can be considered to move on the surfaces of two
concentric spheres.

In figure 33, k is a typical position of one proton
on the surface of one sphere, distant a from the centre
of the second sphere. First we average $1/u^3$, allowing j,
the position of the other proton in the pair, to move over
the surface of the second sphere.

av. value of
$$\frac{1}{u^3} = \frac{1}{4\pi R_1^2} \int_0^\pi \frac{2\pi R_1^2 \sin\theta \cdot d\theta}{u^3}$$

and
$$u\,du = a R_1 \sin\theta \cdot d\theta$$

giving
$$\left\langle \frac{1}{u^3} \right\rangle_{av} = \frac{1}{2aR_1} \int_{a-R_1}^{a+R_1} \frac{1}{u^2} du = \frac{1}{a(a^2 - R_1^2)}$$

Proton k is now allowed to move over the surface of the
first sphere, i.e. a is allowed to vary. Distance e is

the separation of the c. of g's of the 2 molecules
(figure 34).

This gives similarly :

$$\left\langle\left\langle \frac{1}{u^3} \right\rangle\right\rangle_{av/av} = \frac{1}{4\pi R_2^2} \int_0^{\pi} \frac{2\pi R_2^2 \sin\phi \, d\phi}{a(a^2 - R_1^2)}$$

$$= \frac{1}{2cR_2} \int_{c-R_1}^{c+R_1} \frac{da}{a^2 - R_1^2}$$

so that finally the average required is given by

$$\frac{1}{4cR_1R_2} \left\{ \log_e \frac{c^2 - (R_2 - R_1)^2}{(c+R_2+R_1)(c-R_2-R_1)} \right\}$$

where R_1 and R_2 are the radii of the two spheres and c is
the separation of their centres.

For cyclohexane the radii of the 2 concentric spheres are 1.981 A. and 2.488 A.
Round any selected molecule there are the following neighbours:

12 at c. of g. spacing 6.194 A.

6 "   "   "   8.76 A.

24 "   "   "   10.73 A.

12 "   "   "   12.39 A.

The next group of molecules have c = 13.83 A.   From this
group onwards a continuous distribution has been assumed,
as in the calculation of the 'inter' contribution from proton-
proton distances greater than 5 A.

Applying the above formula, and taking the factor
$x = 0.63$ into account, gives a value of 1.32 gauss^2 for the

'Inter' contribution ; since the 'intra' contribution is zero, this is the total second moment for the lattice in which this motion is occurring.

Another, and much simpler, calculation also yields an approximate theoretical value. Here it is supposed that all the protons are at the centres of gravity of the molecules. This yields a value of 1.11 gauss^2 for the second moment. This calculation assumes, of course, that $\langle 1/r_s^3 \rangle$ av = $1/c^3$, and from this consideration alone would lead to a low value. However, the neglected angular variables might well offset this, making, in fact, 1.11 gauss^2 a more realistic value.

The experimental values fall from 1.5 gauss^2 at 190°K to 1.1 gauss^2 at 225°K. The approximate theoretical values, therefore, certainly give weight to the proposal that motion about all axes through the centre of gravity of the molecule is occurring in the solid state at this temperature.

Appendix 3.

Minimum value of the second moment for cyclohexane
if the molecules are fixed in the lattice.

If, in Appendix 2, the protons are placed not at the centres of the spheres but at the ends of diameters so that the distances between the protons of two molecules have their maximum values, then this minimum value can be calculated.

This has been done for values of c (see Appendix 2) up to 12.39 A, and gives a value for the 'inter' contribution of 0.05 gauss^2.   To this must be added, if it is not zero, the 'intra' contribution appropriate to the motion which would effectively place the protons in those positions. Above 240°K the experimental value is definitely less than 0.01 gauss^2, indicating that, in fact, it is certain that molecular diffusion must occur within the lattice, and that this molecular motion is averaging out still more the spin-spin interaction.
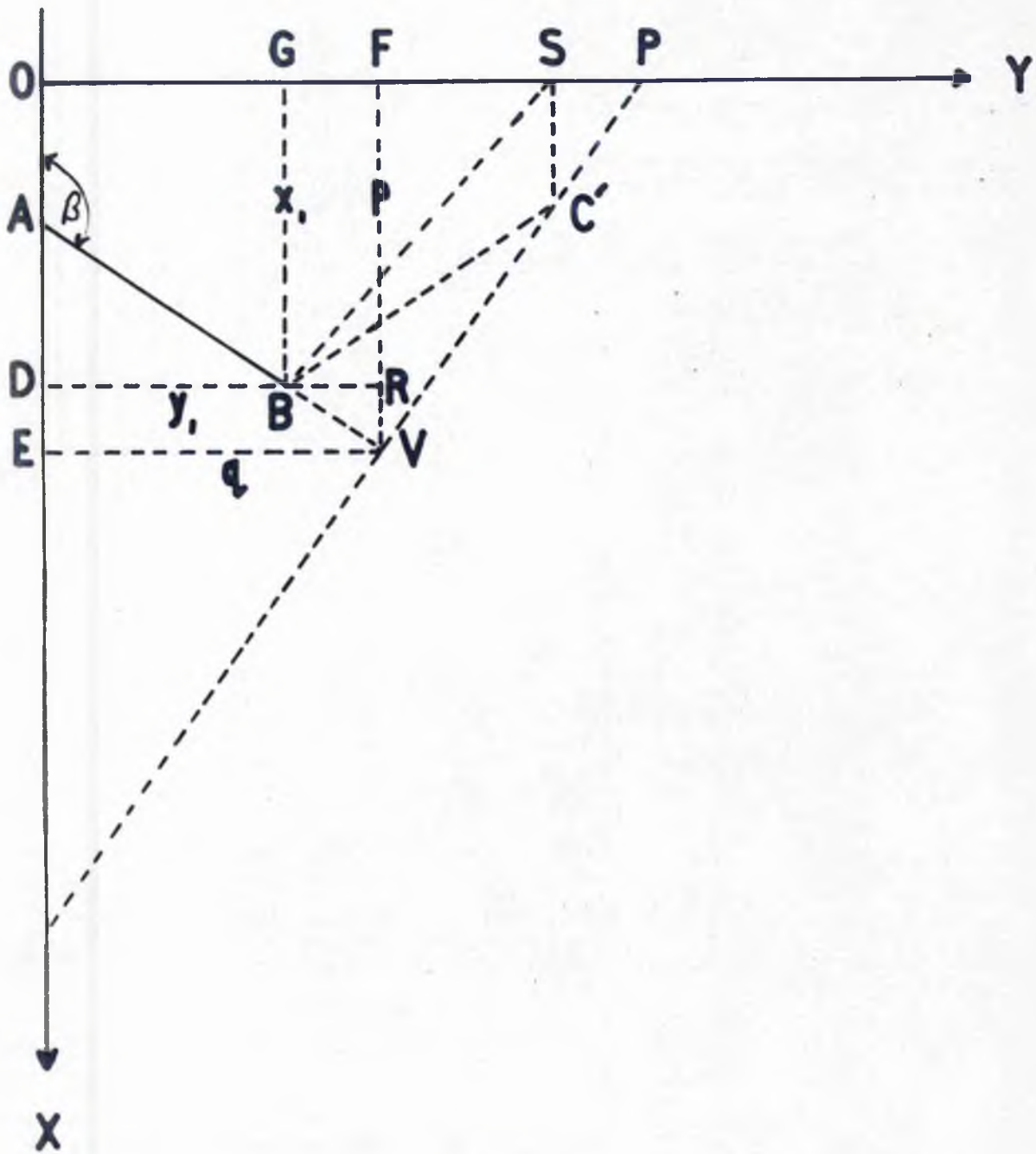
Figure 35.

Appendix 4.

A Molecular Model for Cyclohexene

The following is a corrected version of an analysis appearing in reference 35.

The C = C bond length is 2a, and the C - C bond, 2b. The carbon atoms A,B,E and F are supposed to lie in the plane z = 0, and the bond angles at B and E are made tetra--hedral. Angles FAB and AFE (figure 29) are denoted by β and angles BCD and CDE by γ. We require a relationship between β and γ in terms of the quantities a and b. (Note O, the origin, is placed at the midpoint of AF).

The axis OY (figure 35) is one of 2-fold symmetry; hence if x,y,z are the coordinates of C, then

$$x^2 + z^2 = b^2 \tag{1}$$

Also C must lie on the sphere, centre B (coordinates x_1 y_1 z_1) and radius 2b ; thus

$$(x - x_1)^2 + (y - y_1)^2 + (z - z_1)^2 = 4b^2 \tag{2}$$

Further, since the angles at B are tetrahedral, C must lie on a plane through V and perpendicular to AV. Thus BV $= \frac{1}{3}$ AB, and AV = 8b/3. If OP = d, then

$$y = d + x \cot \beta \tag{3}$$

Substituting for x_1 y_1 z_1 and solving for y gives :

$$y = a \tan \beta \pm \sqrt{\left\{ a^2 \sec^2 \beta - \frac{16}{3} ab \sec \beta + \frac{29}{3} b^2 \right\}} \tag{4}$$

where the positive sign is relevant.

Point S, the centre of the bond OD, lies in the plane $z = 0$, and $\triangle$ BO'S is the projection of $\triangle$ BCS on this plane; hence

$$BS^2 = SC^2 + BC^2 - 2BC.SC.\cos \tau \tag{5}$$

where

$$BS^2 = GS^2 + GB^2 = (y - y_1)^2 + x_1^2 \tag{6}$$

Substituting (4) and (6) in (5) gives the required result :

$$\cos \tau = \frac{1}{4b^2} \left[\frac{28}{3} ab \sec \beta - 2a^2 \sec^2 \beta - \frac{26b^2}{8} - 2a \tan \beta - 4b \sin \beta \sqrt{a^2 \sec^2 \beta - \frac{16}{3} ab \sec \beta + \frac{29}{3} b^2} \right]$$

Appendix 5.

Reduction of the intra-molecular contribution to the second moment due to motion about a diad axis.

In reference 5 Gutowsky and Pake evaluate the reduction factor to be applied to the rigid lattice 'intra' contribution when classical rotation, or n-fold tunnelling $(n \geq 3)$ about a symmetry axis of the molecule, is occurring. This factor is $\frac{1}{4}(3\cos^2 \gamma_s - 1)^2$, where the symbols are those used in figure 32, Appendix 1.

This analysis does not cover the special case of 2-fold tunnelling, which might occur in cyclohexene. The average value of the factor $(3\cos^2 \theta_{jk} - 1)^2$ which appears in the equation for the second moment (see section 2.2) has to be found as follows :

$$\cos \theta_s = \cos \gamma_0 \cos \gamma_s + \sin \gamma_0 \sin \gamma_s \cos (\phi_s - \phi_0)$$

$$\therefore \langle \cos^2 \theta_s \rangle_{av} = \cos^2 \gamma_0 \cos^2 \gamma_s + \frac{1}{2} \sin 2\gamma_0 \sin 2\gamma_s \langle \cos(\phi_s - \phi_0) \rangle_{av}$$

$$+ \sin^2 \gamma_0 \sin^2 \gamma_s \langle \cos^2(\phi_s - \phi_0) \rangle_{av}$$

For a 2-fold axis of rotation, ϕ_s only takes up two values differing by 180 degrees. Thus

$$\langle \cos(\phi_s - \phi_0) \rangle_{av} = \frac{1}{2}(\cos \phi_0 - \cos \phi_0) = 0$$

$$\langle \cos^2(\phi_s - \phi_0) \rangle_{av} = \frac{1}{2}(\cos^2 \phi_0 + \cos^2 \phi_0) = \cos^2 \phi_0$$

and

$$\overline{y}^2 = \left(3\overline{\cos^2\theta_s}^{\phi_s} - 1\right)^2 = \left(3\cos^2\psi_0\cos^2\psi_s + 3\sin^2\psi_0\sin^2\psi_s\cos^2\phi_0 - 1\right)^2$$

Since the specimen is polycrystalline, it is necessary to average ϕ_0 over all values :

$$\overline{y^2}^{\phi_0} = \sin^4\psi_0\left(9\cos^4\psi_s + \frac{27}{8}\sin^4\psi_s - \frac{9}{4}\sin^2\psi_s\cos^2\psi_s\right)$$

$$+ \sin^2\psi_0\left(-18\cos^4\psi_s + \frac{9}{4}\sin^2\psi_s\cos^2\psi_s - 3\sin^2\psi_s + 6\cos^2\psi_s\right)$$

$$+ 9\cos^4\psi_s - 6\cos^2\psi_s + 1$$

Also ψ_0 must be averaged over a sphere of directions, giving :

$$\overline{y^2}^{\phi_0 \psi_0} = \frac{9}{5}\left(\cos^4\psi_s + \sin^4\psi_s + \frac{2}{3}\sin^2\psi_s\cos^2\psi_s\right) - 1 = F(\psi_s)$$

Since $\overline{y^2}^{\psi_0}$ for the rigid lattice has the value 4/5, the reduction factor ρ is :

$$\psi = \frac{F(\psi_s)}{\frac{4}{5}} = \frac{5}{4}\left[\frac{9}{5}\left(\cos^4\psi_s + \sin^4\psi_s + \frac{2}{3}\sin^2\psi_s\cos^2\psi_s\right) - 1\right]$$

which gives $\rho = \left(1 - 3\sin^2\psi_s\cos^2\psi_s\right)$.

Such motion of the cyclohexene molecule about the 2-fold axis OY (figure 29) reduces the 'intra' contribution from

13.8 gauss^2 to 8.0 gauss^2.

7. References

1. N. Bloembergen, E.M. Purcell, R.V. Pound, Phys.Rev.
73, 679, 1948.

2. G.E. Pake, J.Chem.Phys., 16, 327, 1948.

3. Gutowsky, Kistiakowsky, Pake, Purcell, J.Chem.Phys.,
17, 972, 1949.

4. E.R. Andrew, R. Bersohn, J.Chem.Phys., 18, 159, 1950.

5. H.S. Gutowsky, G.E. Pake, J.Chem.Phys., 18, 162, 1950.

6. J.H. Van Vleck, Phys.Rev., 74, 1168, 1948.

7. J.A. Bearden, H.M. Watts, Phys.Rev., 81, 73, 1951.

8. E.R. Andrew, J.Chem.Phys., 18, 607, 1950.

9. W. Heitler, E. Teller, Proc.Roy.Soc., A 155, 629, 1936.

10. I. Waller, Zeits.f.Physik., 79, 370, 1932.

11. G.E. Pake, Amer.J. of Physics, 18, 473, 1950.

12. L.A. Moxon, 'Recent Advances in Radio Receivers'
pub. Camb.U.P., 1949.

13. R.H. Dicke, Rev.Sci.Instrum., 17, 268, 1946.

14. S.W. Punnet, J.Brit.Inst. R.E., 10, 39, 1950.

15. O. Hassel, H. Kringstad, Tidskr.Kjemi.Berg., 10, 128,
1930.

16. K. Lonsdale, H. Smith, Phil.Mag., 28, 614, 1939.

17. R.S. Rasmussen, J.Chem.Phys., 11, 249, 1943.

18. C.W. Beckett, K.S. Pitzer, R. Spitzer, J.A.C.S., 69, 2488, 1947.

19. O. Hassel, B. Ottar, Extr.in Chem.Zentralblatt, 1942, II,2353.

20. L. Pauling, L.O. Brockway, J.A.C.S., 59, 1223, 1937.

21. L.G. Smith, Phys.Rev., 59, 924, 1941.

22. A. Muller, Proc.Roy.Soc., A 120, 437, 1928 : 127, 417, 1930 : 138, 514, 1932.

23. G. Herzberg, Infrared and Raman Spectra of Polyatomic Molecules (D. van Nostrand Company, Inc., New York, 1945, pp. 439-440).

24. W. Gordy, J.W. Simmons, A.G. Smith, Phys.Rev., 74, 243, 1948.

25. L.G. Smith, W.M. Woodward, Phys.Rev., 61, 386, 1942.

26. R. Trambarulo, W. Gordy, J.Chem.Phys., 18, 1612, 1950.

27. O. Hassel, A.M. Sommerfeldt, Zeits.f.Phys.Chem., B40, 391, 1938.

28. G.B. Carpenter, R.S. Halford, J.Chem.Phys., 15, 99, 1947.

29. W. House, Zeits.f.Phys.Chem., A147, 256, 1930.

30. D. Rozental, Bull.Soc.Chem.Belg., 45, 585, 1936.

31. G.S. Parks, H.M. Huffman, S.B. Thomas, J.A.C.S., 52, 1032, 1930.

32. J. Smittenberg, H. Hoog, R.A. Henkes, J.A.C.S., 60, 17, 1938.

33. J.G. Aston, et al., J.A.C.S., 63, 2029, 1941 : 65, 1135, 1943.

34. R.A. Ruehrwein, H.M. Huffman, J.A.C.S., 65, 1620, 1943.

35. J. Boeseken, J. Stuurman, Kon.Acad.Van Weten. Te Amsterdam, 39, 2, 1936.

36. C.W. Beckett, N.K. Freeman, K.S. Pitzer, J.A.C.S., 70, 4227, 1948.

37. M.W. Lister, J.A.C.S., 63, 143, 1941.

38. R.A. Pasternak, Acta Cryst., 4, 316, 1951.

39. H.M. Huffman, M. Eaton, G.D. Oliver, J.A.C.S., 70, 2911, 1948.

40. G.S. Parks, H.M. Huffman, J.A.C.S., 52, 4381, 1930.

41. A.J. Streiff et al., J.Res.Nat.B.Stan., 41, 323, 1948.

42. O. Hassel, J.A. Hveding, Arch.Math.Natur., B45, NR.2, 1942.

43. I.S. Karle, J.Chem.Phys., 20, 65, 1952.

44. E.G. Cox, Proc.Roy.Soc., A135, 491, 1932.

45. B.H. Broome, Physik.Z., 24, 124, 1923 and Z.Krist. 62, 325, 1926.

46. E.D. Eastman, J.A.C.S., 46, 917, 1924.

47. E.G. Cox, see reference 44.

48. G. Bruni, G. Natta, Atti.d.accad.naz.Lincei, 11,1058, 1930.

49. W. Bilts, W. Fisher, E. Winnenberg, Z.Phys.Chem., A 151, 13, 1930.

50. A. Eucken, E. Lindenberg, Ber., 75B, 1953, 1943.

51. W. Heuse, Z.Phys.Chem., A 147, 266, 1930.

52. D. Rosenthal, Bull.Soc.Chim.Belg., 45, 585, 1936.

53. J. Timmermans, Physico-Chemical Constants of Pure Organic Compounds, p. 145, (pub. Elsevier).

54. W. Bilts, Z. Phys.Chem., 151, 1930.

55. A.R. Glasgow Jr., et al., J.Res.Nat.Bur.Stan., 37, 141, 1946.

56. A. Fruhling et al., Ann.der Phys., 6, 401, 1951.

57. I.Ichishima, S. Mizushima, letter J.Chem.Phys., 18, 1686, 1950.

58. S.C. Sirkar, A.K. Ray, Ind.J.Phys., 24, 189, 1950.

59. E.R. Andrew, D. ter Haar.   Private communication.

60. L.O. Brockway, J.M. Robertson, J.Chem.Soc., 1324, 1939.

61. E.R. Andrew.   Private communication.